NASA CONTRACTOR REPORT

NASA CR-1060

AN ANALYSIS OF THE COUPLED CHEMICALLY REACTING BOUNDARY LAYER AND CHARRING IABLATOR

Part I

Summary Report

Roald A. Rindal,

and Carl D. Howe

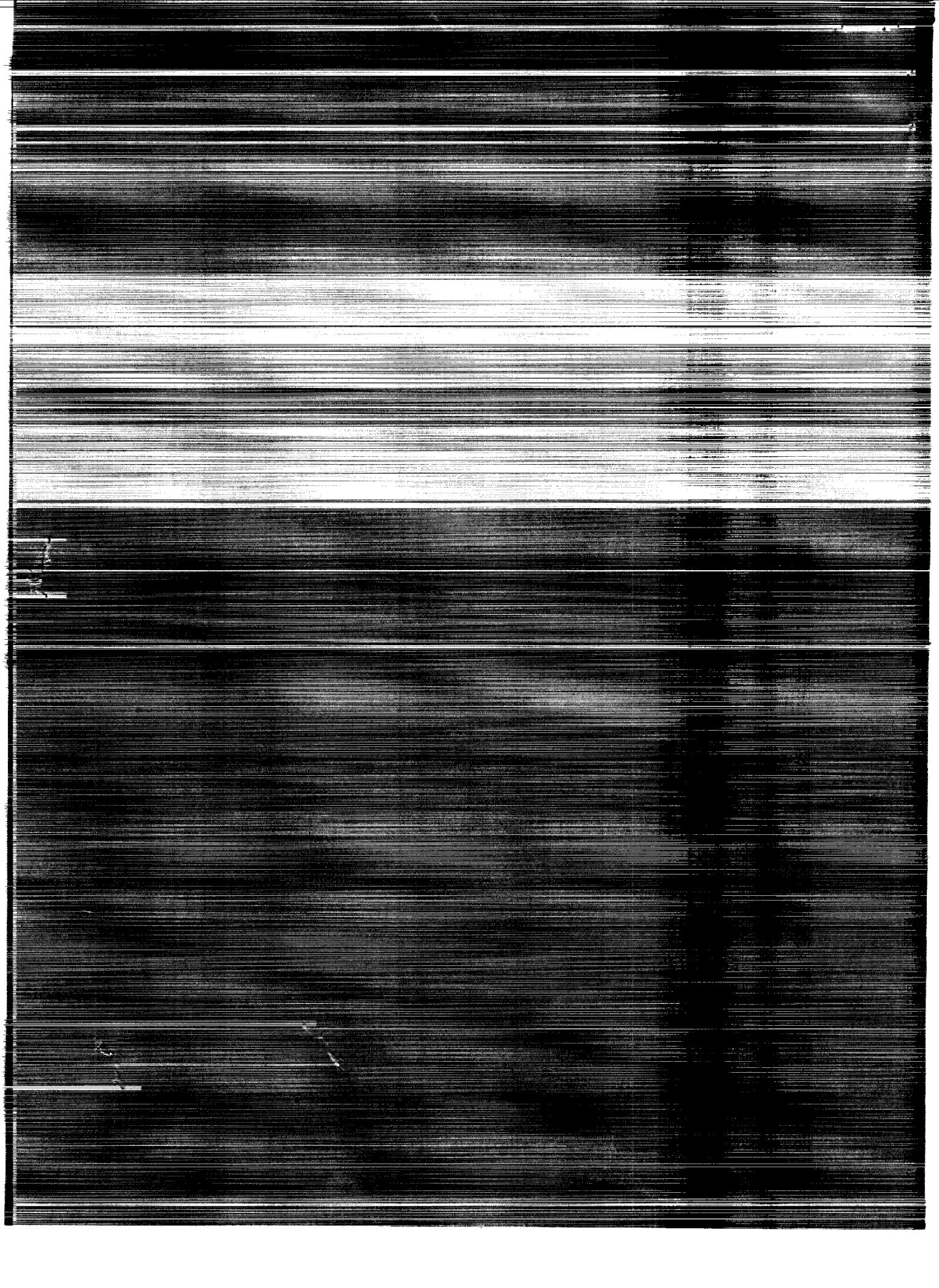

NASA CR-1060

AN ANALYSIS OF THE COUPLED CHEMICALLY REACTING BOUNDARY LAYER AND CHARRING ABLATOR

Part I

Summary Report

By Robert M. Kendall, Eugene P. Bartlett,
Roald A. Rindal, and Carl B. Moyer

Issued by Originator as Aerotherm Report No. 66-7, Part I

Prepared under Contract No. NAS 9-4599 by
ITEK CORPORATION, VIDYA DIVISION
Palo Alto, Calif.

for Manned Spacecraft Center

NATIONAL AERONAUTICS AND SPACE ADMINISTRATION

For sale by the Clearinghouse for Federal Scientific and Technical Information
Springfield, Virginia 22151 – CFSTI price $3.00

FOREWORD

The present report is one of a series of six reports, published simultaneously, which describe analyses and computational procedures for: 1) prediction of the in-depth response of charring ablation materials, based on one-dimensional thermal streamtubes of arbitrary cross-section and considering general surface chemical and energy balances, and 2) nonsimilar solution of chemically reacting laminar boundary layers, with an approximate formulation for unequal diffusion and thermal diffusion coefficients for all species and with a general approach to the thermochemical solution of mixed equilibrium-nonequilibrium homogeneous or heterogeneous systems. Part I serves as a summary report and describes a procedure for coupling the charring ablator and boundary layer routines. The charring ablator procedure is described in Part II, whereas the fluid-mechanical aspects of the boundary layer and the boundary-layer solution procedure are treated in Part III. The approximation for multicomponent transport properties and the thermochemistry model are described in Parts IV and V, respectively. Finally, in Part VI an analysis is presented for the in-depth response of charring materials taking into account char-density buildup near the surface due to coking reactions in depth.

The titles in the series are:

Part I Summary Report: An Analysis of the Coupled Chemically Reacting Boundary Layer and Charring Ablator, by R. M. Kendall, E. P. Bartlett, R. A. Rindal, and C. B. Moyer.

Part II Finite Difference Solution for the In-depth Response of Charring Materials Considering Surface Chemical and Energy Balances, by C. B. Moyer and R. A. Rindal.

Part III Nonsimilar Solution of the Multicomponent Laminar Boundary Layer by an Integral Matrix Method, by E. P. Bartlett and R. M. Kendall.

Part IV A Unified Approximation for Mixture Transport properties for Multicomponent Boundary-Layer Applications, by E. P. Bartlett, R. M. Kendall, and R. A. Rindal.

Part V A General Approach to the Thermochemical Solution of Mixed Equilibrium-Nonequilibrium, Homogeneous or Heterogeneous Systems, by R. M. Kendall.

Part VI An Approach for Characterizing Charring Ablator Response with In-depth Coking Reactions, by R. A. Rindal.

This effort was conducted for the Structures and Mechanics Division of the Manned Spacecraft Center, National Aeronautics and Space Administration under Contract No. NAS9-4599 to Vidya Division of Itek Corporation with Mr. Donald M. Curry and Mr. George Strouhal as the NASA Technical Monitors. The work was initiated by the present authors while at Vidya and was completed by Aerotherm Corporation under subcontract to Vidya (P.O. 8471 V9002) after Aerotherm purchased the physical assets of the Vidya Thermodynamics Department. Dr. Robert M. Kendall of Aerotherm was the Program Manager and Principal Investigator.

ABSTRACT

This report summarizes analyses and computational procedures for predicting the transient in-depth response of charring ablation materials, either coupled to a nonsimilar, laminar, multicomponent, chemically-reacting boundary-layer computational procedure or partially decoupled through the use of convective transfer coefficients. The detailed developments are presented in companion documents. The computational procedure for charring ablators is an implicit finite difference procedure for an ablating surface material with several nonablating backup materials. It considers one-dimensional heat and mass transfer along thermal streamtubes of arbitrary cross-sectional area and permits a multiple-reaction model for gas decomposition and a general thermochemical surface boundary condition. The boundary-layer procedure utilizes a newly developed integral matrix solution procedure. It applies for general chemical systems, allowing rate-controlled surface reactions, and incorporates approximate formulations for mixture transport properties, including unequal diffusion and thermal diffusion coefficients for all species. Analyses are also presented for extending the boundary-layer computational procedure to include mixed equilibrium-nonequilibrium, homogeneous or heterogeneous general chemical systems and to include radiation absorption and emission, and for extending the charring ablation procedure to include char-density buildup due to coking reactions in depth.

TABLE OF CONTENTS

TABLE OF CONTENTS (Continued)

TABLE OF CONTENTS (Concluded)

LIST OF TABLES

LIST OF FIGURES

LIST OF FIGURES (Concluded)

LIST OF SYMBOLS

A	cross-sectional area for a node
A_n	coefficient in Eq. (40)
B'_c	defined as $\dot{m}_c/\rho_e u_e C_M$
B'_g	defined as $\dot{m}_g/\rho_e u_e C_M$
B_i	pre-exponential factor for i^{th} decomposition reaction in charring ablator
B_m	pre-exponential factor for m^{th} reaction constant
B_n	coefficient in Eq. (40)
B_n^*	value of B_n after first pass of Gauss reduction (see Eq. (41))
B_ν	Planck's function (defined by Eq. (26))
c	velocity of light
c_{k_j}	atoms of element k in molecule j
c_t	constant introduced in the approximation for multicomponent thermal diffusion coefficients embodied in Eq. (11). Tentatively established by correlation of data to be -0.5
C	product of density and viscosity normalized by their reference values (defined after Eq. (8))
C_H	Stanton number for heat transfer
C_M	Stanton number for mass transfer
C_n	coefficient in Eq. (40)
C_{p_i}	specific heat of species i
$\overline{C}_p$	specific heat of the gas mixture (defined by Eq. (19))
$\tilde{C}_p$	property of the gas mixture which reduces to $\overline{C}_p$ when diffusion coefficients are assumed equal for all species (defined by Eq. (21))
$\overline{D}$	a reference binary diffusion coefficient introduced by the approximation for binary diffusion coefficients embodied in Eq. (10)
D_i^T	multicomponent thermal diffusion coefficient for species i

LIST OF SYMBOLS (Continued)

D_{ij}	multicomponent diffusion coefficient for species i and j
$\mathcal{D}_{ij}$	binary diffusion coefficient for species i and j
D_n	coefficient in Eq. (40)
D_n^*	value of D_n after first pass of Gauss reduction (see Eq. (41))
E_{a_m}/R	activation energy for m^{th} reaction constant
E_i/R	activation energy for i^{th} decomposition reaction in charring ablator
E_n	error for the n^{th} equation during Newton-Raphson iteration (driven toward zero in the iteration); also exponential integral (defined by Eq. (27))
f	stream function (defined by Eq. (7))
F_i	diffusion factor for species i introduced by the approximation for binary diffusion coefficients embodied in Eq. (10)
G_j	partial molar free energy of species j
h	static enthalpy of the gas; also Planck's constant
$\tilde{h}$	property of the gas mixture which reduces to the static enthalpy h when diffusion coefficients are assumed equal for all species (defined by Eq. (21))
h_c	enthalpy of surface material (e.g., char) removed by combustion, sublimation, or vaporization
h_g	enthalpy of gas which enters boundary layer without phase change <u>at the surface</u> (e.g., pyrolysis gases)
h_i	enthalpy of species i
h_ℓ	enthalpy of surface material (e.g., char) removed in the condensed phase (e.g., by melting with subsequent liquid runoff or by spallation)
h_w	static enthalpy of the gas at the wall
H_j	molar enthalpy of species j
H_r	recovery enthalpy
H_T	total enthalpy
I_{ν_e}	specific radiation intensity at boundary-layer edge
j_i	diffusional mass flux of species i per unit area

j_k	diffusional mass flux of element k per unit area
k	thermal conductivity of solid; also Boltzmann's constant
k_F	forward rate coefficient
K	number of base species (or "elements")
$\tilde{K}_{cg}$	elemental mass fraction of carbon in the pyrolysis gas
$\tilde{K}_{cgE}$	elemental mass fraction of carbon in the pyrolysis gas that would exist if equilibrium were achieved
$\tilde{K}_{c_k}$	total mass fraction of "element" k contained in surface material (e.g., char) removed by combustion, sublimation, or vaporization
$\tilde{K}_{g_k}$	total mass fraction of "element" k contained in gas which enters boundary layer without phase change at the surface (e.g., pyrolysis gases)
K_i	mass fraction of molecular species i
$\tilde{K}_k$	total mass fraction of "element" k irrespective of molecular configuration
$\tilde{K}_{\ell k}$	total mass fraction of "element" k contained in surface material (e.g., char) which is removed in the condensed phase (e.g., by melting with subsequent liquid runoff or by spallation)
K_{p_j}	equilibrium constant for formation of species j
$\dot{m}$	mass flow rate per unit area
$\dot{m}_c$	mass removal rate per unit area of surface material (e.g., char) by combustion, sublimation, or vaporization
$\dot{m}_{coke}$	coking rate
$\dot{m}_g$	mass flow rate per unit area of gas which enters boundary layer without phase change at the surface (e.g., pyrolysis gases); also mass flow rate of pyrolysis gas through an internal charring ablator node
m_i	reaction order for constituent i, see Eq. (39)
$\dot{m}_{r_\ell}$	mass removal rate per unit area of surface material (e.g., char) in the condensed phase (e.g., by melting with subsequent liquid runoff or by spallation)
$\mathcal{M}$	molecular weight of the gas mixture
$\mathcal{M}_i$	molecular weight of species i
n_j	number of moles of species j in a unit mass of the system

N	number of nodal points across the boundary layer selected for the purpose of the numerical solution procedure
N_b	number of base species
N_{bb}	number of base-base species
N_s	total number of species
p_j	partial pressure of species j
P	pressure
Pr	Prandtl number of the gas mixture (defined by Eq. (20))
q_a	diffusional heat flux per unit area
q_{cond}	heat conduction per unit area into the surface material
q_{r_i}	one-dimensional radiant heat flux (normal to surface), that is, the net rate per unit area at which radiant energy is transferred across a plane in the boundary layer parallel to the surface
r_i	net rate of increase of moles of "element" i per unit volume
r_o	local radius of body in a meridian plane for an axisymmetric shape
R	universal gas constant
$\overline{R}_m$	reaction rate for m^{th} reaction
s	distance along body from stagnation point or leading edge; also entropy
S_j	molar entropy of species j
$\overline{Sc}$	reference system Schmidt number (defined by Eq. (16))
T	static temperature
T_{F_ℓ}	fail or flow temperature for condensed-phase component ℓ
u	gas velocity component parallel to body surface
v	gas velocity component normal to body surface
v_j	j^{th} primary variable in the boundary-layer solution procedure
x	coordinate normal to ablating surface, fixed to receding surface
x_i	mole fraction of species i
y	distance from surface into the boundary layer, measured normal to the surface; coordinate normal to ablating surface with origin fixed in space relative to back wall for charring ablator

Z_i	a quantity for species i which is introduced as a result of the approximation for binary diffusion coefficients and reduces to K_i when all diffusion coefficients are assumed equal (defined by Eq. (12))
$\tilde{Z}_k$	a quantity for "element" (or base species) k which is introduced as a result of the approximation for binary diffusion coefficients and reduces to $\tilde{K}_k$ when all diffusion coefficients are assumed equal

GREEK SYMBOLS

α^*	flux normalizing parameter (defined by Eq. (9))
α_H	normalizing parameter used in definition of $\bar{\eta}$ (see Eq. (3))
α_i	moles of "element" i in a unit mass of the system
$\tilde{\alpha}_k$	defined by Eq. (64)
β	streamwise pressure-gradient parameter (defined after Eq. (8))
Γ	volume fraction of resin in plastic (see Eq. (38))
$\Delta f_i, \Delta f_i', \ldots$	corrections for f_i, f_i', ... during Newton-Raphson iteration
ϵ_w	emissivity of wall material
$\eta, \bar{\eta}$	transformed coordinate in a direction normal to the surface (defined by Eqs. (1) and (3))
θ	time; also angle between normal to the surface and direction of incident radiation; also angle between flow vector and a normal to the shock wave in oblique shock relations
κ_ν	mixture absorption coefficient at frequency ν (defined by Eq. (29))
λ	thermal conductivity of gas mixture
μ	shear viscosity of gas mixture
μ_{jm}^P	stoichiometric coefficient of reactant species in Eq. (56)
μ_{jm}^R	stoichiometric coefficient of product species in Eq. (56)
μ_1, μ_2, μ_3	properties of the gas mixture (defined by Eqs. (13) and (21)) which reduce to unity, to m and to $1/m$, respectively for assumed equal diffusion coefficients
ν	spectral frequency; also number of species in chemical system
ν_{ji}	stoichiometric coefficients for the formation reactions of Eq. (45)
$\xi, \bar{\xi}$	transformed streamwise coordinate (defined by Eqs. (2) and (3))

ρ	density
ρ_o	original density of a pyrolyzing component
ρ_r	final density of a pyrolyzing component
$\rho_w v_w$	total mass flux per unit area into the boundary layer
σ	Stefan-Boltzmann constant
σ_{ik}	stoichiometric coefficients for the formation reactions of Eq. (62)
τ_ν	optical thickness at frequency ν (defined by Eq. (25))
φ	angle between a reference line in the surface and the trace of the incident radiation flux on the surface
ϕ_k	"elemental" source term (see discussion following Eq. (8))

SUBSCRIPTS

A,B	denotes pyrolyzing component of resin
e	evaluated at the reference condition, usually taken as zero streamline from inviscid solution (synonymous with boundary-layer edge in the absence of an entropy layer)
g	denotes pyrolysis gas
i	denotes species or nodal point in the boundary layer equations; denotes pyrolyzing component in the charring ablator; denotes base species (or "elements") in chemical state equations
j	denotes species
k	denotes element or base-base species
ℓ	denotes condensed phase component
m	refers to m^{th} kinetic reaction
n	denotes node in charring ablator numerical procedure
p	denotes virgin plastic
w	evaluated at the wall
θ	evaluated within angular interval $\delta\theta$
ν	evaluated within frequency interval $\delta\nu$
1	denotes first (surface) node in charring ablation equations; denotes conditions upstream of the shock in oblique shock relations

LIST OF SYMBOLS (Concluded)

SUPERSCRIPTS

o	denotes standard state
κ	equal to unity for axisymmetric bodies and zero for two-dimensional bodies
*	signifies that quantity is normalized by α^* (e.g., $j_k^* = j_k/\alpha^*$) in boundary layer equations; also refers to condensed phase
'(prime)	represents partial differentiation with respect to $\bar{\eta}$ in boundary layer equations; denotes "new" at $\theta + \Delta\theta$ in charring ablator equations

AN ANALYSIS OF THE COUPLED CHEMICALLY REACTING BOUNDARY LAYER AND CHARRING ABLATOR

SECTION 1

INTRODUCTION

The transient response of charring ablation materials to actual or simulated superorbital reentry depends upon the intimate coupling which exists between the internal heat and mass transfer processes, the surface phenomena, and the boundary layer which envelops the heat shield. In the absence of procedures for obtaining fully coupled solutions, the conventional approach in the past has been to focus attention on the in-depth charring ablator response, utilizing empirical correlations such as heat-of-ablation or ablation-rate-versus-surface-temperature relationships to provide the surface boundary condition. This method has been effective when applied to conditions which do not differ significantly from the test conditions at which the empirical relationships were derived, but there is no valid basis for extrapolation to other conditions since the highly nonlinear coupling between the various phenomena cannot be scaled. A somewhat more sophisticated approach has been to represent the boundary-layer heat and mass transfer processes by convective transfer coefficients while considering detailed chemical interactions and mass and energy balances at the surface. Because detailed surface physics can be retained in the formulation, this method is better suited for application at conditions beyond the range of available experimental data. However, it is still severely limited in this regard since the effects of nonsimilarities between boundary-layer profiles cannot be treated precisely. Thus, mass addition, chemical reactions, and multicomponent diffusion effects can be taken into account only in an approximate manner, and upstream effects, thermal diffusion, and radiation-convection coupling cannot be considered except, possibly, through correlations of boundary-layer solutions.

In the present series of reports, theoretical analyses are presented and computational procedures are described for predicting the one-dimensional transient response of charring (or noncharring) ablation materials intimately coupled to quasi-steady, two-dimensional, nonsimilar, laminar, chemically reacting boundary layers. In addition, procedures are described for obtaining charring ablation solutions with the boundary layer represented by convective transfer coefficients. The physicochemical models which are employed are outlined in the ensuing paragraphs, followed by an introduction to the specific computer codes which have been developed.

Heat and mass transfer within the charring ablator is considered to be one-dimensional, but the thermal streamtubes are allowed to have arbitrary cross-sectional area. A general model for in-depth decomposition is considered. Detailed surface thermochemistry is considered, including selected rate-controlled

reactions, and liquid-layer removal and mechanical spallation are taken into account through the use of a fail temperature for each candidate surface material. An approach for including char-density buildup due to coking reactions is presented, but this has not been incorporated into the computational procedure.

The boundary-layer computer program applies to laminar axisymmetric or planar flow. No similarity approximations are imposed and surface discontinuities (e.g., due to change of ablation materials) are allowed. The procedure applies to any chemical system, considering equilibrium with the exception that selected species can be considered as frozen in the boundary layer while undergoing rate-controlled reactions at the surface. The boundary-layer procedure also considers unequal diffusion and thermal diffusion coefficients for all species through the use of convenient approximations to these coefficients. Additional theoretical developments which have been made but which have not been incorporated into the computer program include a general mixed equilibrium-nonequilibrium, homogeneous or heterogeneous chemical procedure and a model for radiation absorption and emission in the boundary layer.

The convective transfer coefficient approach utilizes the same charring ablation computational procedure (with its general surface thermochemistry, decomposition model, and thermal streamtube approach) and is less restrictive in one sense in that the boundary layer can be turbulent as well as laminar. With regard to other boundary-layer phenomena, it permits consideration of unequal diffusion coefficients, but neglects thermal diffusion and includes nonsimilar effects only if they have been determined from correlations of boundary-layer solutions.

The boundary-layer computational procedure utilizes an entirely new numerical solution procedure which was developed specifically for the present problem. It has come to be known as an integral-matrix method because of the way the problem is formulated and solved. The charring ablation and chemistry routines and the convective transfer coefficient approach are extensions of procedures which have been under continued development by the present authors during the past several years.

The following computer programs have been developed and are described in this series of documents:

1. Charring material ablation (CMA) program
2. Boundary-layer integral-matrix procedure (BLIMP) program
3. Surface thermochemistry programs based on convective transfer coefficients: Aerotherm chemical equilibrium (ACE) and Aerotherm

chemical equilibrium with selected surface reaction kinetics (ACE-KINET)

4. Coupled ablator/boundary layer/environment (CABLE) program

The CMA program can be operated independently for obtaining the in-depth response of charring materials for assigned ablation rates and surface temperatures. The ACE and ACE-KINET programs can be operated independently to compute steady-state ablation of arbitrary material-environment combinations or can be used to provide tables of surface-thermochemistry information as input to the CMA program for transient charring ablation calculations, again for arbitrary material-environment combinations. The BLIMP program can be operated independently to provide boundary-layer solutions for a variety of coupled, partially coupled, or uncoupled steady-state ablation surface boundary conditions. Finally, the CABLE program calls upon the BLIMP and CMA programs as subroutines to provide fully coupled transient charring ablation and boundary-layer solutions.

The analyses and computational procedures for characterizing the laminar chemically-reacting boundary layer, for predicting the in-depth transient response of charring materials, and for evaluating the chemical state are summarized in Sections 2 through 4 and are presented in detail in Parts III, II, and V, respectively. The approximations for multicomponent transport properties are summarized in Section 2.1.2 and reported in detail in Part IV, the approach for characterizing charring ablator response with in-depth coking reactions is summarized in Section 3.5 and described in detail in Part VI, and the radiation model is summarized in Section 2.1.3 and presented in an Appendix to Part III. The coupled boundary-layer and charring-ablation procedures (i.e., CABLE and CMA/ACE and CMA/ACE-KINET combinations) are described in Section 5. Summary, conclusions, and recommendations are presented in Section 6.

SECTION 2

ANALYSIS AND COMPUTATIONAL PROCEDURES FOR LAMINAR CHEMICALLY-REACTING BOUNDARY LAYERS

The boundary layer which envelops an ablating heat shield during superorbital reentry is intimately coupled with the transient ablation processes. In addition:

1. It may be laminar, transitional, or turbulent on different parts of the body and at various flight conditions.

2. It may be highly nonsimilar, especially if there are changes of ablation materials.

3. The surface material may react chemically with the air (or other planetary gas), change phase, and/or be removed mechanically by spallation or liquid-layer runoff.

4. Chemical reactions will generally also occur throughout the boundary layer.

5. The homogeneous and heterogeneous reactions may be kinetically controlled.

6. Incident radiant energy may be absorbed at some wave lengths and emitted at other wave lengths.

7. The molecular species in the boundary layer will be governed by different diffusion coefficients relative to the other molecular species which are present.

8. Thermal diffusion can be significant, especially if there are wide variations of molecular weight (e.g., when hydrogen is present in the boundary layer as a result of the decomposition of a charring ablation material).

9. An entropy layer may be present.

10. At very high entry velocities, the inviscid flow field may be nonadiabatic as a result of radiation cooling.

In the present report, only the laminar boundary layer is considered in detail. Otherwise, all of the features listed above are considered in the theoretical analysis. However, Items 5, 6 and 10 are not presently allowed in the computational procedure, with the exception (with regard to Item 5) that selected species can be considered to be frozen in the boundary layer and to react with finite rates at the surface. The major features contained in the theoretical analyses are summarized in Section 2.1. The numerical solution procedure is introduced in Section 2.2. The computer program, designated BLIMP for boundary layer integral matrix procedure, is described briefly in Section 2.3. The analysis and numerical procedure are presented in considerably more detail in Part III of this series, while a user's guide to the BLIMP program is presented in Ref. 1.

2.1 THEORETICAL ANALYSIS

The boundary-layer analysis which has been developed is based on the following model:

1. Laminar axisymmetric or planar flow with all nonsimilar terms retained and discontinuous wall conditions allowed (e.g., change of heat-shield material)

2. Multicomponent transport properties (including unequal diffusion and thermal diffusion coefficients for all species, based on newly developed approximations for these coefficients)

3. Coupled radiation absorption and emission using a conventional one-dimensional model

4. General boundary conditions, including mass and energy balances at the wall and the presence of an entropy layer

5. Mixed equilibrium-nonequilibrium, homogeneous or heterogeneous chemistry for general chemical systems.

The first four features are discussed in Sections 2.1.1 through 2.1.4, respectively. The chemical model is discussed in Section 4.

2.1.1 Conservation Equations for Nonsimilar, Laminar, Planar or Axisymmetric Boundary Layers

Similarity approximations have been often applied in order to help simplify complex boundary-layer problems. This involves a transformation to a new coordinate system (η,ξ) from the original (y,s) system where y and s are the normal and streamwise coordinate, respectively. The similarity transformation is successful if the ξ-variations of functions of the dependent variables vanish or become of negligible importance, in which case the partial differential equations become ordinary differential equations. The most popular transformation, known among other names as the Levy-Lees similarity transformation (Ref. 2), is given by

$$\eta = \frac{r_o^{\kappa} u_e}{(2\xi)^{\frac{1}{2}}} \int_o^y \rho dy \tag{1}$$

$$\xi = \int_o^s u_e \rho_e \mu_e r_o^{2\kappa} ds \tag{2}$$

where the subscript e refers to the boundary-layer edge, ρ is the density, u is the streamwise velocity, μ is the viscosity, r_o is the local radius of the body measured normal to the body centerline, and κ is zero for planar bodies and unity for axisymmetric bodies.

It can be shown that the similarity transformation is valid at the stagnation point since the terms involving ξ-derivatives vanish at the stagnation point ($\xi = 0$), and is valid within certain restrictions on the surfaces of flat plates, wedges, and cones. These restrictions include:

1. No streamwise variation of surface properties
2. Streamwise variation of boundary-layer-edge properties in accordance with specific relations
3. An inverse-square-root type variation with ξ of surface mass-transfer
4. Transport properties functions of η only
5. Edge conditions functions of ξ only (i.e., no entropy-layer effects)

Furthermore, the similarity assumption is not valid on bodies of arbitrary shape.

The importance of nonsimilar effects is illustrated in Fig. 1 where constant blowing into an incompressible boundary layer over a flat plate is terminated two feet from the leading edge. (This solution was generated with the BLIMP procedure to be described later in this report.) In this example, only Item 3 in the above listing is violated. All results shown in Fig. 1 are for a nonsimilar boundary layer. The point is that a similar solution downstream of injection would show immediate recovery of the wall shear to the asymptotic value, whereas the wall shear is still 13 percent below this value two feet after blowing is terminated.

It is apparent from the above discussion that a similarity assumption is overly restrictive for a general solution procedure. Therefore, in the present analysis, although a similarity transformation is employed because of the normalizing benefits therefrom derived, all nonsimilar terms are retained. That is, no similarity assumptions are made.

The transformation which is employed is similar to the Levy-Lees transformation (Eqs. (1) and (2)), with two exceptions:

1. A coordinate stretching parameter is introduced,

$$\bar{\eta} = \eta/\alpha_H(\xi) , \qquad \bar{\xi} = \xi \tag{3}$$

where $\alpha_H(\xi)$ is a dependent variable determined during the course of the calculation. The purpose of this supplemental transformation is to constrain the maximum and minimum values which the transverse coordinate can assume in a nonsimilar boundary layer.

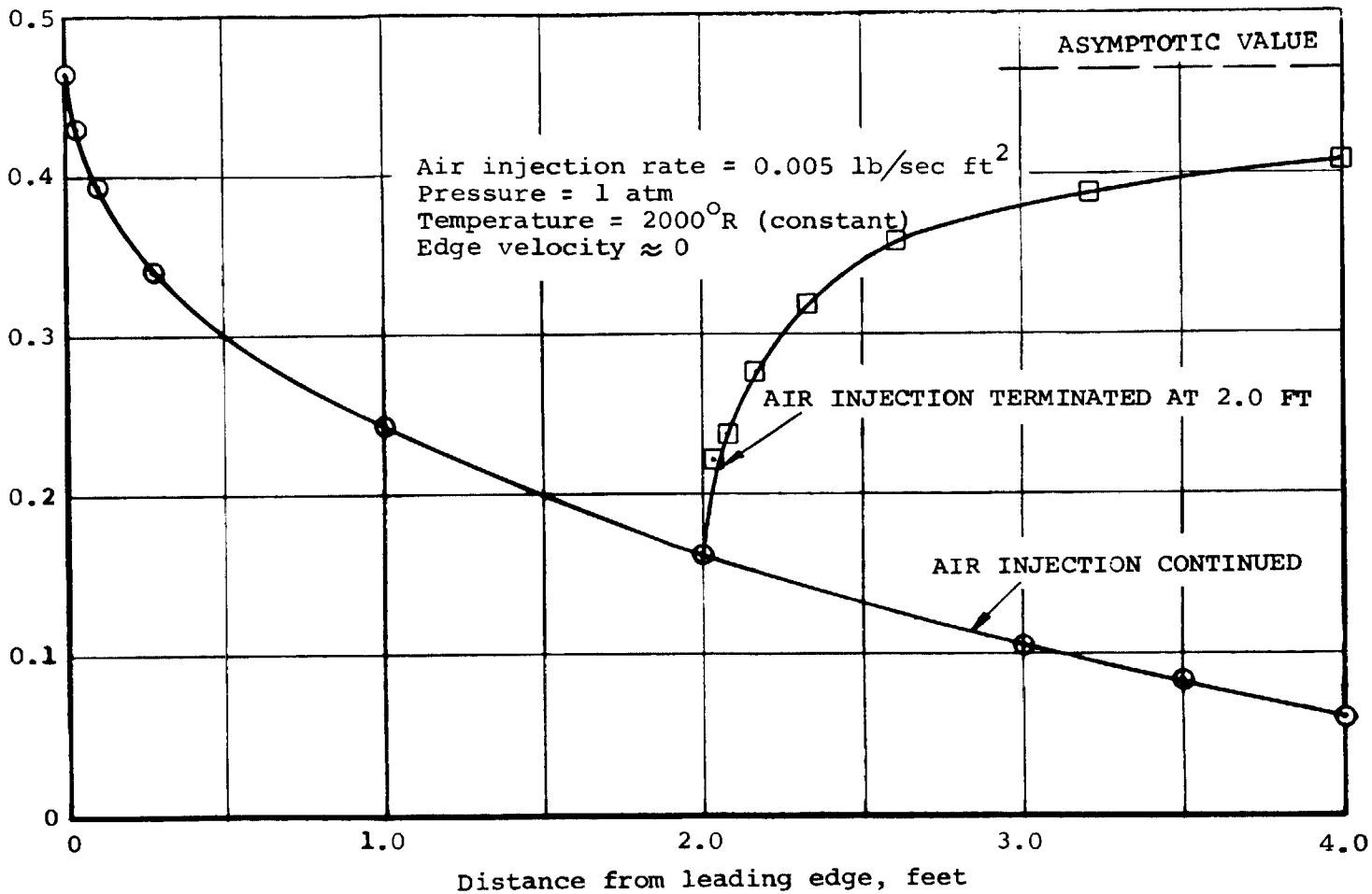

Figure 1. Effect on Wall Shear of Upstream Air-to-Air Injection on a Flat Plate

2. The subscript e refers to the wall streamline value for the inviscid solution, which differs from the boundary-layer-edge condition in the presence of an entropy layer.

Application of this transformation yields the following boundary-layer conservation equations.

Momentum equation

$$ff'' + \left[\frac{Cf''}{\alpha_H}\right]' + \beta\left(\alpha_H^2 \frac{\rho_e}{\rho} - f'^2\right) = 2\left(f' \frac{\partial f'}{\partial \ell n\, \bar{\xi}} - f'' \frac{\partial f}{\partial \ell n\, \bar{\xi}} - f'^2 \frac{d \ell n\, \alpha_H}{d \ell n\, \bar{\xi}}\right) \tag{4}$$

Energy equation

$$fH_T' + \left[-q_a^* + q_r^*\right]' = 2\left(f' \frac{\partial H_T}{\partial \ell n\, \bar{\xi}} - H_T' \frac{\partial f}{\partial \ell n\, \bar{\xi}}\right) \tag{5}$$

Elemental species equations

$$f\tilde{K}_k' + \left[-j_k^*\right]' + \alpha_H \phi_k = 2\left(f' \frac{\partial \tilde{K}_k}{\partial \ell n\, \bar{\xi}} - \tilde{K}_k' \frac{\partial f}{\partial \ell n\, \bar{\xi}}\right) \tag{6}$$

where the prime denotes partial differentiation with respect to $\bar{\eta}$, f is the stream function defined by

$$f - f_w = \alpha_H \int_0^{\bar{\eta}} \frac{u}{u_e}\, d\bar{\eta} \tag{7}$$

such that $f' = \alpha_H u/u_e$, f_w is given by

$$f_w = -(2\bar{\xi})^{-\frac{1}{2}} \int_0^{\bar{\xi}} \frac{\rho_w v_w d\bar{\xi}}{\rho_e u_e \mu_e r_o^{\nu}} \tag{8}$$

$\rho_w v_w$ is the total mass flux into the boundary layer, H_T is the total enthalpy, $\tilde{K}_k$ is the mass fraction of base species k independent of molecular configuration, $C \equiv \rho\mu/\rho_e\mu_e$, $\beta \equiv 2d \ell n\, u_e/d \ell n\, \bar{\xi}$, ϕ_k is the source term for base species k which arises in nonequilibrium systems

(see Section 4), q_a is the diffusive heat flux, q_r is the net one-dimensional radiant heat flux, j_k is the diffusive mass flux of base species k, and the asterisk signifies normalization by division by α^*, defined by

$$\alpha^* \equiv \rho_e u_e \mu_e r_o^{\varkappa} / (2\bar{\xi})^{\frac{1}{2}} \tag{9}$$

Expressions for q_a and j_k including approximate formulations for unequal diffusion and thermal diffusion coefficients are presented in Section 2.1.2, whereas a relation for q_r based on a one-dimensional model is presented in Section 2.1.3.

2.1.2 Diffusive Fluxes in a Multicomponent Boundary Layer Based on Approximations for Unequal Diffusion and Thermal Diffusion Coefficients

Consideration of unequal diffusion and thermal diffusion coefficients for all species adds considerable complexity to the boundary-layer solution if these coefficients are treated in a precise manner (i.e., first-order kinetic theory for the binary diffusion coefficients and second-order kinetic theory for multicomponent thermal diffusion coefficients). On the other hand, the assumption of equal diffusion coefficients for all species and the neglect of thermal diffusion (or the use of constant thermal diffusion factors) are overly restrictive. Therefore, convenient approximations for these coefficients have been developed and introduced into the boundary-layer equations. The approximations per se are described in detail in Part IV and are briefly reviewed in this section. Expressions for diffusive heat and mass fluxes incorporating these approximations are developed in Part III and summarized herein.

The approximation for binary diffusion coefficients* is of the form

$$\mathscr{D}_{ij} = \frac{\bar{D}}{F_i F_j} \tag{10}$$

where $\bar{D}$ is a reference diffusion coefficient and F_i is a diffusion factor for each species in the mixture. Thus, the $\nu(\nu - 1)/2$ diffusion coefficients pertinent to a molecular set of ν species are replaced by $\bar{D}$ and ν diffusion factors F_i.** The primary advantage of this approximation is that it enables explicit expression of the diffusional mass flux of species i, j_i, in terms of gradients and properties of species i and of the system as a whole. This, in turn, permits the Shvab-Zeldovich transformation to be made without introducing the concentration-dependent multicomponent diffusion coefficients, D_{ij}. This transformation reduces the number of species

*Such a bifurcation approximation was first proposed by Bird (Ref. 3).
**Thus, the procedure is exact for binary or ternary systems and amounts to a correlation of diffusion coefficient data for larger systems.

conservation equations from one for each of the molecular species (e.g., 20 to 70) to one for each element (e.g., 3 to 5). A thorough study of the accuracy of the approximation, presented in Part IV, shows that diffusion coefficients obtained using this technique are generally within a few percent of the values predicted by kinetic theory.

It is convenient to consider F_i to be unity for some reference species such as molecular oxygen. Then the $\overline{D}$ is not too unlike the self-diffusion coefficient for that species. The F_i for the other species in the system of interest are then obtained by means of a least-squares fit of actual diffusion coefficient data. The F_i might be expected to depend upon temperature, pressure, and concentrations. However, the F_i are, in fact, independent of pressure, since the pressure dependence of $\mathcal{D}_{ij}$ can be fully absorbed into the $\overline{D}$. Furthermore, satisfactory accuracy can be obtained while considering the F_i to be independent of temperature and concentrations. Thus, the F_i can be considered as a set of constants for a given set of molecular species. In addition, it has been found that the F_i for a given species i will in general be nearly the same when species i is considered as part of two different sets of molecular species, being given approximately by $F_i = (\mathcal{M}_i/26)^{0.461}$ where $\mathcal{M}_i$ is the molecular weight of species i.

The approximation for multicomponent thermal diffusion coefficients, D_i^T, is based on a correlation of binary thermal diffusion data and a generalization to multicomponent systems, satisfying the requirement that $\sum D_i^T = 0$, recognizing that D_i^T is independent of fluxes, and assuming that thermal diffusion of species i behaves as though it were in a system of species i and a species representative of the mixture as a whole. The resulting equation is given by

$$D_i^T = \frac{c_t \rho \overline{D} \mu_2}{\mu_1 \mathcal{M}} (Z_i - K_i) \tag{11}$$

where K_i is mass fraction of species i, Z_i is defined as

$$Z_i = \frac{\mathcal{M} K_i}{\mu_2 F_i} \tag{12}$$

μ_1 and μ_2 are system properties defined by

$$\mu_1 \equiv \sum_{i=1}^{\nu} x_i F_i \qquad \mu_2 \equiv \mathcal{M} \sum_{i=1}^{\nu} \frac{K_i}{F_i} \tag{13}$$

with x_i the mole fraction of species i, and c_t an empirically determined parameter which was found from the correlation of binary thermal diffusion data to be nearly constant (-0.5). This approximation permits consideration of multicomponent thermal diffusion coefficients for all molecular species with very little computational effort.

The approximation for binary diffusion coefficients is also introduced into approximate expressions for multicomponent viscosity and thermal conductivity of the Sutherland-Wassiljewa type (see Ref. 4) to simplify them still further. For example, the resulting expression for viscosity is given by

$$\mu = \frac{\rho \bar{D}}{\mathcal{M}} \sum_{i=1}^{\nu} \left[\frac{x_i \mathcal{M}_i / C_1 F_i}{C_2 x_i F_i + \mu_1} \right] \tag{14}$$

where C_1 and C_2 can be considered as constants. Since the F_i and $\bar{D}$ can be determined in advance for a particular chemical system by a correlation of diffusion data from any desired source, it follows that reasonably accurate descriptions for the mixture transport properties can be utilized without introducing any molecular-interaction models into the input format of the boundary-layer program. The development of this and the other approximate expressions for multicomponent transport properties is presented in Part IV.

The diffusive heat and elemental mass fluxes for a multicomponent boundary layer are substantially simplified by introduction of the approximations for binary diffusion coefficients and multicomponent thermal diffusion coefficients. The diffusive mass flux of species i is given by

$$j_i^* = \frac{j_i}{\alpha^*} = - \frac{C}{\alpha_H \overline{Sc}} \left[Z_i' + (Z_i - K_i) \left[\ell n \left(\mu_2 T^{c_t} \right) \right]' \right] \tag{15}$$

with $\overline{Sc}$ a system property defined by

$$\overline{Sc} \equiv \frac{\mu_1 \mu \mathcal{M}}{\rho \bar{D} \mu_2} \tag{16}$$

The diffusive flux of the k^{th} base species is similarly given by

$$j_k^* = \frac{j_k}{\alpha^*} = -\frac{C}{\alpha_H \overline{Sc}}\left[\tilde{Z}_k' + (\tilde{Z}_k - \tilde{K}_k)\left[\ell n\left(\mu_2 T^{C_t}\right)\right]'\right] \tag{17}$$

The diffusive heat flux is given by

$$q_a^* = \frac{q_a}{\alpha^*} = -\frac{C}{\alpha_H}\left(\frac{f'f''u_e^2}{\alpha_H^2} + \frac{\overline{C}_p T'}{Pr}\right) - \sum_j j_j^*\left(h_j + \frac{c_t RT}{m_j}\left(1 - \frac{F_j}{\mu_1}\right)\right)$$

$$= -\frac{C}{\alpha_H}\left[\frac{f'f''}{\alpha_H^2}u_e^2 + \frac{\overline{C}_p}{Pr}T' + \frac{1}{\overline{Sc}}\left(\tilde{h}' - \left(\tilde{C}_p + \frac{c_t^2 R}{\mu_1\mu_2}\right)T'\right.\right.$$

$$\left.\left. + c_t RT\mu_3' + (\tilde{h} - h + c_t RT\mu_3)\left[\ell n\left(\mu_2 T^{C_t}\right)\right]'\right)\right] \tag{18}$$

where $\overline{C}_p$ is the frozen specific heat defined by

$$\overline{C}_p \equiv \sum_i K_i C_{p_i} \tag{19}$$

with C_{p_i} the specific heat of species i, Pr is the Prandtl number defined by

$$Pr \equiv \frac{\overline{C}_p \mu}{\lambda} \tag{20}$$

with λ the thermal conductivity of the mixture, h is the static enthalpy, h_i is the static enthalpy of species i, and $\tilde{h}$, $\tilde{C}_p$, and μ_3 are defined by

$$\tilde{h} \equiv \sum_{i=1}^{\nu} Z_i h_i \qquad \tilde{C}_p \equiv \sum_{i=1}^{\nu} Z_i C_{p_i} \qquad \mu_3 \equiv \sum_{i=1}^{\nu} \frac{Z_i}{m_i} \tag{21}$$

In the absence of thermal diffusion and with the diffusion coefficients assumed equal, the F_i can be set equal to unity. Then the $Z_i = K_i$, $\tilde{h} = h$, $\tilde{C}_p = \overline{C}_p$, and the expression for j_i reduces to Fick's law.

Finally, it is shown in Part IV that the last term on the right-hand-side of Eq. (15) is small compared to the other terms in the equation. Thus, with fair approximation

$$j_i^* = \frac{j_i}{\alpha^*} \approx -\frac{C}{\alpha_H \overline{Sc}} Z_i' \tag{22}$$

and the Z_i' become the driving potentials for diffusion. This observation serves as the basis for the development of convective transfer coefficients including unequal diffusion coefficients for all species. These relations are also presented in Part IV. However, the more precise Equation (15) is utilized in the boundary-layer computational procedure.

2.1.3 Radiant Heat Flux in an Absorbing and Emitting Boundary Layer

As indicated previously, the boundary-layer energy equation contains a term representing the net radiative flux which must be known at every point at which the boundary-layer equations are evaluated. This term is important at lunar reentry velocities (at maximum heating conditions it is comparable to the diffusive flux), and it becomes dominant at still higher reentry velocities. A model for the radiant heat flux is presented in Appendix E of Part III and is summarized in this section. This model is not presently included in the computational procedure, but is seen as the eventual replacement for the present radiation model which assumes that the incident radiation passes, unattenuated, through the boundary layer.

The radiation flux term accounts for the net energy extracted from the local radiation field and added to the internal energy of the boundary-layer gases. The energy in the radiation field originates, for the most part, from emission in the hot shock-layer gases and subsequent transmission into the boundary-layer region. Scattering need not be considered since it does not contribute measureably unless particulate matter is present. The atoms, ions, and molecules present in the boundary layer absorb energy from the radiation field and distribute it among their internal energy levels. This is a highly frequency-dependent process, and any meaningful analysis must allow for it. Finally, the excess energy in internal energy levels is redistributed by interparticle collisions. This is an efficient process, and when local thermodynamic equilibrium exists (as is assumed here), it occurs instantaneously.

In forming the flux integrals, it is consistent and adequate to employ the conventional one-dimensional approximation, viz., local net radiant heat flux a function of y only. The resulting expression for the radiant heat flux is similar to that of Cess (Ref. 5) except for a change in the edge boundary condition. The present model considers a boundary layer of finite thickness with an angular-dependent incident flux; whereas, Cess considered an absorbing media which extends to infinity. The resulting expression for the net radiant heat flux toward the surface at the nodal point i in the boundary layer is given by

$$q_{r_i} = \int_0^\infty q_{r_{i_\nu}} \, d\nu \tag{23}$$

where ν is the frequency and where the spectral flux, $q_{r_{i_\nu}}$ is given by

$$q_{r_{i_\nu}} = 2\pi \int_{\tau_{\nu_i}}^{\tau_{\nu_e}} B_\nu(T) E_2(t - \tau_{\nu_i}) \, dt - 2\pi \int_0^{\tau_{\nu_i}} B_\nu(T) E_2(\tau_{\nu_i} - t) \, dt$$

$$- 2\pi e_{\nu_w} B_\nu(T_w) E_3(\tau_{\nu_i}) - 4\pi (1 - e_{\nu_w}) E_3(\tau_{\nu_i}) \int_0^{\tau_{\nu_e}} B_\nu(T) E_2(t) \, dt$$

$$+ \int_0^{\pi/2} \left[q^+_{r_{\nu,\theta_e}} \right] \left[e^{-(\tau_{\nu_e} - \tau_{\nu_i})/\cos\theta} - 2(1 - e_{\nu_w}) E_3(\tau_{\nu_i}) e^{-\tau_{\nu_e}/\cos\theta} \right] d\theta \tag{24}$$

In Eq. (24), τ_{ν_i} is the optical depth defined by

$$\tau_{\nu_i} \equiv \int_0^{y_i} \rho\kappa_\nu \, dy \tag{25}$$

$\rho\kappa_\nu$ is the mixture absorption coefficient, $B_\nu(T)$ is the Planck function defined as

$$B_\nu(T) \equiv \frac{2h}{c^2} \frac{\nu^3}{(e^{h\nu/kT} - 1)} \tag{26}$$

with the symbols h,c and k having their usual definitions, $E_n(t)$ is the exponential integral defined by

$$E_n(t) \equiv \int_0^1 \mu^{n-2} \, e^{-t/\mu} \, d\mu \tag{27}$$

e_{ν_w} is the hemispheric surface emissivity, and

$$q^+_{r_{\nu,\theta_e}} = \cos\theta \sin\theta \int_0^{2\pi} I_{\nu_e}(\theta,\varphi) \, d\varphi$$

$$0 < \theta < \pi/2 \tag{28}$$

with $I_{\nu_e}(\theta,\varphi)$ the angular-dependent specific intensity at the edge of the boundary layer, θ the angle between the normal to the surface and the direction of incident radiation, and φ the angle between a reference line in the surface and the trace of the incident flux on the surface.

The mixture absorption coefficient, $\rho\kappa_\nu$, is obtained by summing (at a fixed frequency) the contributions from all atomic, ionic and molecular species in the boundary layer. Thus, $\rho\kappa_\nu$ is given by

$$\rho\kappa_\nu = \sum_j \rho\kappa_\nu \tag{29}$$

The calculation of q_{r_i} proceeds as follows. A set of frequency points is selected so that the continuum spectra is accurately represented. Thus, 20 to 30 points are usually adequate to represent the $0.25 \leq h\nu \leq 20$ ev. frequency range of interest. Using the given concentration and temperature distributions, the mixture absorption coefficients and the Planck function are calculated at each spatial nodal point for each of the frequencies. The integrals required for each of the optical depths (Eq. (25)) and the spectral fluxes (Eq. (24)) are obtained. This"continuum flux" is obtained by integrating the spectral flux over frequency (according to Eq. (23)).

Atomic and ionic lines are usually important in reentry problems, in which case, a correction to this continuum flux is required. The calculation of the line contribution to the total flux proceeds as follows. The frequency range of interest is divided into increments, each of which includes a group of important lines. Each frequency increment is small enough so that the frequency variation of the continuum spectra can be neglected. Other than this requirement, the frequency increments selected for the lines are unrelated to the frequency points used for the continuum flux calculation; furthermore, the frequency increments for the lines do not have to be connected or have to span the entire frequency range. A set of frequency points is selected for each line group so that the rapid variation of the line spectra is accurately described. This usually requires about 20 to 30 points per line group. The contribution from each line group is calculated using the same equations and procedures described in the preceding paragraph and then combined with the continuum flux to obtain the total flux.

2.1.4 Generalized Boundary Conditions

The wall boundary conditions of interest admit the addition of chemically active species arising from the pyrolysis of an internally decomposing material, surface combustion or phase change, and liquid-layer removal. In this case, the surface mass flux, surface enthalpy, and surface elemental mass fractions are supplied through surface chemistry considerations and energy and elemental mass balances.

The surface energy and elemental mass balances can be supplied by transient internal conduction solutions such as those described in Section 3. The procedure for accomplishing this will be discussed in Section 5. The resultant equation for the surface energy balance is given by

$$\dot{m}^*_g h_g + \dot{m}^*_c h_c - \sum_\ell \dot{m}^*_{r_\ell} h_\ell - (\rho_w v_w)^* h_w - q^*_{a_w} + q^*_{r_w} - q^*_{cond} = 0 \qquad (30)$$

where the asterisk signifies normalization by division by α^* (Eq.(9)), $\dot{m}_g$ is the mass flow rate per unit area and h_g the enthalpy of gas which enters the boundary layer without phase change at the surface (e.g., pyrolysis gases), $\dot{m}_c$ is the mass removal rate per unit area and h_c the enthalpy of surface material (e.g., char) by chemical reactions or phase change, $\dot{m}_{r_\ell}$ is the mass removal rate per unit area and h_ℓ the enthalpy of surface material (e.g., char) in the condensed phase (e.g., by melting with subsequent liquid runoff or by mechanical spallation), h_w is the enthalpy of the gas phase at the wall, $q^*_{a_w}$ is the normalized diffusive heat flux away from the wall (Eq. (18) evaluated at the wall), q_{r_w} is the net radiative flux to the wall (Eq. (23) evaluated at the wall), and $q_{cond} = \lambda_w(\partial T/\partial y)_w$ is conduction into the surface material (with λ_w the thermal conductivity of the surface material). The elemental mass balances are given by

$$\dot{m}^*_g \tilde{K}_{g_k} + \dot{m}^*_c \tilde{K}_{c_k} - \sum_\ell \dot{m}^*_{r_\ell} \tilde{K}_{\ell k} - (\rho_w v_w)^* \tilde{K}_{k_w} - j^*_{k_w} = 0 \qquad (31)$$

where the subscripts g, c, r and w and the asterisks have the same meaning and $j^*_{k_w}$ is the normalized diffusive net mass flux of elemental species k away from the wall, given by Eq. (17) evaluated at the wall.

The boundary-layer edge condition is allowed to be nonisentropic such as results from an entropy layer or radiation cooling of the inviscid flow field. The former is accomplished by defining the reference condition as the $f = 0$ streamline of the inviscid flow field and specifying the edge boundary condition as a function of f as well as ξ and time. This is discussed in Part III.

2.2 NUMERICAL SOLUTION PROCEDURE

A boundary-layer solution procedure has been developed for the problem described in Section 2.1, that of a nonsimilar, laminar, multicomponent, boundary layer, with general equilibrium or nonequilibrium chemistry, radiation absorption and emission, and a transient charring ablation wall boundary condition.

As discussed elsewhere in this report, these features are not all included in the currently operational computer code; however, it is significant that the numerical procedure has been formulated with this ultimate problem in mind and that features presently not included can be added in a convenient manner. The solution procedure, which has come to be known as an integral-matrix method, is described in detail in Part III and is discussed summarily in this section.

In developing the laminar boundary-layer solution procedure, the emphasis was on achieving a procedure adaptable to this general environment. It was also required that the procedure have the versatility to treat a variety of boundary conditions. Additional goals of the procedure were simplicity, accuracy, and computational speed. Simplicity relates to problem formulation and is probably best measured (negatively) by the amount of judgement required during the solution procedure and by the amount of algebra required to achieve formulation. Accuracy is meant to imply that the procedure will have the capability, in a practical limit, of yielding exact solutions.

In developing this procedure it was desirable to consider the characteristics of existing techniques. The iterative initial value approach seemed inappropriate since the inclusion of radiation with its integro-differential character can not be accomplished in a particularly convenient fashion. In addition, Refs. 6 and 7 indicate a rather complex convergence process. The "accuracy" requirement eliminates several methods such as simple integral methods, perturbation solutions and semi-analytical methods. Explicit finite difference methods tend to require excessive computational time. Of the remaining solution procedures, three types may be considered: implicit finite difference (e.g., Ref. 8), matrix (e.g., Ref. 9), and integral relations (e.g., Refs. 10 and 11).

In light of the goals set for the procedure to be adopted, certain specific requirements seemed appropriate. In particular, minimization of the number of entries into the conservation equations required to obtain a solution was judged to be of prime importance as a consequence of the relatively large times associated with state calculations for a general chemical environment. In the streamwise direction, large steps are necessitated by the desire to couple the boundary-layer procedure to a transient internal-conduction or ablation solution.

For a given accuracy, the number of entries into the conservation equations necessary for solution in the surface normal direction is controlled primarily by the nature of the functions which relate the dependent variables (and their derivatives) to the independent variable. Thus the continuous functions typically used in integral relations approaches require fewer entries than the

discontinuous functions implied by most finite difference approximations. In order to permit relatively flexible profiles, sets of connected cubics were selected to represent enthalpy, velocity, and concentration parameters. The first and second derivatives of these cubics were made continuous at the connecting points. These spline functions, as they are commonly known, are conveniently supplied through truncated Taylor series expansions for f, H_T, $\tilde{K}_K$ and their derivatives in terms of their higher derivatives at the same and the neighboring nodal points.

If the general integral relations approach is followed, weighting functions must be selected. In the present study this selection was based primarily on the complexity of the resultant algebra. Based on studies (discussed in Part III) using Dirac delta weighting functions (i.e., a differential approach*) and step weighting functions similar to those used by Pallone (Ref. 10) indicated, when other aspects of the procedure were unchanged, no apparent superiority with regard to accuracy or stability. Because all of the complexities introduced by the generalization of the thermodynamic and transport properties of the system occur within divergence terms, square-wave weighting functions produce markedly simpler algebra and, consequently, were adopted for the present procedure.

In the past when relatively large spacing in the streamwise direction has been desired, iterative procedures have generally been used to assure accuracy and stability. In many instances (e.g., Refs. 7 and 9) these procedures have treated the solution in a manner resembling those used for similar solutions but with the addition of finite difference representations for the nonsimilar terms, a procedure which eliminates the necessity of special starting techniques. Using this basic approach, the specific treatment adopted in the current method follows most closely the matrix procedure used by Leigh (Ref. 9) wherein the iteration is a consequence of the solution of a set of linear and nonlinear algebraic relations. Whereas a special successive approximation procedure was used by Leigh, the general Newton-Raphson technique is used in the present procedure. This technique results in linearized coupling between all relations required to characterize the boundary layer, and thus assures a more rapid and stable iterative convergence. In addition, coupling to a transient conduction solution becomes straightforward, and features such as nonequilibrium chemistry and gaseous radiation can be conveniently added.

*This correspondence is pointed out by Dorodnitsyn (Ref. 11).

An efficient method for solution of this matrix equation is utilized which takes advantage of the linear Taylor series expansions and of the zeros in the matrix. This will be discussed in Section 2.3.1.

Several computer results are presented in Part III which demonstrate that the integral matrix method is capable of yielding accurate numerical solutions with a minimum number of entries into the conservation equations (7 to 11 spline segments have consistently yielded 3 to 4 place accuracy). It is flexible and versatile as the number and spacing of spline points can be varied at will and the number and type of chemical elements and molecular species can be selected arbitrarily. Finally, it can be applied to radiation problems since it considers simultaneously all points across the boundary layer at a given streamwise station.

2.3 BOUNDARY LAYER INTEGRAL MATRIX PROCEDURE (BLIMP) COMPUTER PROGRAM

The BLIMP program is a computer code for solving a nonsimilar laminar boundary layer utilizing the integral matrix solution procedure introduced in Section 2.2 and described in detail in Part III. The procedure also serves as a subroutine for coupling the boundary layer to a transient charring ablation routine (to be discussed in Section 5). Thermal diffusion and unequal diffusion are included using the approximations introduced in Section 2.1.2 and described in Part IV. The boundary layer can be considered as nonreacting, as equilibrium, or as a mixed equilibrium-frozen system with specific rate-controlled heterogeneous (surface) reactions or surface catalyzed reactions. The nonreacting boundary-layer option utilizes rather general laws for specification of enthalpy, viscosity, and Prandtl numbers as functions of temperature. The other options utilize the chemical procedures introduced in Section 4 and described in detail in Part V. (The generalized nonequilibrium procedure introduced in Section 4 and described in detail in Part V and the radiation model introduced in Section 2.1.4 and discussed in detail in Appendix E of Part III are not presently included.) The computational procedure is discussed briefly in Section 2.3.1, the most significant operational considerations are summarized in Section 2.3.2, and a sample problem solution is presented in Section 2.3.3.

2.3.1 Computational Procedure

The integral-matrix solution procedure outlined in Section 2.2 is utilized in the BLIMP program. In essence, this involves simultaneous solution at each streamwise station of $(7 + 3K)N + 1$ linear and nonlinear algebraic equations for the primary dependent variables (α_H, f_i, f_i', f_i'', f_i''', H_{T_i}, H_{T_i}', H_{T_i}'', and K sets of $\tilde{K}_{k_i}$, $\tilde{K}_{k_i}'$, and $\tilde{K}_{k_i}''$), where K is one less* than the number of elements (or base species), N is the number of spline points, α_H

*The remaining element is determined from overall conservation considerations.

is the boundary-layer thickness normalizing parameter, f is the stream function, H_T is the total enthalpy, $\tilde{K}_k$ is the mass fraction of element k, the subscript i refers to the spline point, and the prime refers to partial differentiation with respect to η, the normal boundary-layer coordinate.* The boundary-layer conservation equations, integrated with a weighting factor of unity between neighboring points and zero elsewhere, provide $(2+K)(N-1)$ of the equations, the Taylor series expansions which express, for example, f_{i+1} in terms of f_i, f_i', f_i'', f_i''', and f_{i+1}''', provide $(5+2K)(N-1)$ equations, and the boundary conditions and α_H constraint provide the remaining $8+3K$ equations.

The solution of these equations is achieved by use of the general Newton-Raphson procedure. Thus, the nonlinear equations (the boundary-layer conservation equations and some of the boundary conditions) are linearized with respect to the primary dependent variables, and the errors introduced by the linearization are driven toward zero by iteration. This yields a matrix of equations of the form

$$\sum_j \frac{\partial E_n}{\partial V_j} \Delta V_j = - \text{ERROR}(E_n) \tag{32}$$

where E_n represents the n^{th} equation, V_j signifies the j^{th} primary dependent variable (f_1, f_2, ...), $\text{ERROR}(E_n)$ represents the error in the n^{th} equation resulting from the previous iteration, and ΔV_j is the correction to be added to the variable V_j for the next iteration. In order to reduce the nonlinear equations to the form of Eqs. (32), it is necessary to express the corrections for all other dependent variables in terms of corrections on the primary variables. For example, the correction on density is expressed as

$$\Delta\rho_i = \sum_{k=1}^{K} \frac{\partial \rho_i}{\partial \tilde{K}_{k_i}} \Delta\tilde{K}_{k_i} + \frac{\partial \rho_i}{\partial h_i} \Delta h_i \tag{33}$$

since the pressure is constant across the boundary layer. The derivatives with respect to h and $\tilde{K}_k$ are state properties determined at each η_i by the chemistry routine. The Δh_i is given by

*The streamwise derivatives do not appear as primary variables as they are expressed in terms of local conditions and known upstream conditions by means of two- or three-point finite-difference relations.

$$\Delta h_i = \Delta H_{T_i} - \frac{u_e^2 f_i'^2}{\alpha_H^2}\left(\frac{\Delta f_i'}{f_i'} - \frac{\Delta \alpha_H}{\alpha_H}\right) \tag{34}$$

The corrections on primed quantities (e.g., $\Delta\rho_i'$) are considerably more complicated and introduce second derivatives.

Direct inversion of the entire matrix of $(7 + 3K)N + 1$ equations during each iteration would rapidly become unwieldy as the number of spline points and/or elements is increased. Therefore, it is significant that the solution procedure takes advantage of the fact that the majority of the equations are inherently linear and that the matrix is sparse in an ordered manner.

The first step in this process is to utilize the Taylor series expansions and linear boundary conditions to express some of the corrections (termed "linear corrections") in terms of the remaining corrections (termed "nonlinear corrections"). These are then substituted, in effect, into the nonlinear equations, thereby reducing the matrix to $(K + 2)(N - 1) + 3$ equations in terms of $(K + 2)N + 3$ "nonlinear corrections." (A total of $K + 2$ nonlinear wall boundary conditions are not included at this point since it is more convenient for some coupled problems to introduce them after the major matrix inversion.) This matrix equation is then reduced further in terms of $K + 2$ "reduced nonlinear corrections " (Δf_w, ΔH_{T_w} and the $\Delta\tilde{K}_{k_w}$) by inversion of a $(K + 2)(N - 1) + 3$ matrix. The Δf_w, ΔH_{T_w} and $\Delta\tilde{K}_{k_w}$ are then determined from the $K + 2$ remaining wall boundary conditions.

The sequence of events in the actual calculational procedure is summarized in Fig. 2. This illustrates the computations which are performed for every new case, for each new time, and for each new station. For each station, there is a master iteration as indicated in the figure. For each iteration, the calculation proceeds through the boundary layer (for the given streamwise station) from the wall to the boundary-layer edge. This is followed by the major matrix inversion, which expresses the "nonlinear corrections" in terms of the "reduced nonlinear corrections." The reduced nonlinear corrections are then provided by surface considerations, as mentioned previously. The "nonlinear corrections" and finally the "linear corrections" are then evaluated, and the primary variables are corrected. The iteration is completed when the corrections are sufficiently small that the errors in all linear and nonlinear equations are acceptably small. The results for the streamwise location are then printed out (including all desired nodal data) and the solution proceeds to the next time, or to the next station (in which case it returns to the first time), or to the next case.

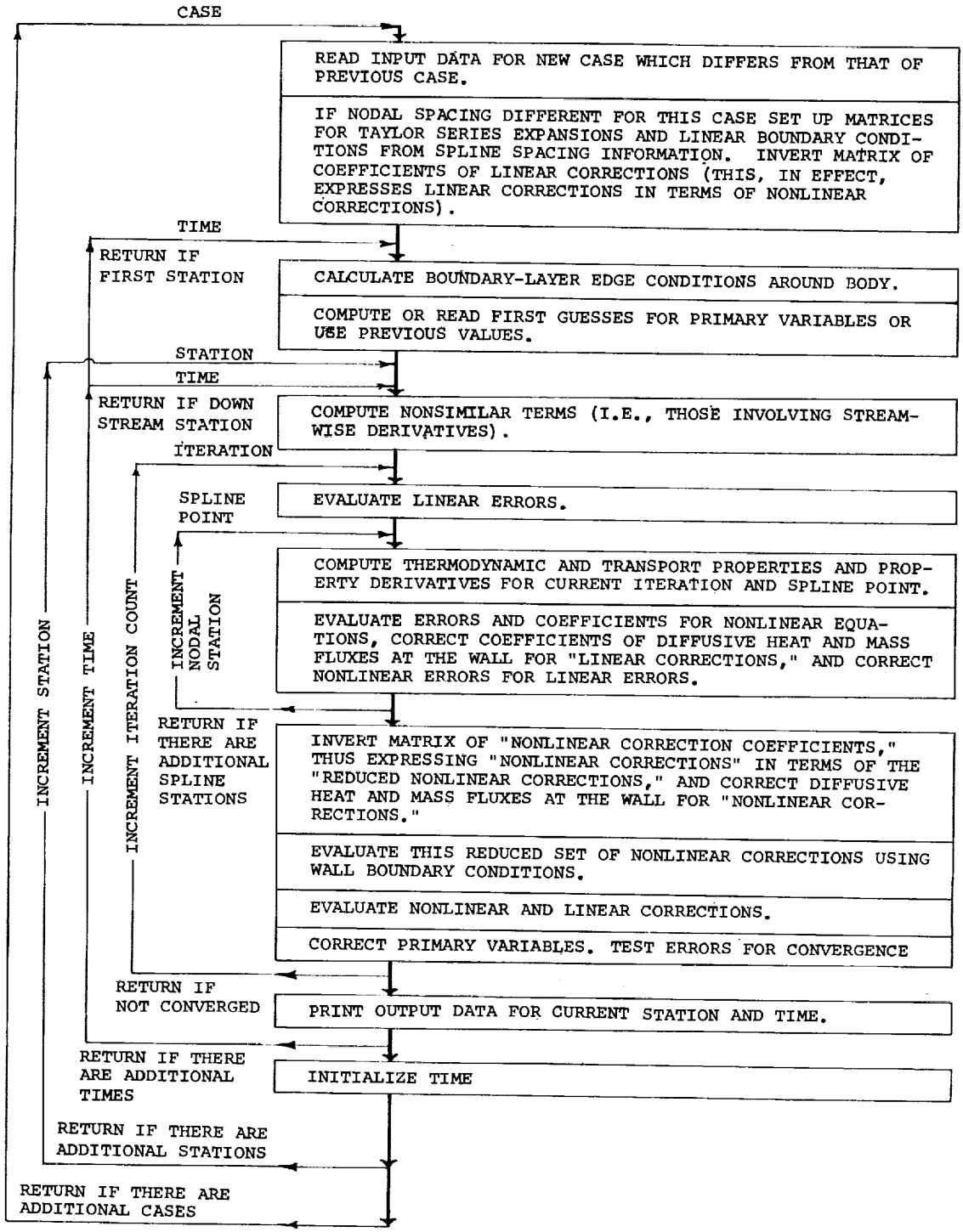

Figure 2. Schematic of BLIMP program.

2.3.2 Operational Considerations

In this section, such operational considerations as program options, input requirements and output capabilities, storage requirements, and computational times are discussed briefly.

2.3.2.1 Program options

The BLIMP program has been designed for versatility and generality within the constraint of the physicochemical model which has been adopted. Therefore, the user has many options at his disposal. The ablation material, environmental gas, molecular species, and number and spacing of spline segments can be chosen arbitrarily. In addition, the more significant options are as follows:

1. Body shape:
   (a) axisymmetric blunt (e.g., sphere cone),
   (b) axisymmetric sharp (e.g., cone),
   (c) planar blunt (e.g., leading edge),
   (d) planar sharp (e.g., wedge).
2. Treatment of upstream effects:
   (a) nonsimilar boundary layer with two- or three-point difference representations of upstream information, with possible discontinuities,
   (b) similar boundary layer.
3. Chemical model:
   (a) nonreacting (homogeneous) boundary layer with variable properties,
   (b) equilibrium boundary layer,
   (c) mixed equilibrium-frozen boundary layer with rate-controlled surface reactions or surface catalyzed reactions.
4. Transport properties:
   (a) thermal diffusion and unequal diffusion coefficients,
   (b) unequal diffusion coefficients but neglecting thermal diffusion,
   (c) equal diffusion and neglecting thermal diffusion.
5. Surface boundary condition:
   (a) specified wall enthalpy (or temperature), wall total mass flux (or f_w) and elemental concentrations,
   (b) specified wall component mass fluxes (i.e., char, pyrolysis gas and edge gas) and wall enthalpy (or temperature),

(c) specified wall component mass fluxes with surface equilibrium,

(d) coupled steady-state wall mass balances and either wall energy balance or assigned wall temperature (providing component fluxes and surface equilibrium).

(e) coupled mass and energy balance at the wall as provided by a transient charring (or noncharring) conduction solution (providing component fluxes and surface equilibrium).

6. Edge boundary condition:

(a) given total enthalpy, total pressure behind the shock, and pressure distribution around the body,

(b) assigned boundary-layer-edge conditions including the possibility of an entropy layer.

2.3.2.2 Input And Output Data

The input requirements for the BLIMP program are surprisingly few and simple considering the numerous options and the general applicability of the program. The options enumerated in Section 2.3.2.1 are controlled by a single control card. Thermodynamic properties are provided by a thermochemical data deck (one card for each element and three cards for each molecular species). A program is available for generating these data in the proper form. Multicomponent transport properties require only a set of diffusion factors, F_i. Body shape is specified by nose radius and cone angle for sphere-cones or by $r_o(s)$ for general axisymmetric bodies. The boundary-layer grid is established by a single set of η-values plus the specification of a u/u_e at one of the nodes (the $\alpha_H(\xi)$ constraint), which can be invariant from problem to problem as a consequence of the α_H parameter. In the absence of an entropy layer, boundary-layer edge conditions can be established from stagnation pressure, stagnation enthalpy, and pressure ratio around the body for the times of interest. For the case of surface mass and energy balances with surface equilibrium, no further input data is required with the exception of material property data. In the other extreme of a completely specified (uncoupled) wall boundary condition, it is necessary to input T_w (or h_w) and either 1) $\dot{m}_g$ and $\dot{m}_c$ or 2) $\tilde{K}_{k_w}$ and $\rho_w v_w$ (or f_w), all for the times and streamwise stations of interest.

The number of points across the boundary layer and the spacing between points, the number of streamwise stations and the distance between streamwise stations, and the number and type of elements (or base species) and candidate molecular and ionic species can all be selected arbitrarily. The size of

these arrays affect only dimension statements. It has been found (see Part III) that nominal 3-place accuracy can be obtained with about 7 spline points and 4-place accuracy with about 11 spline points if the spacing is optimized (e.g., $\bar{\eta}$ of 0, 0.2, 0.5, 0.9, 1.4, 2.0, 2.7, 3.5, 4.4, 5.4, and 6.5) and that poorly chosen nodal spacing can lead to convergence failures.

The output from the BLIMP program consists of three parts: 1) a brief convergence history, listing α_H, f''_w, damping factor, and maximum errors for each iteration; 2) data for current streamwise station (blowing rate, surface mass ablation rate, pyrolysis gas generation rate (or transpiration rate), mechanical removal rate, blowing parameters, elemental mass diffusive fluxes at the wall, wall heat flux, surface shear, skin friction coefficient, heat transfer coefficient, elemental mass transfer coefficients, momentum thickness, displacement thickness, shape factor, enthalpy thickness, elemental mass thicknesses, and Reynolds number per foot); and nodal data (distance from wall, η, stream function, velocity ratio and its first and second derivatives with respect to η, total enthalpy and its first and second derivatives with respect to η, elemental mass fractions and their first and second derivatives with respect to η, mole fractions of all molecular species, static enthalpy, temperature, density, viscosity, frozen specific heat, thermal conductivity, Prandtl number, molecular weight, and reference Schmidt number). A sample output is presented in Figure 3.

2.3.2.3 Storage Requirements and Computational Time

The BLIMP program contains something in excess of 4000 instructions, including COMMON statements. The number of nodal points and the number of elements are the most critical dimensioned variables, in regard to both storage requirements and computational speed. To illustrate, the largest single block of numbers is the matrix of "nonlinear correction coefficients," discussed previously, which is dimensioned $[3 + (K + 2)N]$ by $[3 + (K + 2)N]$. Furthermore, this matrix has to be inverted during each iteration. It is therefore significant that the solution procedure requires a relatively small number of spline points and usually converges in three or four iterations.* When dimensioned for seven nodal points, five elements plus electrons, 30 species, and 20 streamwise stations, the program fits on the Philco 212 without overlay but requires overlays on the IBM 7094 computer. By reducing the number of elements to four and molecular species to 25, it fits on the IBM 7094 without overlay but requires overlays on the smaller CDC 3200 computer

The computational speed of the procedure is illustrated by the following examples. Equilibrium solutions for a sphere-cone configuration with coupled water injection into air involving 16 chemical species and seven

*The relatively slow convergence in Fig. 3 (9 iterations) was a consequence of the 0.6 damping factor which was employed in this particular problem.

TIME .44000+04 SECONDS - - - STREAMWISE DIMENSION .00000 FEET - - -

ITERATED VALUES ITS ALPH	PPRW	DAMP	MAX LIN ERROR		MAX ERRORS IN CONSERVATION EQS, MOMENTUM		ENERGY		C3		CO		H2O		OSI	
1 1.105	.3012	.5000	2.-07	2	7.3-03	4	-5.3+02	2	-2.2-03	2	2.4-03	2	-1.8-03	2	-2.7-08	
2 1.108	.3008	.6000	1.-07	2	5.3-03	4	-2.5+02	2	-1.9-03	2	2.0-03	2	-1.5-03	7	9.4-08	
3 1.109	.3006	.6000	2.-07	2	3.1-03	4	-8.6+01	2	-1.2-03	2	1.3-03	2	-9.9-04	7	7.4-08	
4 1.109	.3004	.6000	1.-07	2	1.6-03	4	-2.1+01	2	-8.4-04	2	8.9-04	2	-5.2-04	7	3.1-08	
5 1.109	.3003	.6000	1.-07	2	7.0-04	3	-6.5+00	2	-2.9-04	2	3.1-04	2	-2.3-04	7	1.8-08	
6 1.109	.3003	.6000	1.-07	2	2.8-04	3	-6.4+00	2	-1.1-04	2	1.2-04	2	-9.2-05	7	8.3-09	
7 1.109	.3003	.6000	4.-07	2	9.7-05	3	-4.1+00	2	-3.6-05	2	3.9-05	2	-2.9-05	7	3.4-09	
8 1.109	.3003	.6000	1.-07	4	3.4-05	3	-2.2+00	4	-1.3-05	4	1.4-05	4	-1.0-05	2	1.8-09	
9 1.109	.3003	.6000	4.-07	4	1.7-05	4	1.1+00	4	-6.6-06	4	7.2-06	4	-5.5-06	1	-1.6-09	

ALPHA	XI (LB /SEC)**2	ROKAP (FT)	PRESSURE (ATM)	EDGE VELOCITY (FT/SEC)	BETA	FLUX NORMALIZING PARAMETER	DIFFUSIONAL HEAT FLUXES TOT ENTH (BTU/SEC SQ FT)	
1.109+00	0.000	-0.000	5.628-04	0.000	5.000+01	3.479+04	2.988+00	2.997+00

WALL SHEAR (LB/SQ FT)	MECH REM	MASS FLUXES PYROL GAS (LB/SEC SQ FT)	CHAR	TOTAL GAS	ELEMENTAL MASS DIFFUSIVE FLUXES (LB/SEC SQ FT) FOR HYDROGE	CARBON	NITROGE	OXYGEN	SILICON
0.000	0.000	1.044-04	3.479-09	1.044-04	-6.098-06	-3.587-05	4.892-05	-6.950-06	-5.222-10

MOM TRANS COEFF, RHO*UE*CF/2	HEAT TRANS COEFF, RHO*UE*CH	BLOWING PARAMETERS (BASED ON CH) FOR PYROL GAS	CHAR	TOTAL GAS	ELEMENTAL MASS TRANSFER COEFFICIENTS, RHOE*UE*CM (LB/SEC SQ FT) FOR HYDROGE	CARBON	NITROGE	OXYGEN	SILICON
1.854-04	1.979-04	5.273-01	1.758-05	5.274-01	1.763+04	1.763-04	1.763-04	1.763-04	1.762+04

MOMENTUM THICKNESS, THETA (FT)	DISPLACE, THICKNESS, DELSTAR (FT)	SHAPE FACTOR, DELSTAR /THETA	ENTHALPY THICKNESS, LAMBDA (FT)	REYNOLDS NUMBER PER FOOT	MASS THICKNESSES (FT) FOR HYDROGE	CARBON	NITROGE	OXYGEN	SILICON
1.482-01	2.790-02	1.855-01	2.463-01	0.000	2.287+01	2.287-01	2.287-01	2.287-01	2.288+01

NODAL INFORMATION

DISTANCE FROM WALL (FT)	ETA	F	FP (=U/UE)	FPP	FPPP	TOTAL ENTHALPY,G (BTU/LB)	GP (BTU/LB)	GPP (BTU/LB)	STATIC ENTHALPY (BTU/LB)	TEMP (DEG R)
0.000	0.000	-3.000-01	0.000	3.003-01	1.920+01	-1.053+02	1.672+03	7.047+03	-1.053+02	2.410+03
4.265-02	3.543-01	-2.493-01	1.897-01	3.730-01	7.082+02	1.540+03	3.610+03	-5.169+01	1.540+03	4.177+03
1.033-01	1.109+00	-8.449-02	4.068-01	4.093-01	6.009+02	3.593+03	3.904+03	1.112+03	3.593+03	4.884+03
1.922-01	1.683+00	2.033-01	6.292-01	3.685-01	-2.074+01	6.005+03	4.936+03	2.613+03	6.005+03	7.602+03
3.081-01	2.217+00	6.026-01	8.000-01	2.449-01	-2.384+01	8.906+03	5.102+03	-2.015+03	8.906+03	8.391+03
5.758-01	3.326+00	1.595+00	9.582-01	7.051-02	-7.620+02	1.322+04	2.588+03	-2.592+03	1.322+04	9.230+03
1.188+00	5.543+00	3.795+00	1.000+00	-1.922-14	1.280+02	1.498+04	0.000	1.871+02	1.498+04	9.878+03

DISTANCE FROM WALL (FT)	DENSITY, RHO (LB/CU FT)	VISCOSITY, MU LB/SEC FT	RHO*MU /RHOE*MUE, C	SPECIFIC HEAT (BTU/LB R)	THERMAL COND (BTU /SEC FT R)	PRANDTL NUMBER	MODIFIED SCHMIDT NUMBER	MOLECULAR WEIGHT
0.000	6.209-06	3.287-05	1.775+00	4.074-01	3.706+05	3.613-01	6.348-01	1.942+01
4.265-02	3.426-06	4.628-05	1.379+00	4.360-01	5.893+05	3.448-01	6.222-01	1.857+01
1.033-01	2.645-06	5.005-05	1.151+00	4.293-01	7.232+05	2.971-01	6.069-01	1.676+01
1.922-01	1.699-06	6.979-05	1.031+00	4.135-01	8.375+05	3.446-01	6.323-01	1.676+01
3.081-01	1.491-06	8.028-05	1.041+00	3.978-01	7.243+05	4.409-01	6.815-01	1.623+01
5.758-01	1.277-06	9.255-05	1.028+00	3.791-01	5.780+05	6.091-01	7.378-01	1.539+01
1.188+00	1.166-06	9.863-05	1.000+00	3.749-01	5.347+05	6.851-01	7.519-01	1.494+01

DISTANCE FROM WALL,FT

	0.000	4.265-02	1.033-01	1.922-01	3.081+01	5.758-01	1.188+00

ELEMENTAL FRACTIONS AND THEIR FIRST AND SECOND DERIVATIVES WITH RESPECT TO ETA

C3	2.034-01	1.583-01	1.013-01	3.341-02	-3.775+02	-1.373-01	-1.764-01
	-6.885-02	-9.259-02	-1.134-01	-1.297-01	-1.203+01	-5.849-02	0.000
	-4.977-02	-3.589-02	-3.934-02	-1.950-02	5.371+02	5.773-02	-4.986-03
CO	-6.876-05	4.879-02	1.105-01	1.841-01	2.612+01	3.690-01	4.114-01
	7.458-02	1.003-01	1.229-01	1.406-01	1.303+01	8.336-02	0.000
	5.391-02	3.887-02	4.262-02	2.113-02	-5.819+02	-6.254-02	5.380-03
H2O	3.090-01	2.725-01	2.260-01	1.707-01	1.128+01	3.186-02	0.000
	-5.601-02	-7.533-02	-9.229-02	-1.056-01	-9.785+02	-4.759-02	0.000
	-4.049-02	-2.920-02	-3.201+02	-1.587-02	4.370+02	4.697-02	-4.040-03
OSI	4.651-06	4.099-06	3.401-06	2.570-06	1.698+06	4.798-07	0.000
	-8.426-07	-1.134-06	-1.389-06	-1.589-06	-1.473+06	-7.164-07	0.000
	-6.096-07	-4.401-07	-4.813-07	-2.395-07	6.577+07	7.068-07	-6.062-08
N2	4.876-01	5.205-01	5.622-01	6.118-01	6.637+01	7.364-01	7.650-01
	5.028-02	6.762-02	8.284-02	9.475-02	8.783+02	4.272-02	-0.000
	3.635-02	2.621-02	2.873-02	1.424-02	-3.923+02	-4.216-02	3.627-03

MOLE FRACTIONS

C3	9.217-30	2.809-27	3.170-25	2.681-13	2,582+12	1.644-13	0.000
CO	3.274-01	2.788-01	2.059-01	1.548-01	8.592+02	9.869-03	0.000
H2O	2.737-03	2.172-02	1.172-03	3.581-10	1.570+11	1.465-13	0.000
OSI	2.048-06	1.724-06	1.292-06	5.298-08	5.786+09	2.948-10	0.000
N2	3.385-01	3.448-01	3.365-01	3.264-01	2.398+01	1.032-01	3.552-02
C*	0.000	0.000	0.000	0.000	0.000	0.000	0.000
C	4.744-21	1.016-12	1.500-10	1.972-03	1.431+02	1.678-02	0.000
CN	1.096-15	1.024-11	2.036-10	4.003-05	1.253+04	5.267-05	0.000
C2N2	9.649-19	1.515-20	7.402-20	2.723-13	5.540+13	2.456-14	0.000
CO2	1.461-03	6.381-03	1.678-03	5.914-07	1.184+07	5.242-09	0.000
N	1.492-14	1.197-06	4.376-05	9.101-02	2.896+01	5.973-01	7.450-01
NO	4.816-11	3.218-04	1.706-03	2.363-04	1.899+04	1.093-04	4.940-05
O	8.891-13	3.021-03	5.641-02	1.140-01	1.689+01	2.185-01	2.194-01
O2	3.693-15	1.673-04	1.247-03	1.474-06	7.959+07	4.072-07	1.856-07
HO	6.727-09	4.141-03	5.371-03	7.103-06	1.935+06	2.319-07	0.000
H	4.866-05	1.833-01	3.693-01	3.176-01	2.033+01	5.409-02	0.000
H2	3.364-01	1.693-01	2.172-02	1.079-05	1.276+06	3.042-08	0.000
CHN	2.116-08	6.449-10	4.227-10	1.203-08	5.546-09	1.711-10	0.000
CHO	3.999-09	8.663-08	4.894-08	3.755-09	9.286+10	2.056-11	0.000
CH3	4.476-13	5.668-15	4.733-16	6.060-18	3.702+19	4.005-22	0.000
CH4	4.799-11	1.265-16	7.697-19	9.739-24	9.339+26	9.636-30	0.000
C2H	3.345-19	2.357-18	1.489-17	1.638-11	2.319+11	5.264-13	0.000
C3H	4.180-24	4.727-26	2.849-25	1.922-16	1.787+16	9.880-19	0.000
HSI	9.157-21	9.121-17	7.074-16	1.922-15	4.712+14	2.050-15	0.000
O2SI	4.411-11	2.681-09	1.166-09	6.664-14	3.109+15	7.128-17	0.000
SI2	3.182-26	1.291-24	2.779-23	6.326-18	1.070+18	3.246-20	0.000
SI	1.416-15	6.574-12	1.140-10	9.242-09	6.197+07	1.662-07	0.000
C2H2	7.814-15	1.872-18	6.240-19	2.887-16	7.358+17	1.474-19	0.000
CSI*	0.000	0.000	0.000	0.000	0.000	0.000	0.000
O2SI*	0.000	0.000	0.000	0.000	0.000	0.000	0.000

Figure 3. Typical Output from BLIMP Program. Stagnation Point Solution for Apollo Heat-Shield Material. Surface Equilibrium with Assigned Component Mass Fluxes

nodal points were obtained in approximately 2.5 minutes on an IBM 7094. These solutions included evaluation of edge conditions, a similar solution at the stagnation point, and nonsimilar solutions at ten additional stations. Problems with five elements and 30 species take nine seconds per iteration on the IBM 7094 using overlays and 2 seconds per iteration on the Philco 212 without overlays.

2.3.3 Sample Problem Solution

The BLIMP program has been used to study a variety of problems. Several solutions are presented in Part III. A typical result is shown in Fig. 4. Profiles of velocity ratio, temperature, and shear function across a boundary layer into which a large quantity of Apollo heat-shield material is being injected are presented in Fig. 4(a). Mole fraction profiles are shown in Fig. 4(b). These results were obtained for an assigned surface temperature and assigned component fluxes ($\dot{m}_g$ and $\dot{m}_c$) and utilized a 30-component chemical model. A converged solution was obtained in seven iterations, starting with an air boundary-layer solution with the same wall temperature and same edge conditions but with no mass injection.

2.4 SUMMARY

The transformed nonsimilar laminar boundary-layer equations have been presented for a multicomponent boundary layer. These equations incorporate an approximate formulation for unequal diffusion and thermal diffusion coefficients for all species, a mixed equilibrium-nonequilibrium chemistry model and a one-dimensional model for radiation absorption and emission with angular dependent incident radiation at the boundary-layer edge. The formulation is suitable for coupling with a transient charring ablation solution and for matching with an entropy layer and a nonadiabatic inviscid flow field.

A numerical procedure is then described for solving the above problem. Cubic spline functions are used to relate the velocity ratio, total enthalpy, and elemental mass fractions to the transverse boundary layer coordinate. The boundary-layer equations are integrated between neighboring nodes. This integration is primarily for algebraic convenience, the smoothness of the weighting function having been found to be relatively unimportant with regard to accuracy and convergence stability considerations. The streamwise derivatives (nonsimilar terms) are represented by conventional three-point finite-difference relations.

A boundary-layer computer program, termed the boundary layer integral matrix procedure (BLIMP), has been developed which utilizes this numerical procedure for solution of the nonsimilar, equilibrium, multicomponent, planar or axisymmetric, laminar boundary layer. This program applies to general

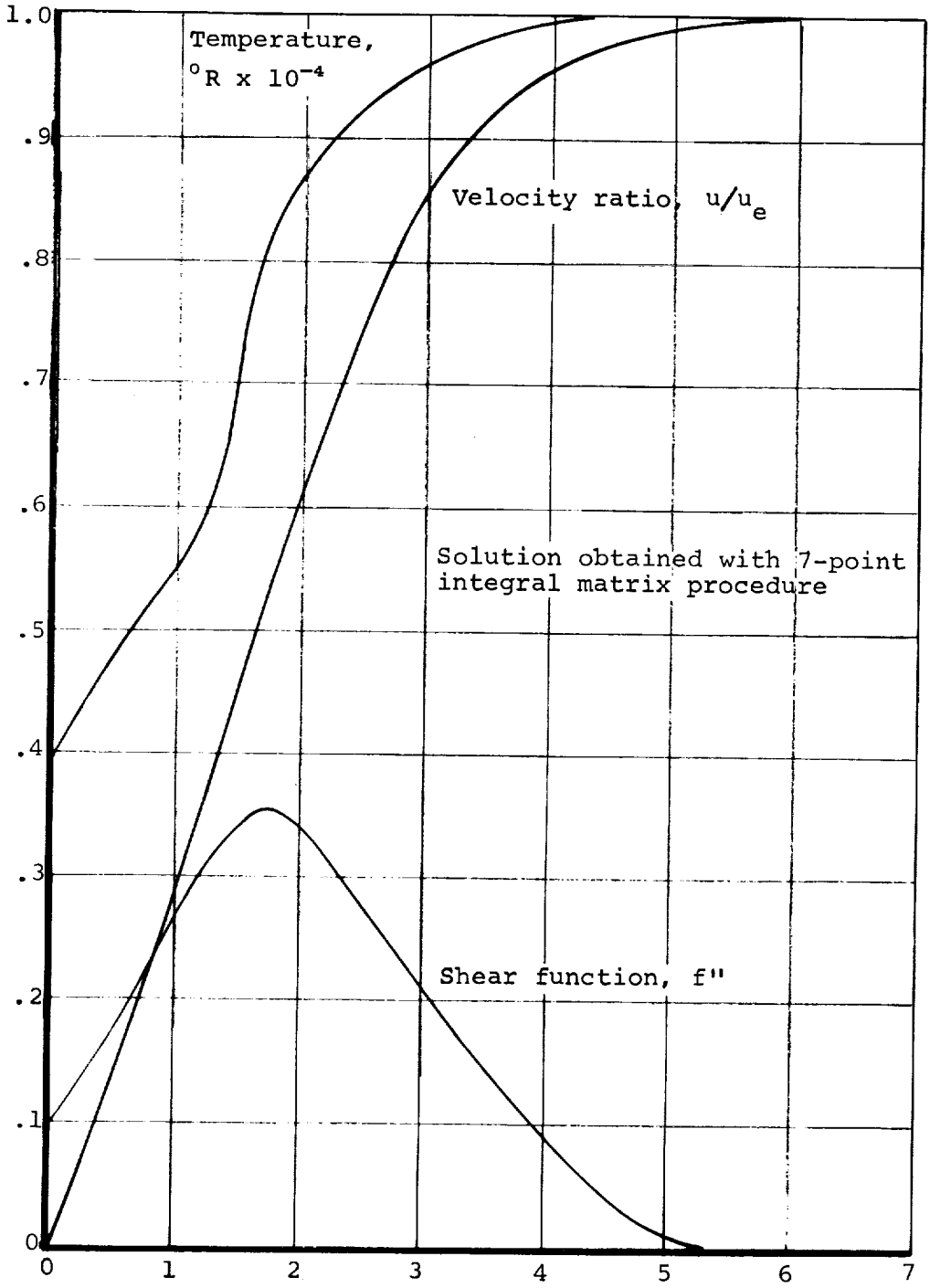

(a) Velocity Ratio, Temperature, and Shear Function

Figure 4. Boundary-Layer Profiles Over the Apollo Heat-Shield Material: Assigned Wall Temperature and Component Mass Fluxes ($\dot{m}_g$ and $\dot{m}_c$)

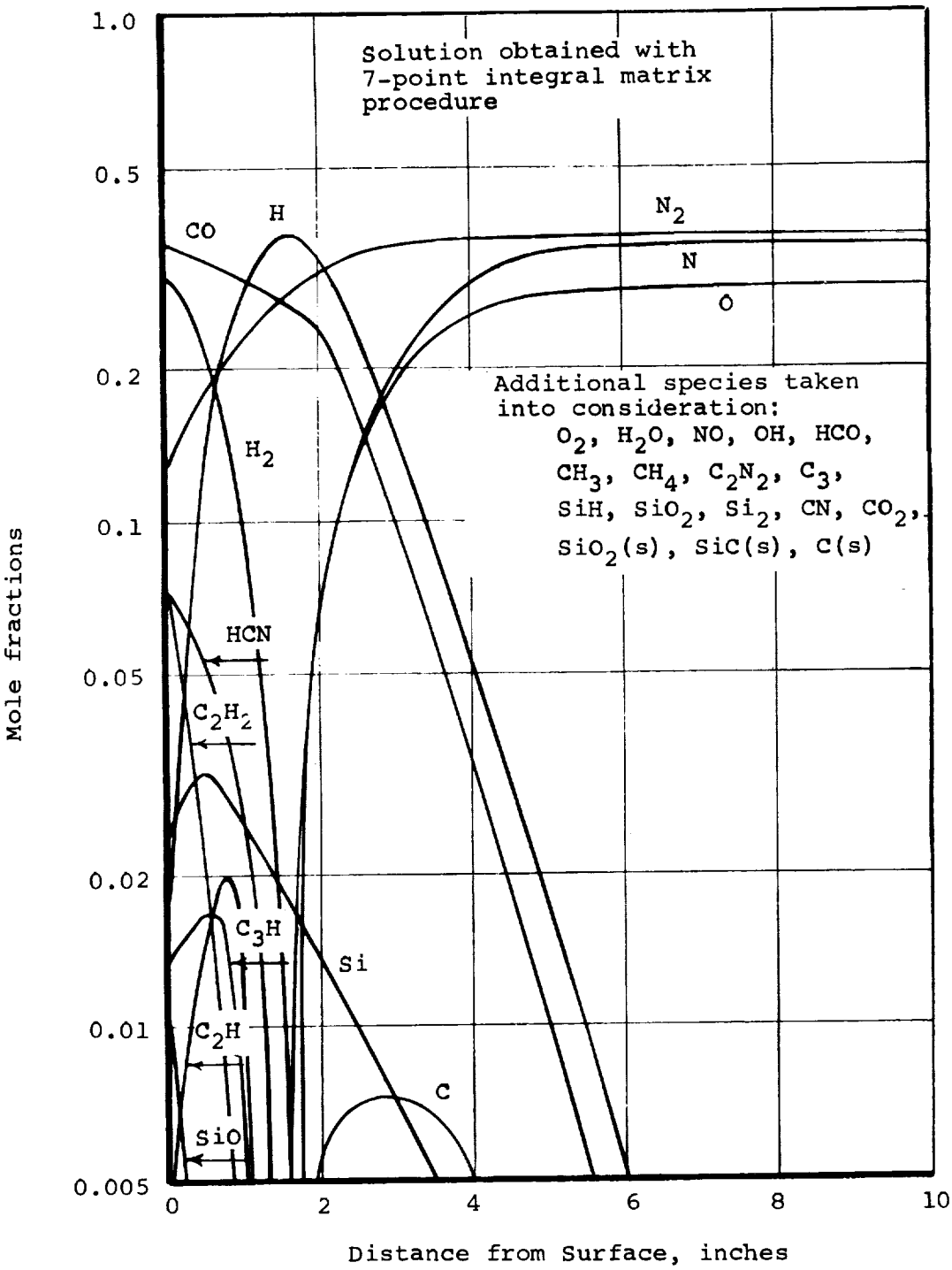

(b) Mole Fractions

Figure 4.. Concluded

chemical systems and treats a variety of surface boundary conditions, including coupling to a transient charring ablation computational procedure. Accurate solutions have consistently been obtained with relatively few nodal points and convergence has been rapid, with the result that computational speed is a program virtue.

SECTION 3
ANALYSIS AND COMPUTATIONAL PROCEDURE FOR CHARRING MATERIAL RESPONSE

3.1 INTRODUCTION

Analysis of a complete transient ablation problem necessarily involves a computation of the internal thermal response of the ablating material. A substantial part of the total effort under the present program has been devoted to the development of a computer code for in-depth response prediction of a charring material, suitable for coupling to the boundary layer program (BLIMP) described in Section 2 above. This section of the summary report describes the in-depth program (CMA) and related analysis. Section 5 below describes aspects of coupling procedures.

3.2 PROBLEM DEFINITION

3.2.1 General Description

The basic problem is to predict the temperature and density histories of a thermally decomposing material exposed to some defined environment which supplies heat and which may chemically erode the material surface.

The general prediction problem may conveniently be divided into two parts: the construction of a scheme for computing the in-depth behavior, and the specification of the heated surface boundary condition. The present report is mainly concerned with the first problem, although the second topic is also given extensive discussion. It may be noted in passing that for quasi-steady ablation problems (constant wall temperature, steady recession rate, invariant temperature profile with respect to the moving surface), the details of the in-depth solution are not necessary for determining the surface temperature and the recession rate. The transient problem, on the other hand, does require a complete in-depth solution, and hence is a much more elaborate problem.

The physical problem may be illustrated as follows:

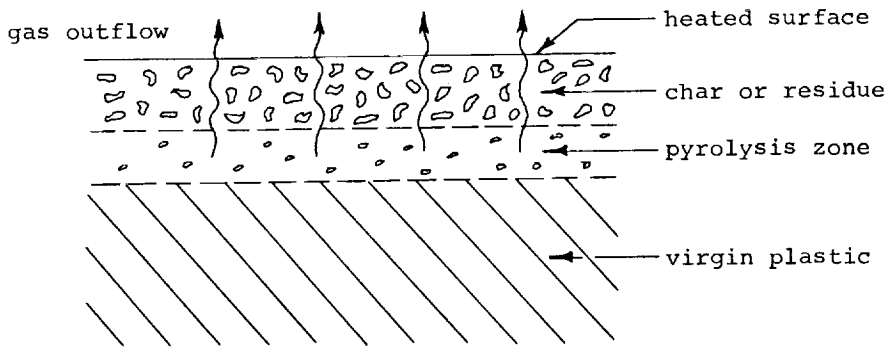

As the material is heated, one or more components of the original composite virgin material pyrolyzes and yields a pyrolysis gas, which percolates away from the pyrolysis zone, and a porous residue, which for most materials of interest is a carbonaceous char, possibly reinforced with refractory fibers or cloth.

Superimposed on this basic problem may be a number of even more complex events. The pyrolysis gases percolating through the char may undergo further chemical reactions among themselves and may react with the char, either eroding it or depositing additional residue upon it ("coking"). The char itself may collapse or fragment from mechanical or thermal stresses, and the refractory reinforcements may melt or suffer mechanical damage. Finally, various constituents of the residue structure may react chemically with each other, changing the nature of the char, and various mechanical forces may remove material from the surface.

Despite these complexities, it is found that the "simple physics" described by

$$\text{virgin plastic} \rightarrow \text{char} + \text{gas}$$

underlies a wide range of problems of technical interest, and for a great many materials, such as carbon phenolic, graphite phenolic, and wood, constitute all the events of interest. Such events as coking, mechanical erosion, melting, and subsurface reactions (other than pyrolysis) are less common and generally characterize specific problems.

Therefore in any effort to compute the in-depth response of pyrolyzing materials the first order of business is to characterize the heat conduction

and the primary pyrolysis reaction which have useful generality. Particular details of special char chemical systems can then be superimposed upon this general computational scheme as required. The present effort has been mostly devoted to the general conduction pyrolysis problem. The numerical details will be described below.

3.2.2 Differential Equations

For the basic in-depth solution, it is assumed that thermal conduction is one-dimensional; however, the cross-section area (perpendicular to the conduction flux) is allowed to vary with depth in an arbitrary manner. This corresponds to a thermal stream tube. Furthermore, it is assumed that any pyrolysis gases formed are in thermal equilibrium with the char. Coking or further chemical erosion are not presently included in the computational procedure and thus are excluded from the present discussion. An analysis has been developed for including these effects, however, and is discussed in Section 3.5 below. Thus, in the present discussion, it is assumed that the pyrolysis gases do not react chemically with the char in any way. Finally, any pyrolysis gas formed is assumed to pass immediately out through the char, that is, it has zero residence time in the char. Cracking or other chemical reactions involving only the pyrolysis gases may be simulated with an appropriate gas enthalpy-temperature relation.

The one-dimensional energy differential equation for this problem is readily formulated as

$$\frac{\partial}{\partial \theta} (\rho h A)_y = \frac{\partial}{\partial y} \left(kA \frac{\partial T}{\partial y} \right)_\theta + \frac{\partial}{\partial y} (\dot{m}_g h_g)_\theta \tag{35}$$

where ρ is the density, k is the thermal conductivity, A is area, h is enthalpy, and $\dot{m}_g$ the local gas flow rate.

The conservation of mass equation is

$$\left(\frac{\partial \dot{m}_g}{\partial y} \right)_\theta = A \left(\frac{\partial \rho}{\partial \theta} \right)_y \tag{36}$$

Evaluation of this expression requires a specification of the decomposition rate $\partial\rho/\partial\theta)_y$. A great amount of laboratory pyrolysis data suggests that the decomposition rate may be taken as an Arrhenius type of expression

$$\left(\frac{\partial \rho}{\partial \theta} \right)_y = - B\, e^{-E/RT}\, \rho_o \left(\frac{\rho - \rho_r}{\rho_o} \right)^n \tag{37}$$

and for even greater generality it has been found useful and sufficient to consider up to three differently decomposing constituents

$$\rho = \Gamma(\rho_A + \rho_B) + (1 - \Gamma)\rho_C \tag{38}$$

where each component is governed by a relation of the form of Eq. (37)

$$\left.\frac{\partial \rho_i}{\partial \theta}\right)_\theta = - B_i e^{-E_i/RT} \rho_{o_i} \left(\frac{\rho_i - \rho_{r_i}}{\rho_{o_i}} \right)^{m_i}, \quad i = A,B,C \tag{39}$$

For example $(\rho_A + \rho_B)$ might be the density of resin (or analogous binder) in the ablating material, ρ_C would be the density of the reinforcement and Γ the volume fraction of resin in the virgin plastic composite.

It is possible to handle the decomposition in other ways than by Eq. (37). A popular simplification is to treat density as a function of temperature only. An even more drastic simplification converts the virgin material to complete char at one particular "charring temperature." Other techniques specify some char thickness as a function of time or of heating rate. All of these simplifications are, of course, open to objection. Equation (37) is not only the most realistic physically, but is usually easy to handle in computation.

3.2.3 Boundary Conditions

Suitable boundary and initial conditions for the set of Eqs. (35) through (39) may be readily formulated. The boundary conditions at the front and back faces of the ablating material are usually surface energy balances. Of these, the front or "active" surface boundary condition is the most complex. It is handled in slightly different ways depending on which boundary layer treatment is being coupled to the in-depth response program.

Basically, the surface energy balance may be pictured as

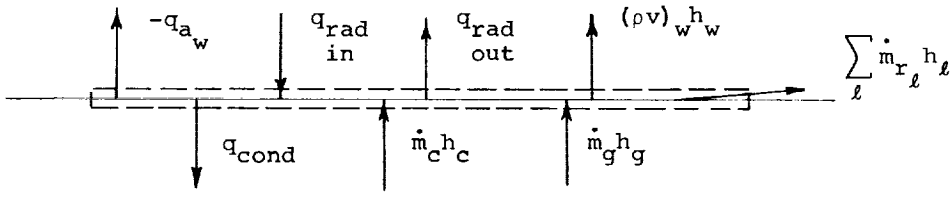

where the indicated control volume is fixed to the receding surface (see Eq. (30)). Energy fluxes leaving the control volume include conduction into the material, radiation away from the surface, energy in any flow of condensed phase material such as liquid runoff, and gross blowing at the surface. Energy inputs to the control volume include radiation in from the boundary layer and enthalpy fluxes due to char and pyrolysis gas mass flow rates. The final input in the sketch is denoted $-q_a$. It includes all diffusive energy fluxes from the gas-phase boundary layer (given by Eq. (18)). If the in-depth response computation is being coupled to an exact boundary-layer solution, the term $-q_a$ is obtained from that solution procedure and is, of course, a complex function of the boundary-layer structure. If, on the other hand, the in-depth response is being coupled to a simplified boundary-layer scheme, such as a convective film coefficient model, then the term $-q_a$ assumes the form of a correlation equation. Section 5 below contains a further discussion of this aspect of the total computation for these two approaches.

For the present, it suffices to note that computation of the surface energy balance requires the following information from the in-depth solution:

a. The instantaneous pyrolysis gas rate delivered from in-depth to the surface, $\dot{m}_g$

b. A relation between the surface temperature and the rate of energy conduction into the material, q_{cond}.

With these two pieces of information the surface considerations allow deteration of char consumption rate $\dot{m}_c$ and surface temperature T_w. It will be useful to keep in mind that, from this point of view, the purpose of the in-depth solution at any instant is to provide information about $\dot{m}_g$ and $q_{cond}(T_w)$. In some circumstances, of course, it is of interest merely to specify the heated surface temperature and recession rate. In this case, no surface energy balance is required.

It is usually of interest to have only one ablating surface. The backwall or nonablating wall boundary condition may be modeled with a film coefficient heat transfer equation.

3.3 FINITE DIFFERENCE SOLUTION PROCEDURE

3.3.1 Introduction

Section 3.2.2 above sets forth the governing differential equations whose solution is required to define the internal response of the charring material. As in many other problems, however, the differential equations

cannot be solved in general, and it is necessary instead to solve finite difference equations* which model the differential equations and, the analyst hopes, retain the same mathematical properties as the original differential equations. A number of plausible difference equations can be proposed, and without the benefit of actual experience it is generally impossible to select any particular differencing scheme as superior to any other. In the past few years a few general differencing principles have been made reasonably clear, however, so that the analyst is not completely in the dark. The following section offers some background on this topic.

3.3.2 Differencing Philosophy

This section sets down the general principles upon which the finite differencing of the governing equations is based. These principles have proved sound and useful, particularly for complex problems.

In common with all difference procedures, the area of interest (here, the charring material) is divided into a number of small zones, each considered to be homogeneous. All derivatives in the governing differential equations are then replaced by some difference expression from zone to zone. These zones, called nodes, thus provide the basic conceptual structure upon which the differencing procedure is based.

The following principles of differencing and nodal sizing have been followed in the present programming effort:

(1) The nodes have a fixed size. This avoids the slight additional computation complexity of shrinking nodes, and more importantly, makes principle (2) easier to satisfy, in addition to preserving a useful nodal spacing throughout the history of a given problem.

(2) Since the nodes are fixed in size, not all of them can be retained if the surface of the material is receding due to chemical or mechanical erosion. From time to time a node must be dropped, and experience shows that it is much more preferable to drop nodes from the back (non-ablating) face of the material rather than from the front face. This means that the nodal network is "tied to the receding surface," and that material appears to be flowing through the nodes. This involves a transformation of differential equations (35) and (36) to a moving coordinate system and somewhat complicates the algebra of the difference equations modeled on these differential equations.

*It is possible, of course, to use simpler schemes than finite difference equations. Integral analysis approaches, for example, have been tried. However, those techniques which have been employed have been of insufficient accuracy to be generally useful.

Disposing of nodes from the front surface, however, often leads to undesirable oscillations.

(3) The difference forms of derivatives are kept simple and are formed so as to provide a direct physical analog of the differential event leading to the derivative. This approach may be contrasted to those approaches which seek elaborate difference approximations to derivative expressions. Experience shows that the scheme advocated here, while sometimes at a minor disadvantage in accuracy, greatly simplifies the attainment of a major objective: a difference scheme which conserves energy and mass. Many of the more elaborate difference schemes fail to meet these "simple" but crucial conservation criteria, and hence frequently converge to erroneous or spurious solutions.

(4) The difference equation for energy is formulated in such a way that it reduces to the difference equation for mass conservation when temperatures and enthalpies are uniform. Any lack of consistency between the energy and mass equations complicates, and may entirely defeat, convergence to a meaningful result.

(5) The difference energy equations are written to be "implicit" in temperature. That is, all temperatures appearing are taken to be "new" unknown temperatures applicable at the end of the current time step. It is well established that implicit procedures are generally more economical than explicit procedures, at least for the majority of ablation problems of interest in the current work.

(6) In contrast to point (5), the decomposition relations are written as "explicit" in temperature. To implicitize temperature in these highly nonlinear equations necessarily involves either a time-consuming iteration procedure or an elaborate linearization.

(7) Since experience has shown that material decomposition rates are strongly dependent on temperature, it is highly desirable to perform the mass balance operations in a different, tighter network than that used for the energy balance equations. For greatest generality and utility, the number of these mass balance "nodelets" per energy balance "node" are freely selectable.

3.3.3 Array of Difference Equations

The actual derivation of the necessary finite difference equations is a complicated and tedious mass of detail best left to the detailed development given in Part II of the present series. For this summary report, only the

final result of the energy equation differencing is of interest, since the coupling procedure description given in Section 5 below requires an understanding of this step.

With an implicit temperature formulation, it may readily be seen from the energy differential equation (35) that the difference form of the energy equation for a given node at any time step will involve the "new" unknown temperature of that node and the two adjacent nodes. The equation for the last node, however, will have only two unkowns, since the adjacent temperature for that node is the known reservoir temperature. Similarly, the first node equation involves only two unknown temperatures, but it also includes the unknown quantity q_{cond}, which ultimately will be determined by the surface energy balance.

If we arrange all the energy relations in order we obtain an array of the form

$$
\begin{aligned}
B_1 T'_1 + C_1 T'_2 &= q_{cond} \\
A_2 T'_1 + B_2 T'_2 + C_2 T'_3 &= D_2 \\
A_3 T'_2 + B_3 T'_3 + C_3 T'_4 &= D_3 \\
A_4 T'_3 + B_4 T'_4 + C_4 T'_5 &= D_4 \\
&\vdots \\
A_N T'_{N-1} + B_N T'_N + 0 &= f(T_{res})
\end{aligned}
\tag{40}
$$

where the coefficients A_N, B_N, C_N, and D_N are given by complicated algebraic expressions involving nodal thickness, thermal conductivities, gas flow rates, and old temperatures.

3.3.4 Reduction of Array

It is now possible to see clearly what needs to be done for each time step $\Delta\theta$ of the solution in order to prepare for coupling to the surface

energy balance. First, using the current values of ρ_n, surface recession rate, and T_n, the mass relations (38) and (39) can be solved for each node n, yielding "new" gas flow rates $\dot{m}_{g_n}$.

This information may then be used to compute the coefficients of the tri-diagonal energy equation matrix. Once this matrix is set up, the required surface energy relation $q_{cond} = q_{cond}(T_w)$ may be obtained directly, as described in the next section.

The next step in the solution procedure is to eliminate one unknown temperature from each equation in the array (Eq. (40)). This can be done by eliminating T_N from the next to last equation and proceeding sequentially upward to the top equation, eliminating the highest-indexed unknown temperature from each equation of Set (40) in turn. The resulting reduced set has the form

$$
\begin{aligned}
B_1^* T_1' &= q_{cond} \\
A_2 T_1' + B_2^* T_2' &= D_2^* \\
A_3 T_2' + B_3^* T_3' &= D_3^* \\
A_4 T_3' + B_4^* T_4' &= D_4^* \\
&\vdots \\
A_N T_{N-1} + B_N^* T_N' &= F_4(T_{res})
\end{aligned}
\qquad (41)
$$

3.3.5 Coupling to Surface Energy Balance and Final Step

The top equation of this set relates q_{cond} to T_1', where T_1' is the new surface temperature. This is the required relation for use in the surface energy balance coupling to whatever boundary-layer model is being used, as discussed in Section 5 below. This coupling operation balances the surface energy terms and thus determines the new surface temperature T_1'. Since T_1' is now known, the second equation of Set (41) yields T_2' directly, then the third equation yields T_3', and so on until the new temperature set is complete.

As a final step, new values for temperature dependent properties can be selected for each node and the entire system is then ready for a new time step, beginning with the decomposition event.

3.4 CHARRING MATERIAL ABLATION (CMA) PROGRAM

The Charring Material Ablation Program is a coded procedure for calculating the in-depth thermal response of a charring, ablating material. The solution is obtained through the difference equations discussed in the preceding subsections. The program is described briefly in Section 3.4.1 and some sample problem solutions are presented in Section 3.4.2. Complete decriptions, user's manual, and flow charts are given in Refs. 12, 13, and 14.

3.4.1 Program Description

3.4.1.1 Program Objectives

The program produces in-depth temperature and density histories, plus surface recession rate as a function of time. In addition to this basic output, the program outputs a number of integrated energy terms and various material property data of interest. Section 3.4.1.5 below gives a more detailed description of the program output.

3.4.1.2 Program Capabilities

The Charring Material Ablation Program is an implicit, finite-difference computational procedure for computing the one-dimensional transient transport of thermal energy in a three-dimensional isotropic material which can ablate from a front surface and which can decompose in depth. Decomposition reactions are based on a three-component model. The program permits up to eight different backup materials of arbitrary thickness. The back wall of the composite material may transfer energy by convection and radiation.

In one program configuration, the ablating surface boundary condition may take one of three forms:

Option 1 - Film coefficient model convection-radiation heating with coupled mass transfer, including the effects of unequal heat and mass transfer coefficients (non-unity Lewis number) and unequal mass diffusion coefficients. Surface thermochemistry computations need not presume chemical equilibrium at the surface, and may allow for melting and liquid phase removal at the surface. Chemical state programs for providing this thermochemical surface boundary condition are discussed in Section 4.4.

Option 2 - Specified surface temperature and surface recession rate

Option 3 - Specified radiation view factor and incident radiation flux, as functions of time, for a stationary surface.

Any combination of the first three options may be used for a single computation. Option 3 is appropriate to cooldown after termination of convective heat input and is often useful in conjunction with Options 1 and 2.

In another configuration, the program may be coupled to the boundary layer integral matrix procedure (BLIMP) program. In this arrangement, the total assembly is designated the CABLE program and is described in Section 5 below.

The program permits the specification of a number of geometries. In the most general case, area may vary arbitrarily with depth. Special cases include:

(1) Plane

(2) Cylindrical or annular, with heated surface either inner or outer

(3) Spherical or spherical shell, with heated surface either inner or outer.

The rear surface of the last node may be specified as insulated, or may experience convective and radiative heat transfer to a "reservoir" at a specified reservoir temperature if a rear surface convection coefficient and an emissivity are input.

Material properties such as thermal conductivity, specific heat, and emissivity are input as functions of temperature for virgin plastic and char. For partially decomposed material, the program performs an appropriate averaging to determine effective material properties.

3.4.1.3 Solution Procedure

The basic solution procedure is by the finite difference approach discussed in Section 3.3. For each time step, the decomposition relations are solved and then the in-depth energy fluxes constructed in general terms. These are then harmonized with a surface energy balance (if a surface energy balance option is being used) and the in-depth temperatures determined. New material property values are set up and the solution is ready for the next time increment.

3.4.1.4 Output Information

The CMA program outputs instantaneous mass ablation rates and blowing parameters for char and pyrolysis gas, total integrated mass ablation of char

and pyrolysis gas, total recession and recession rates of surface, of the char line, and of the pyrolysis line. It also outputs the surface energy flux terms, namely, the energy convected in, energy radiated in, energy reradiated out, chemical generation, and conduction away (q_{cond}). Further, it describes how the input energy of q_{cond} is "accommodated" or "partitioned" in the solid material. Part of the energy is consumed in decomposing the plastic, part is consumed in sensible enthalpy changes of the solid, and part is "picked-up" by the pyrolysis gases as they pass through the car. Thermocouple and isotherm output can also be called for. A typical output is presented in Figure 5.

3.4.1.5 Storage Requirements and Computational Time

The storage requirements for the CMA program depend strongly upon the coupling mode in use. Coupling to a film coefficient model for the surface energy balance (option 1) involves considerable table storage such that the program will barely fit a 32,000-word machine with full table sizes. In certain cases a reduction in table sizes will allow the program to fit on a smaller machine. As a subroutine to the CABLE program or use of Option 2 or Option 3 eliminates the need for storing extensive boundary condition tables. In these cases, the CMA program requires less than 8000 words of storage.

Computation time depends, of course, on the problem being computed, but experience to date indicates that CMA computations run in roughly 1/3 of real time for "typical" charring material problems, for machines of the IBM 7094 speed class.

3.4.2 Sample Problem Solutions

As an illustration of the general performance of the charring material computer program, Figure 6(a) presents a graphic representation of the in-depth density history for a nylon-phenolic material exposed to a typical reentry environment. Figure 6(b) shows some in-depth thermocouple temperature response predictions for the same problem. Figure 7, from a different problem, shows a machine made plot generated by a plot routine coupled to the CMA program.

3.4.3 Concluding Remarks for the Charring Material Ablation Program

The preceding sections have described the analysis and an associated computer program for the calculation of the in-depth response of a charring or pyrolyzing material. The general objective of the development effort has been to produce a computation scheme which accounts for those physical events common to a wide range of technically important applications, so that the resulting program has as much generality and flexibility as possible. To this end, the analysis accounts for the basic in-depth pyrolysis problem, which

AEROTHERM CHARRING MATERIAL THERMAL RESPONSE AND ABLATION PROGRAM

10K-1.00-.00

- - - - - - - - - - - - - 4386.7999 SECONDS - - - - - - - - - - - - -

TIME STEP	SURF ITER	PROB OPTN	SURFACE RAD (IN)	H WALL (BTU/LB)	H EDGE (BTU/LB)	HEAT COEFF (LB/SQ FT-SEC)	CH/CHO
44	2	0	.0000	-1074.36	.00	.0002	1.00000

---ABLATION RATES---

B PRIME	B PRIME G	M DOT CHAR (LB/SQ FT-SEC)	M DOT GAS	M CHAR (LB/ORIG SQ FT)	M GAS
.18737	.18737	.000000	.000045	.000000	.000150

---RECESSIONS/RECESSION RATES---
(IN) / (IN/SEC)

SURFACE	CHAR (.08)	PYROLYSIS (.92)
.0000000/ .0000000	-.0000000/-.0000000	.0000000/-.0000000

---SURFACE ENERGY FLUX TERMS---
CURRENT RATES (BTU/SQ FT SURFACE-SEC)
AND INTEGRATED VALUES (BTU/ORIG SQ FT)

	CONVECTED IN	RADIATED IN	RADIATED OUT	CHEMICAL GENERATION	CONDUCTION AWAY
RATE	.241+01	.000	.000	.000	.241+01
TOTAL	.702+02	.000	.000	.000	.701+02

---INTERIOR ENERGY TERMS---
CURRENT RATES (BTU/SQ FT SURFACE-SEC)
AND INTEGRATED VALUES (BTU/ORIG SQ FT)

	PYROL GAS PICK UP	DECOMP ABSORPTION	CONVECTION WITH SOLIDS	STORAGE IN SOLID	LOSS AT REAR FACE
RATE	.425-02	.166-02	-.000	.237+01	.329-07
TOTAL	.134-01	.151-02	.000	.699+02	.444-06

NODE	MAT	TEMP (DEG R)	DENSITY (LB/CU FT)	ENTHALPY (BTU/LB)	NODE	MAT	TEMP (DEG R)	DENSITY (LB/CU FT)	ENTHALPY (BTU/LB)
1	0	1380.08	33.766	-2063.55	20	1	635.44	34.000	-2358.73
2	0	1337.48	33.851	-2079.56	21	1	619.87	34.000	-2363.62
3	0	1298.90	33.946	-2110.81	22	1	606.47	34.000	-2367.84
4	0	1186.88	33.984	-2140.65	23	1	594.94	34.000	-2371.46
5	1	1121.84	34.000	-2167.87	24	1	585.06	34.000	-2374.57
6	1	1063.43	34.000	-2192.70	25	1	576.59	34.000	-2377.23
7	1	1011.11	34.000	-2214.93	26	1	569.36	34.000	-2379.51
8	1	964.22	34.000	-2234.86	27	1	563.18	34.000	-2381.45
9	1	922.00	34.000	-2251.64	28	1	557.93	34.000	-2383.10
10	1	883.87	34.000	-2266.68	29	1	553.47	34.000	-2384.51
11	1	849.46	34.000	-2280.26	30	1	549.69	34.000	-2385.70
12	1	818.42	34.000	-2292.51	31	1	546.49	34.000	-2386.70
13	1	790.42	34.000	-2303.55	32	1	542.89	34.000	-2387.83
14	1	765.16	34.000	-2313.52	33	1	539.52	34.000	-2388.89
15	1	742.38	34.000	-2322.50	34	1	537.01	34.000	-2389.68
16	1	721.84	34.000	-2330.61	35	1	535.17	34.000	-2390.26
17	1	698.53	34.000	-2338.88	36	1	533.84	34.000	-2390.68
18	1	674.39	34.000	-2346.48	37	1	532.43	34.000	-2391.12
19	1	653.49	34.000	-2353.05	38	1	531.65	34.000	-2391.37

Figure 5. Typical Output from CMA Program. Stagnation Point Solution for Apollo Heat-Shield Material During SA 202 Trajectory

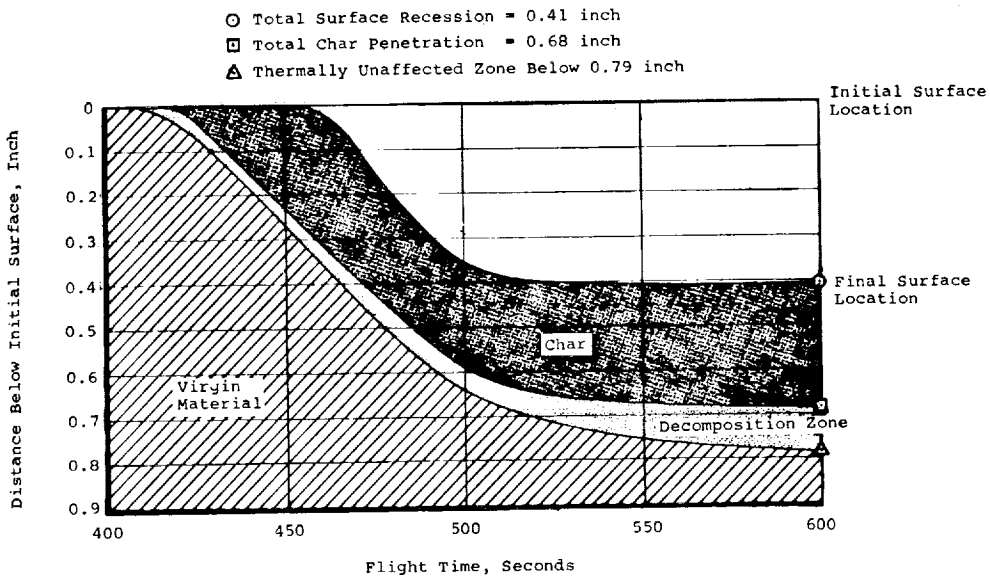

(a) Predicted Degradation Depth Histories

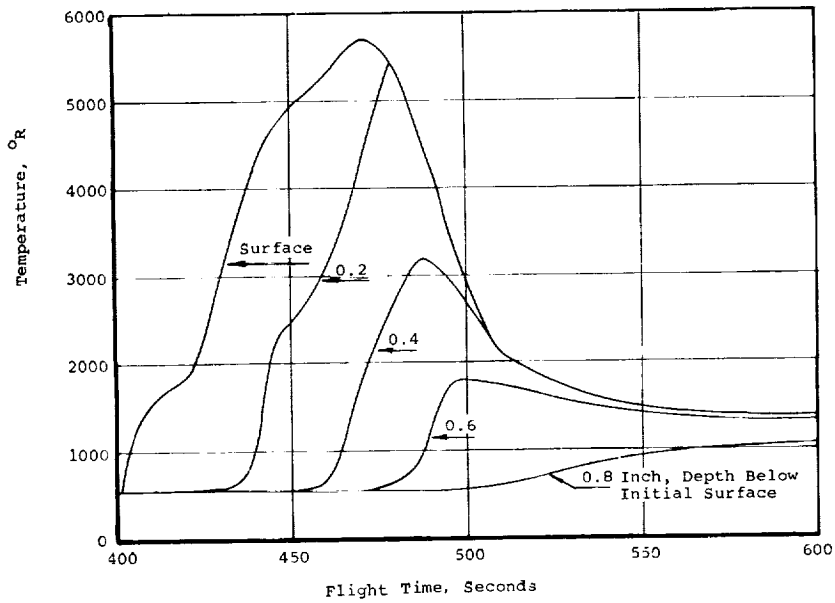

(b) Predicted Temperature Histories at Surface and Selected Thermocouple Locations

Figure 6. Nylon Phenolic Reentry Problem

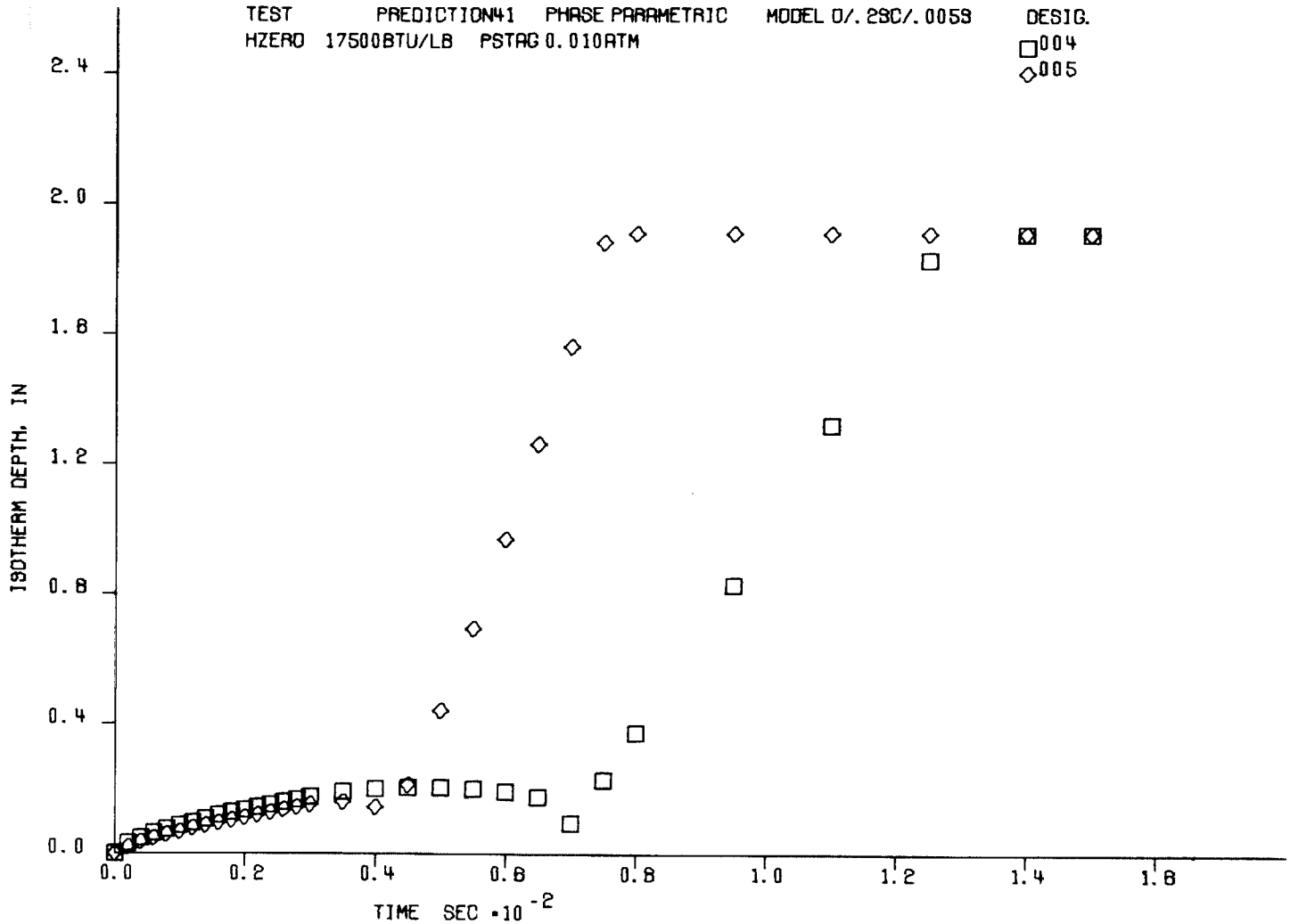

Figure 7. Typical Machine Plotted Isotherm Depths

is observed to be common to a wide range of problems, and excludes coking (char densification), thermal expansion, condensed phase char rate-controlled reactions, and mechanical damage mechanisms. All of these are specific to particular materials or material types. For such materials, the basic program can be modified to include these special effects.

The basic program generates a one-dimensional in-depth solution, but the cross-sectional area of the material analyzed may vary with depth (thermal stream tube). Pyrolysis may occur through three distinct Arrhenius-type kinetic reactions.

An important feature of the program is the range of physically realistic boundary conditions available for the heated surface. These include

(1) Specified temperature and recession rate

(2) Radiation energy balance with zero recession and no convection (cool down or soak out)

(3) Coupling through a film coefficient model to surface thermochemistry solution including general heterogeneous equilibrium, or heterogeneous equilibrium modified by certain rate controlled reactions, both models including the effects of the melting and total removal of surface species formed at temperatures above their melt or fail temperatures

(4) Coupling to a general, nonsimilar, multicomponent boundary-layer solution including heterogeneous kinetic effects, with surface melting or failing.

This range of possibilities offers opportunities for economy during routine in-depth studies or during computations for which film coefficient models are adequate, while preserving the capability of doing very accurate coupled, simultaneous boundary layer and in-depth solutions.

Other features of particular importance which are worth stressing may be enumerated as follows:

Simple difference formulation. The difference equations employed to effect the in-depth solution are kept simple and are designed to conserve energy and mass without fail. This helps avoid convergence to spurious solutions.

Implicit temperature formulation for energy, explicit temperature formulation for decomposition. This approach keeps the energy solution stable and economical and avoids the complexities of a totally implicit solution.

Three-component Arrhenius expression for pyrolysis kinetics. This expression is believed sufficiently general to accurately represent the degradation kinetics of most ablation materials of interest.

Freely selectable pyrolysis gas kinetics model. The history of the pyrolysis gas as it passes through the char is a key aspect of any solution. The analysis scheme used here does not involve any particular assumption about the pyrolysis gas history, but employs only an input temperature-enthalpy relationship. This relationship may be derived from any model the user feels applicable.

Final conclusions about the general accuracy and utility of the CMA in-depth routine will be deferred until Section 5.2.4 below where the program can be considered as coupled to a thermochemical boundary condition. For the present it may merely be noted that the in-depth aspects alone of the solution have been subjected to extensive scrutiny for cases of known surface temperature and recession rate. Agreement with both analytical solutions and with in-depth thermocouple data has generally been excellent, although, of course, when dealing with charring ablators, adjustments in thermal conductivity and pyrolysis gas enthalpy data are frequently necessary to force agreement between predictions and thermocouple data. These two parameters have such powerful effects on the solution that the thermocouple data must be supplemented by in-depth observations to detect any omissions in the analytical model. The chief possibilities here are coking and reinforcement-char chemical reactions; both effects have occasionally been observed. The conclusion remains, however, that the program accurately models the fundamental pyrolysis and energy transport events it was intended to model.

In conclusion, the in-depth analysis presented here and programmed as the CMA program has been applied to a wide range of materials of technical interest with excellent results. The program appears to be thoroughly checked out and fully operational.

3.5 SUBSURFACE COKING REACTIONS

The CMA program described above is a mathematical analog of the surface and subsurface thermochemical events which are common to most reinforced organic ablation materials. These events consist basically of (1) energy and mass transfer in a material which experiences subsurface decomposition of an organic polymer into a pyrolysis gas and a char residue, and (2) the energy, mass, and chemical species transfer at the ablating surface which dictate the magnitude of surface recession. As discussed earlier, additional complications may be of importance when consideration is given to certain particular types of ablation materials. These complications may include such events as subsurface reactions between reinforcing fibers and the carbonaceous

char, mechanical failure of the char layer resulting from pressure gradient and thermally induced stresses, and the thermal cracking of pyrolysis gas products resulting in carbon deposition in the char layer beneath the heated surface. Phenomenological models have been postulated and some experimental data has been obtained for both subsurface fiber-carbon interactions (Ref. 15) and mechanical failure of the char layer (Ref. 16). Little attention has been directed toward the construction of a phenomenological model to represent subsurface pyrolysis gas cracking with attendant carbon precipitation upon the char layer (coking).

An analysis has been conducted and finite difference relations suitable for computer coding have been developed for representing the response of a charring ablation material which may undergo subsurface "coking" of the pyrolysis gas. Coking reactions, as employed here, refer to the precipitation of carbon from the hydrocarbon-containing gaseous pyrolysis products with attendant deposition upon the char, and the reverse reaction evidenced by erosion of the carbonaceous char accompanied by the addition of carbon to the gaseous pyrolysis products. Forward and reverse coking reactions are of interest because the permeability of the char layer is decreased by coking which may result in high gas pressure in depth. High pressure in depth may give rise to excessive char stress which may produce catastrophic failure of the char layer. The technique considers internal pressure build-up resulting from pyrolysis product flow through a char layer of variable permeability.

Details of the development and finite difference formulation are presented in Part VI of the present series. A brief description of the adopted phenomenological model and some comments regarding the finite difference formulation are given in the following two subsections.

3.5.1 Description of the Physical Process

The physical process to be characterized represents an extension to that represented in the CMA program described above, in that after the pyrolysis gas is formed, further mass transfer between the pyrolysis gas and char may occur. The resultant change in pyrolysis gas and char composition is evaluated and the effect of this change upon subsequent events, both below and at the heated surface are considered. The generalized model selected to represent the charring material is described first. Thisis followed by a description of the type of reactions that may be considered and the rate equations selected to represent the rate at which these reactions may proceed.

In its undecomposed state the ablation material is taken to be composed of two basic types of constituents: (1) inert, and (2) reactive. The inert constituents will consist of materials which are not permitted to undergo molecular changes in depth, e.g., silica or other metal oxide reinforcements.

The reactive constituents may consist of organic materials, carbon or graphite reinforcements, and water of crystalization of reinforcing fibers, for example. Carbon and graphite are included in the list of reactive constituents because they may be vaporized in depth or be eroded chemically by the gaseous products of other reactive constituent pyrolysis products. The following, idealized, irreversible reaction characterizes the initial decomposition of the composite.

$$\text{Inert} + \text{Reactive} \rightarrow \text{Inert} + \text{Carbon(S)} + \text{Gas(O)} \qquad (42)$$

As noted from this relation, the inert constituent does not take part in the reaction, but is simply transported from a constituent in the virgin plastic to a constituent in the initial decomposed material. The reactive constituents, on the other hand, do undergo a change in molecular configuration and phase; however, the products of this initial reaction may consist of only two constituents, solid carbon, and an initial pyrolysis gas (gas(O)). The reaction should be looked upon as one which splits the virgin material into three distinct parts, each having a fixed quantity of chemical elements.

The initial off-gas elemental composition may then be obtained by subtracting the quantity of chemical elements contained in a laboratory-produced char from the chemical elements contained in the virgin plastic. After the initial decomposition gas is formed, it will percolate through the char layer toward the heated surface. This will result in an increased gas temperature and decreased pressure. The change in pressure and temperature will cause the initial gas products (gas (O)) to undergo numerous chemical reactions as they pass through the char. The reactions considered fall into three general categories:

1. Decomposition of the gas including thermal decomposition of high-molecular-weight hydrocarbons and dissociation of CO_2, H_2O, and H_2 for example.
2. Further decomposition of the hydrocarbons resulting in precipitation of carbon (coking) on the adjacent char passages resulting in char density buildup.
3. Chemical erosion of the char layer (below the heated surface) by the gases including carbon vaporization resulting in a char density reduction near the heated surface.

The three reaction regimes are represented in the following sketch for decomposition of a hypothetical material.

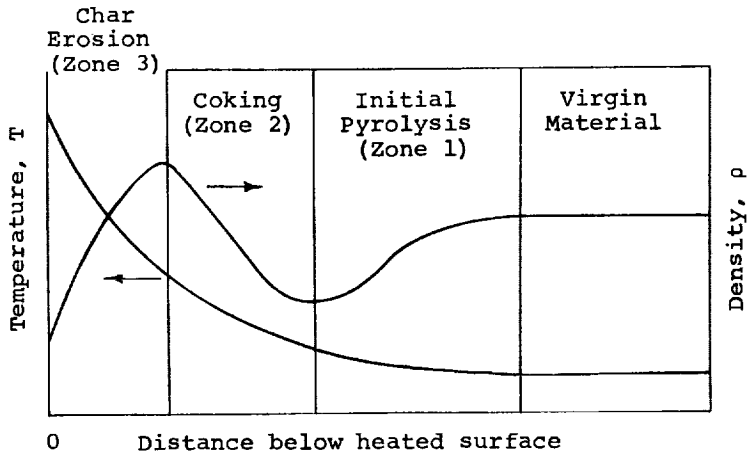

The classification of reactions above corresponds to the order in which the various types of reactions would be expected to occur as the gas passes through the char. The first class of reactions may be looked upon simply as the gas reacting with itself so no change in the concentration of chemical elements in the gas results. The second two classes of reactions, however, will result in a transfer of carbon elements between the gas and the porous char. With regard to the elemental composition change these reactions may be considered reversible.

$$\text{gas(O)} \underset{3}{\overset{2}{\rightleftharpoons}} \text{gas} + \text{carbon(S)} \tag{43}$$

where the forward reaction corresponds to moderate temperature, type 2 reactions, and results in a precipitation of carbon from the initial pyrolysis gas. The subsequent, type 3, high temperature reactions result in char erosion with attendant addition of carbon to the gas.

An understanding of the detailed kinetic mechanisms required to characterize these reactions is not presently in hand; however, some qualitative information is available upon which a crude model may be formulated. The specific information relating to each reaction type is presented briefly and the physical model adapted to characterize each reaction regime is described in the following paragraphs.

Type 1 Reactions - If the subsurface composition is computed on the basis of chemical equilibrium considerations, a far more dense char is predicted to occur than is observed from char density measurements (Ref. 17). It may be concluded either that condensed phase carbon is formed but does not stick to

the char, or that the high molecular weight hydrocarbons do not decompose according to the dictates of chemical equilibrium. The latter possibility seems more probable but conclusive experimental evidence on this matter is lacking.

Type 2 Reactions - A certain amount of experimental evidence exists (Refs. 18 and 19) which indicates that char densification may occur between the organic decomposition zone and the heated surface. It appears that this char densification is a result of deposition of condensed phase carbon from the hydrocarbons in the organic pyrolysis gas products. This seems reasonable since, as indicated above, the gases contain far more carbon than would exist if equilibrium were achieved. As the gases approach the heated surface their temperature is increased and the rate at which equilibrium is approached increases. In the present study, the coking rate is expressed as the product of a forward rate coefficient and a carbon mass fraction "coking potential."

$$\dot{m}_{coke} \propto k_F(\tilde{K}_{cg} - \tilde{K}_{cgE}) \tag{44}$$

where the forward rate coefficient is expressed in Arrhenius form, and the driving potential is represented by the difference between the elemental carbon mass fraction of the gas and that which would exist if equilibrium were achieved. The coking rate equation has the following features:

1. It is simple enough to be included practically in a charring ablation solution.
2. It approaches the coking rates which would be predicted by more detailed complete equations when kinetics are relatively slow or fast.
3. It is based upon parameters which may be controlled in a laboratory experiment to derive data on the coking process.

As noted from the postulated "coking" rate equation, the coking rate will approach zero as the pyrolysis gas approaches chemical equilibrium with the char. This marks the onset of regime 3 which is characterized by addition of carbon to the gas from the char.

Type 3 Reactions - In the event local char layer temperatures much in excess of 4500°R are achieved, it is probable that chemical equilibrium will be achieved between the pyrolysis gas and the char, in which case the coking potential will reach zero. For this reason type 3 reactions are presumed to occur in chemical equilibrium and sufficient carbon will be added to the gas from the char to maintain this equilibrium. This char erosion will result in a char density decrease which may, in an extreme case, cause the char density to approach zero.

3.5.2 Solution Procedure

The differential and finite difference formulation of the energy, mass, and momentum transfer events associated with the above phenomenological model is accomplished in much the same manner as with the CMA program described earlier. The primary feature which distinguishes between the two formulations is associated with the treatment of the subsurface species conservation equations and evaluation of the char material state. The species conservation equations include evaluation of the pyrolysis gas elemental carbon content as results from the integrated effect of coking events.

In order that the energy exchanges associated with coking reactions be properly evaluated it is necessary to accurately assess the thermodynamic state of both the pyrolysis gas and the char material. This is accomplished by expressing the pyrolysis gas enthalpy as a function of pressure, temperature, and elemental carbon content. The char state is expressed in terms of temperature and the relative quantities of each constituent; inert, reactive, and carbon. Because the ablation material composition depends upon the relative quantity of each of three constituents it is not possible to express the material state in terms of temperature and density alone, as in the CMA program. Because of this, it is most convenient to express both the energy and mass conservation equations in terms of nodal mass rather than nodal density.

In addition to the inclusion of energy and mass transfer events associated with subsurface coking relations, an empirical expression is included for evaluating the pressure distribution through the char layer as results from pyrolysis gas flow through the char layer of variable permeability.

3.6 CONCLUDING REMARKS

The above sections have described the basic physical problems of the charring ablator and have given the governing differential equations. The finite difference solution procedure for solving for the in-depth response of a charring ablator was sketched out. The manner in which this in-depth solution could be coupled to either a film coefficient boundary-layer model or to a complete boundary-layer solution was indicated; this subject will be dealt with in greater detail in Section 5 below. Sample solutions were cited illustrating the general applicability of the analysis in its computer program form.

A supplementary analysis was described which broadened the physical problem to include the effects of carbon deposition from the pyrolysis gases (coking) and the reverse char erosion effect. The resulting solution procedure differs in detail from the no-coking procedure, since a new physical quantity (carbon content) must be traced, but the general level of problem complexity is not appreciably higher than in the no-coking problem. The coking analysis has not been programmed for machine computation.

SECTION 4

ANALYSIS AND COMPUTATIONAL PROCEDURES FOR EVALUATION OF CHEMICAL STATE

4.1 INTRODUCTION

In the study of high energy boundary layer phenomena, thermochemical processes can be of dominant importance. This is particularly true when these boundary layers interact with chemically active surfaces. In the present study, interest is directed toward the prediction of thermochemical response of a heat shield during superorbital reentry. The requirements for evaluating the chemical state of homogeneous and heterogeneous systems in this problem are extensive. These requirements include the determination of the chemical state after normal or oblique shock wave compression, during the isentropic expansion of the inviscid shock layer gases, within the boundary layer, and at the chemically active surface. In the last two instances, these state calculations are coupled with complex mass balance relations. Many chemical state solution procedures have been documented to treat reasonably standard closed systems, such as those associated with expansion processes. For open systems only a few direct solution procedures have been documented. Because of the number of requirements imposed upon the chemical state routines in the present study, the general treatment of a variety of chemical systems became a major effort. The inclusion of a general kinetic model, ionization, and the extensive bookkeeping associated with the downstream introduction of new species, is of major importance in the formulation of the general problem necessary for thoroughly treating the coupled boundary layer problem.

The chemical state procedures adopted as a part of this effort are described in Part V of this series of reports and summarized in the following sections. The basic relations are presented in Section 4.2, whereas in Section 4.3 the solution procedure is discussed. These techniques have been built in greater or lesser extent into the equilibrium surface thermochemistry (EST) program, the Aerotherm chemical equilibrium (ACE) program and certain special modifications of it, and the chemical state subroutines to the BLIMP program. Section 4.4 specifies the status of these routines and the extent to which the general formulation presented herein has been implemented. In brief, the procedures are presently limited to equilibrium, except that selected species can be considered as frozen across the boundary layer and to undergo rate-controlled surface-catalyzed reactions or reactions with the surface material.

4.2 ANALYTICAL APPROACH

In this section, the analytical approach utilized to specify the chemical state of a system are summarized. Basically four types of relations can be

considered in a general open system. These are the equilibrium relations applying to those reactions which can be considered as generally equilibrated, the nonequilibrium relations for those reactions which can be (but are not necessarily) out of equilibrium, the mass balance relations, and those additional state constraints imposed on the system.

4.2.1 Equilibrium Relations - Totally Equilibrated Systems

In a chemical system there will exist, in the general case, a set of independent equilibrium reactions. All other equilibrium reactions will be equivalent, both physically and mathematically, to this independent set. It can be shown that in a completely equilibrated system the number of independent equations is usually equal to the number of molecules less the number of elements. The modification of these relations for systems that are not completely equilibrated will be considered in Section 4.2.2.

The selection of this set of independent reactions can be done arbitrarily, but it is convenient to establish some consistent technique. Most such techniques are based on the pre-selection of a set of species usually equal in number to the number of elements. The formation reactions of all other species from this base set represent the independent set of equilibrium reactions. The base species must be selected in such a fashion that no reaction can be written wherein reactants and products are all base species. Thus in the O,H system, HO and H_2O_2 represent an invalid base set whereas HO and O, HO and H, etc., represent valid sets. It has been reasonably common practice to select the monatomic gases as base species, since the formulation of the formation reactions is particularly convenient. There are advantages, however, in selecting a more general set, particularly when chemical kinetics are important. Considering a set of base species N_i, formation reactions for the remaining N_j species are of the form

$$\sum_i \nu_{ji} N_i \rightleftarrows N_j \tag{45}$$

where the ν_{ji} are the stoichiometric coefficients of the formation reactions. Mathematically, the ν_{ji} are obtained implicitly from the c_{kj} (the atoms of element k in molecule j) by

$$\sum_i c_{ki}\nu_{ji} = c_{kj} \tag{46}$$

The set of independent formation reactions (Eq. (45)) for j ranging from N_b to N_s, where N_b is the number of base species and N_s is the total number of species, can be used to formulate a set of equilibrium

constraints. At equilibrium, the second law requires that these independent reactions occur without change in free energy. Therefore

$$G_j = \sum_i \nu_{ji} G_i \tag{47}$$

where the G_j are the partial molar free energies of the species. It is shown in Part V of this series of reports that equilibrium constant relations can be expressed as

$$\ell n\, K_{p_j} = -\frac{\Delta G_j^o}{RT} = \ell n\, p_j - \sum_i \nu_{ji}\, \ell n\, p_i \tag{48}$$

where p_j is the partial pressure of the j^{th} species, T is temperature, R is the universal gas constant, the standard state free energy change of the formation reaction for species j is defined by

$$\Delta G_j^o = G_j^o - \sum_i \nu_{ji} G_i^o \tag{49}$$

and the partial pressure of condensed species is taken as one atmosphere. The standard state free energy is a function of temperature only and is obtained for each molecular species from

$$G_j^o = H_j^o - TS_j^o \tag{50}$$

where enthalpies are obtained relative to some chemical base state, often the elements in their most natural form at 298°K and one atmosphere (JANAF base state).

The stationary condition of the free energy at equilibrium expressed in Eq. (47) is consistent with the minimum free energy statement often utilized in seeking the equilibrium state. Although the formulation followed here differs from those followed in free energy minimization approaches, the ultimate numerics can reduce to an identical iterative solution procedure.

The solution of the set of algebraic equations (Eq. (48)) must be considered in conjunction with other constraints including the pressure balance

$$\sum_j p_j = P \tag{51}$$

where the summation is over all gas phase species. The detailed solution procedure will be considered only after all required relations have been discussed.

4.2.2 Mixed Equilibrium-Nonequilibrium Relations

When some reactions fail to equilibrate it is necessary to approach the selection of the independent set of equilibrium reactions with greater caution. In a general chemical system, certain sets of molecules can be treated as always equilibrated. Between these sets certain independent equilibrium and kinetically controlled interchange reactions may exist. A procedure for treating mixed equilibrium-nonequilibrium systems is presented in this section.

The following rules are established in order to organize the logic:

1. Every species is assigned to one and only one set.
2. A set may contain as few as one species.
3. Each set has its own base species, i.e., that minimum number of species from which all other members of the set may be formed.
4. Within each set all possible reactions between member species are equilibrated.
5. Equilibrium interchange reactions involve species from more than one set.

Consider, for example, eight species of the O-H system: O, H_2O; H; H_2; O_2, O_3; HO, H_2O_2 where five sets are divided by semicolons. For these sets, the following base species are appropriate: O, H_2O; H; H_2; O_2; HO where only the first set requires more than one base species. At this juncture only two independent equilibrium reactions have been formulated, namely

$$\left.\begin{aligned} 1.5\ O_2 &\rightleftarrows O_3 \\ 2\ HO &\rightleftarrows H_2O_2 \end{aligned}\right\} \qquad (52)$$

Two independent equilibrium interchange reactions might be included in this system, for example

$$\left.\begin{aligned} H + OH &\rightleftarrows H_2 + O \\ O + OH &\rightleftarrows O_2 + H \end{aligned}\right\} \qquad (53)$$

The effect of these reactions is to reduce the number of base species by two. For example H_2 and O_2 can be deleted. The remaining base species and the array of formation reactions coefficients, ν_{ji}, are therefore

i \ j	1 O	2 H_2O	3 H	4 OH	5 H_2	6 O_2	7 H_2O_2	8 O_3
1 O	1	0	0	0	-1	1	0	1.5
2 H_2O	0	1	0	0	0	0	0	0
3 H	0	0	1	0	1	-1	0	-1.5
4 OH	0	0	0	1	1	1	2	1.5

in the general relation of Eq. (45).

If it is assumed that all other interchange reactions are frozen the formulation of the equilibrium-nonequilibrium aspects of the program are complete. In the totally equilibrated chemical system, conservational constraints are often applied to the elements. In the system just presented, however, additional conservational constraints are required. In general these constraints take the form

$$\sum_j \nu_{ji} n_j = \alpha_i \tag{54}$$

where n_j is the number of moles of species j in a unit mass of system and α_i is a conserved variable relating to the "elemental" composition of a unit mass of the system. One such constraint is applied for each base species. In effect, the base species become the "elements" of the system, and their total masses can be treated as the conserved variable of the system. This generalized concept of the conserved "elements"* of the system is extremely important to the present development.

In the general nonequilibrium system, certain kinetically controlled reactions will be important. For example, in the H-O system

$$\left.\begin{aligned} H + H + M &\rightarrow H_2 + M \\ O + O + M &\rightarrow O_2 + M \\ H + H + O &\rightarrow H_2O \end{aligned}\right\} \tag{55}$$

*The term "element" (in quotes) is used to refer to those atoms or groupings of atoms (i.e., grouped according to the base species formulae) which according to the equilibrium relations are conserved.

are three reactions of possible interest, M being any third body. The rates of these reactions can be related to the partial pressures of the reactants and products, the ultimate equilibrium constraint appropriate to the reaction, and the kinetic coefficient. With the general kinetic reaction in the form

$$\sum_j \mu^R_{jm} N_j \rightarrow \sum_j \mu^P_{jm} N_j \tag{56}$$

its rate, $\bar{R}_m$, can be expressed generally by

$$\bar{R}_m = k_{F_m} \left[\exp \sum_j \mu^R_{jm} \ell n\, p_j - \exp\left(\sum_j \mu^P_{jm} \ell n\, p_j - \ell n\, K_{p_m} \right) \right] \tag{57}$$

where k_{F_m} is the forward rate constant. The net effect of these reactions is the modification of the "elemental" makeup of the system. The kinetic reactions cause a net increase rate (moles per unit volume)

$$r_i = \sum_m \sum_j (\mu^P_{jm} - \mu^R_{jm}) \nu_{ji} \bar{R}_m \tag{58}$$

of "element" i. It is this relation which is introduced into the conservational equations in order to establish the local state of the reacting chemical system.

The forward rate constant k_{F_m}, hopefully based on experimental data, is represented with an Arrhenius type function

$$k_{F_m} = B_m \exp\,(E_{a_m}/RT) \tag{59}$$

where the exponential factor establishes the probability of a collision having energy in excess of the activation energy E_{a_m} and the factor B_m represents a multitude of phenomena associated with the probability of success of a single collision (e.g., collision orientation).

When kinetically controlled reactions approach equilibrium, difficulty is often encountered in the treatment of the relevant conservational equations. To understand the nature of this difficulty, and thus the means of avoiding it, it is instructive to consider the simple time dependent character of the H-O system previously described. Recalling that α_i represents the moles of

"element" i in a unit mass, and that r_i represents the rate of production of moles of "element" i per unit volume, it follows that

$$\frac{d\alpha_i}{d\theta} = \frac{r_i RT}{P\mathcal{M}} \tag{60}$$

At this point it is necessary to introduce another new concept. From the base species, a subset of N_{bb} base-base species can be obtained much as if all specified kinetic reactions were permitted to equilibrate. For this example O and H will be selected for this honor and the "formation reaction" for the remaining base species written as

$$\left.\begin{aligned} 2H + O &\rightarrow H_2O \\ H + O &\rightarrow OH \end{aligned}\right\} \tag{61}$$

or, more generally,

$$\sum_k \sigma_{ik} N_k \rightarrow N_i \tag{62}$$

The reactions (Eqs. (61)) equilibrate if the third of the kinetic reactions of Eq. (55) and either of the other two reactions have infinite rates. As shown in Part V of this series of reports, N_{bb} of the Eqs. (60) can be replaced by

$$\frac{d\tilde{\alpha}_k}{d\theta} = 0 \tag{63}$$

where

$$\tilde{\alpha}_k \equiv \sum_i \sigma_{ik} \alpha_i \tag{64}$$

For each base species i which is also a base-base species k, an equation of the form of Eq. (63) replaces the corresponding one of the form of Eq. (60). The other Eqs. (60) are maintained unaltered in the system of equations and still contain the kinetic expressions. These are referred to as the reactive mass balance equations. In the general case, a given reaction, m, will affect more than one of these equations. The consequences of this when such a reaction approaches equilibrium are discussed in Part V of this series of reports. By combining equations in a manner based on the a priori

selection of a set of controlling reactions, these consequences can be circumvented in an effective fashion.

4.2.3 Mass Balance Relations

In the preceding sections the equilibrium and nonequilibrium relations have been summarized for a general chemical state. These relations are in themselves insufficient until other relations, in particular the mass balance relations, are imposed. In the case of kinetic control, the time dependence of the system must be equated to flow rates and other rate dependent parameters entering the mass balances. Likewise, in diffusional systems the local state is determined by mass balance relations associated with mass transfer processes. In the following subsections the mass balance relations appropriate to various systems are summarized.

4.2.3.1 Expansion of Isolated Systems

In the expansion of a fixed mass, closed, adiabatic system it is usually appropriate to trace its state history as a function of static pressure. If the process is reversible, the entropy is constant and the local state is not a function of the time history of the expansion. Such systems satisfy the simple mass balance constraint

$$\alpha_i = \text{constant} \tag{65}$$

This equation implies either total equilibrium or a mixed equilibrium-frozen chemical process. If, however, finite reaction rates are important, the path ceases to be reversible, entropy rises, and the time history of the expansion must be considered. If the pressure is a known function of time, the expansion can be treated as

$$\text{state} = f(\alpha_i, s, P) \tag{66}$$

where the state includes such terms as $d\alpha_i/d\theta$ and $ds/d\theta$. The rate of change of the "elemental" composition is obtained from Eqs. (57) and (58), whereas the rate of increase in entropy is given by

$$\frac{ds}{d\theta} = R \sum_m \left[\ell n \, K_{p_m} - \sum_j (\mu_{jm}^P - \mu_{jm}^R) \ell n \, p_j \right] \overline{R}_m \frac{RT}{P\overline{m}} \tag{67}$$

This derivative is well behaved, even as equilibrium is approached and may be evaluated explicitly if desired. The α_i derivatives, however, must be

treated implicitly if any hope for near equilibrium solutions is to be maintained. Once a particular formulation is adopted the techniques suggested in the nonequilibrium presentation (Section 4.2.2) can be introduced in order to assure consistent solution validity. Because of the simplicity of the mass balance relation for this process, it is practical to include the kinetic mass balances directly with the iterative solution of the chemical state. This state calculation includes the relations previously presented together with the entropy constraint, namely

$$\sum_j p_j S_j = P\mathcal{M}s \tag{68}$$

4.2.3.2 State Calculations for Open Systems

The evaluation of the state in a general open system involving diffusive and convective mass and energy fluxes is most generally performed as a subordinate solution. For example, in the boundary-layer solutions of current interest, state solutions are required at several interacting locations. In this application, state solutions are required based on assigned "elemental" mass fractions (or α_i), enthalpy and pressure, i.e.

$$\text{state} = f(\alpha_i, h, P) \tag{69}$$

This solution provides to the boundary-layer solution the detailed state including thermodynamic, transport and radiative properties as well as the production rates $d\alpha_i/dt$. The last term must be included with the general mass balance relations of the boundary-layer program.

The specific relations used to achieve the state solution are the equilibrium equations (Eq. (48)), the mass balance relations (Eq. (54)), the pressure constraint (Eq. (51)) and an enthalpy constraint

$$\sum_j p_j H_j = P\mathcal{M}h \tag{70}$$

which involve no greater complexity than the conventional isolated system equilibrium solution. The coupling between this solution and the boundary-layer solution requires not only the evaluation of the production rates, $d\alpha_i/dt$ but also the rate of change of these rates with respect to the independent parameters on the right-hand-side of Eq. (69). The rates are determined with Eqs. (58) and the derivatives by use of relations developed in Part V of this series of reports.

Again, the problem of stability threatens when equilibrium approaches. However, by following the approach previously presented, the kinetic terms

can be treated separately while all other terms of the mass-balance equations are being collected. These equations can then be rearranged and combined with the kinetic relations in such a way that controlling reactions again affect only one equation at each location. Because of the overall implicit character of the boundary-layer solution, this procedure will, on convergence, yield valid stable solutions. It has been found, however, that the introduction of equilibrium type relations into the set of boundary-layer equations can destroy the linearity of the system. Therefore the approach of equilibrium by the kinetic equations included in the boundary-layer mass balances would probably delay convergence and necessitate the inclusion of certain iteration constraints.

4.2.3.3 Surface State Solutions

A more complex set of mass balance relations are introduced when surface state solutions are sought. Coupling between boundary layer, internal conduction, and surface mechanical removal solutions may be involved in these relations. In effect all the other mass balance solutions become subordinate to this solution. Two types of boundary-layer representations have been developed, a transfer coefficient correlation of mass transfer using the Z-potential and the expression of the fluxes at the wall in a form compatible with the boundary layer nodal solution procedure. The governing equations, including heterogeneous reaction kinetics, are presented in Part V of this series of reports.

One of the most elusive aspects of surface-state solutions is the adequate specification of the mechanical-chemical surface constraint. The present formulation is based on the following set of constraints for condensed phase species.

$$p_\ell = 0 \quad \text{if} \quad T < T_{F_\ell} \tag{71}$$

and

$$\sum_i \nu_{\ell i} \ell n\, p_i \leq \ell n\, K_{p_\ell} \tag{72}$$

with the equality applying to one species with $T_{F_\ell} \geq T$. The first equation implies that a particular condensed species cannot leave the surface until the surface temperature is at or above that species fail or flow temperature, T_{F_ℓ}. The second relation states that all present condensed species are in equilibrium with the base species. The inequality applies to non-present

condensed species and prohibits a super-saturated vapor state. This is equivalent to saying that at 100°C

$$P_{H_2O} \leq 1 \text{ atm} \tag{73}$$

The requirement that one species be at or below its fail temperature establishes the structural limitation of the surface. A typical result might show a surface at 2500°K with the equilibrium holding for SiC* and SiO_2^*, but if SiO_2^* has been assigned a fail temperature of, say, 2300°K, P_{SiO_2} will be positive indicating liquid removal of SiO_2^*. The SiC*, with a fail temperature greater than 2500°K, represents the surface constraining species.

4.2.4 Oblique Shock Relations

In the case of an oblique shock wave, constraints of Eqs. (51), (68), and (70) do not apply and are replaced by the conventional equations for conservation of energy, mass and momentum across the oblique shock. Presuming knowledge of the upstream conditions, these relations yield as unknowns only h, ρ, and P downstream of the shock. These relations can be further reduced to

$$\sum_j p_j + (\rho_1 u_1 \cos\theta_1)^2 \frac{RT}{P\mathcal{M}} = P_1 + \frac{(\rho_1 u_1 \cos\theta_1)^2}{\rho_1} \tag{74}$$

$$\sum_j p_j H_j + \frac{1}{2} (\rho_1 u_1 \cos\theta_1)^2 \frac{(RT)^2}{P\mathcal{M}} = P\mathcal{M}\left[h_1 + \frac{u_1 \cos\theta_1)^2}{2}\right] \tag{75}$$

where the non-subscripted variables are downstream of the shock. The first of this pair of equations replaces the more conventional pressure constraint and the latter the enthalpy constraint.

4.2.5 Summary

In this subsection an attempt has been made to formalize the basic relations so as to simplify the generation of an orderly solution. Unfortunately dealing with nonlinear equations such as these is never straightforward and is subject to many pitfalls. In the next subsection, the procedures as adopted in the current solution technique are described.

4.3 NUMERICAL SOLUTION PROCEDURE

The solution to a set of simultaneous nonlinear algebraic equations can be either trivially simple or agonizingly difficult, depending on the linearity

of the system and the depth of coupling existing between the equations. None of the problems formulated in Section 4.2 fall into the first class and some fall into the latter. The basic formulation adopted is relatively conventional and will be described first, followed by some discussion of the pitfalls that can be encountered and devices adopted to circumvent them.

4.3.1 Basic Formulation

The most direct method of solving a set of nonlinear algebraic equations is the Newton-Raphson procedure. Its application is straightforward in concept but in reality many choices occur during the formulation of a specific problem, choices which can affect the success or failure of a specific solution. The method itself is the extension of Newton's iterative method to multi-dimensional problems. Errors are evaluated for each of the equations based on a set of trial values for the unknown independent variables. The rates of change of these errors with respect to these independent variables are analytically determined, also based on the trial values. In the formulation which has been followed, $\ell n\ p_j$, p_ℓ, $\ell n\ T$, and $\ell n\ (P\mathcal{M})$ are taken as the set of independent variables, but corrections are often in terms of p_j, $1/T$ and $P\mathcal{M}$. In some systems this choice yields linear mass balance equations which if once satisfied will never deviate.

4.3.2 Solution Convergence

In general, the convergence of the set of equations appropriate to a particular problem depends on a number of factors in addition to the formulation of the derivatives. In addition to the selection of correction coordinates, initial estimates and correction restraints are major factors.

4.3.2.1 Correction Restraints

In highly nonlinear application of the Newton-Raphson technique, a variety of constraints with regard to independent variable corrections are necessary. These constraints all manifest themselves in a damping factor which limits the extent which the solution is advanced down the correction vector. When corrections exceed the constraint limits, a damping factor is introduced which is applied uniformly to all variables.

4.3.2.2 Initial Guesses

It is obvious that a good first guess can save time in any iterative solution. In the present formulation these guesses are generally based on previous solutions and only the initial stagnation or shock solution does not have the benefit of prior solution. This solution is readily obtained from practically any first guess, since the stagnation state is usually at relatively elevated

temperatures and has a fixed "elemental" composition. In the subroutine version of the chemical state program used in conjunction with the boundary-layer procedure, first guesses are generally based on solutions at the same boundary layer transverse location stored during prior iterations in the boundary-layer program or from solutions at the preceding axial station.

Because of the introduction of new species by the wall material it is necessary to initialize their compositions when the corresponding elements appear in the state solutions. Likewise if a species disappears, e.g., as the edge of the boundary layer is approached or because the sequence of boundary-layer iterations results in the termination of surface mass addition, it is necessary to zero the species in a fashion that will not result in a singular solution for the rest of the equations.

Bookkeeping becomes a major factor in the state programs if efficient and stable repetitive utilization is to be made of the routines. This bookkeeping establishes optimum first guesses, determines which atomic elements are present and zeros or initializes the appropriate molecular species.

4.4 CHEMICAL STATE PROGRAMS

To treat the solution of chemical state problems, two equilibrium programs are currently in operation, namely, the equilibrium surface thermochemistry (EST) program and the Aerotherm chemical equilibrium (ACE) program. For nonequilibrium systems a special version of the ACE program is utilized with the KINET subroutine. Ultimately, this latter combination will be generalized into the general nonequilibrium ablation thermochemistry (GNAT) program. In this section, the current capabilities of these routines is summarized, together with brief descriptions of the input required and output obtained for operation under various program options.

4.4.1 The Aerotherm Chemical Equilibrium (ACE) Program

The ACE program is the more recent and more general of the two equilibrium programs. The program operates either as a separate routine or as a subroutine to the boundary layer integral matrix procedure (BLIMP). Some options apply in both cases, but certain bookkeeping aspects are modified in order to streamline the subroutine version. The principal options are as follows:

1. Oblique shock relations
2. Assigned enthalpy, pressure and elemental composition
3. Assigned entropy, pressure and elemental composition
4. Assigned temperature, pressure and elemental composition

5. Surface balances with assigned temperature or assigned surface equilibrium

The equations actually involved in these calculations have been summarized in the preceding subsections and developed in Part V of the current report series. All of the options are formulated for a general chemical system. Consideration of any molecular, ionic or atomic species requires only the inclusion of the basic thermochemical data appropriate for that species. These basic data are obtained, for example, from the JANAF Thermochemical Data Tables and include entropy, heat of formation and specific heat curve-fit data.

Of the options listed, only the first and last require further definition of the requisite input. The oblique shock option accepts the upstream velocity, density and static enthalpy and the shock angle as basic input along with the elemental composition. The output includes the state of the gases downstream of the shock and the isentropic stagnation state.

The surface mass balance options require as a minimum input the normalized pyrolysis gas and char recession rates as well as the elemental composition of these components and the pressure. If surface equilibrium is to be suppressed, temperature must also be assigned. Two forms of surface mass balances are included in the ACE program. For coupling with the BLIMP program, special linearized flux relations are developed by a truncated Taylor series expansion about the current trial wall fluxes and wall state (see Section 2.3.1). For use with transfer coefficients, the program requires the specification of edge composition and, further, if the unequal diffusion model is to be used, the diffusion factors, F_i, must be specified unless the logarithmic proportionality of these factors to molecular weight is utilized (see Section 2.1.2). When liquid-layer removal is contemplated, it is necessary to specify the maximum temperature at which each condensed species can structurally support the surface. The output from the surface mass balance options include the total definition of the surface state including temperature, condensed-material removal rate, and the condensed species which structurally maintains the surface. Output from this option is also obtained on cards suitable for direct use with the CMA program if transfer coefficient mass balances are performed.

For most options a rather complete state of the system is generated which includes compositions, thermodynamic and transport properties, and major property and composition derivatives. It is these derivatives which permit the analytic treatment of the complex boundary-layer equations in the BLIMP program.

4.4.2 The Equilibrium Surface Thermochemistry (EST) Program

The EST program has the advantage of seniority and experience but includes no options excluded from the ACE program. Thus the advantages of EST involve better diagnostic output, more formalized input and output, and, on some occasions, greater convergence stability. EST is designed primarily for the surface mass balance options but also can be used for assigned temperature, elemental composition and pressure solutions. It does not include the condensed phase removal model, and is limited to the transfer coefficient mass balance relations. A typical output (from Ref. 20) is shown in Fig. 8.

4.4.3 The ACE-KINET Program

For nonequilibrium solutions, the KINET subroutine adds to the surface mass balance option of ACE the ability to treat specific heterogeneous or homogeneous surface-catalyzed reactions. Special KINET routines are prepared for specific systems and include a predetermined set of kinetically controlled reactions. The routine currently in use treats the heterogeneous oxidation of graphite by CO_2, O_2, H_2O, and the surface catalyzed water gas shift reaction in the H, C, O, N system. A typical result for graphite phenolic ablation (Fig. 9) shows the significant low-temperature effect of the kinetic relations. The basic data required for specifying the kinetic rates of each reaction are activation energy, pre-exponential factor, and reaction order. The output is identical to the ACE program but does not include nonequilibrium state derivatives.

4.5 SUMMARY AND CURRENT STATUS

In the preceding subsections, an approach for determining the equilibrium or nonequilibrium chemical state has been summarized for a number of open and closed thermodynamic systems. An effort has been made to provide a relatively general approach to the problems associated with such solutions and to indicate means of circumventing them. A brief discussion of the mechanics of the solution served to introduce the program and subprograms involved in the computer analysis. Some of these routines are quite general in their present formulation, others are directed toward specific systems.

Currently all equilibrium aspects of the program are fully operational for general chemical systems. This includes the various closed and open system options, the shock wave relations, the surface coupled boundary layer mass balances, bookkeeping involved with treating appearing and disappearing atomic elements, and the property and property derivative calculations. The KINET routine currently treats only the heterogeneous reactions associated with graphite oxidation. The generalization of this routine following the approach presented in this section is a major recommendation of this report.

ABLATING SURFACE THERMO-CHEMICAL EQUILIBRIA

PREPARATION OF TABLE FOR GRAPHITE PHENOLIC ABLATION IN ARC PLASMA GENERATOR

7/6/64

RELATIVE ELEMENTAL COMPOSITIONS, ATOMIC WTS/UNIT MASS

AT.NO.	ELEMENT	ATOMIC WT	PYRO.GAS	CHAR LAYER	B/L EDGE GAS
1	HYDROGEN	1.00800	0.1070182	-0.	-0.
2	HELIUM	4.00300	-0.	-0.	0.0570572
6	CARBON	12.01100	0.0505157	0.0832570	-0.
7	NITROGEN	14.00800	-0.	-0.	0.0441962
8	OXYGEN	16.00000	0.0178364	-0.	0.0095312

PRESSURE,ATM 9.00000E 00 SURF.TEMP,K 3559.68 ENTH,CAL/GM 1.78067E 03
MDOT P.G./CM 5.00000E-02 MOL.WEIGHT 13.2584 HW(1+M/CM) 2.22583E 03
MDOT CHAR/CM 2.00000E-01 SPEC.HEAT 0.51900 SURFACE C* 22

- - - - MOLE FRACTION -	SPECIE - - - -						
0.0005308	C	0.0000178	CH	0.0161998	CHN	0.0000000	CHNO
0.0000035	CHO	0.0000004	CH2	0.0000000	CH2O	0.0000004	CH3
0.0000000	CH4	0.0045728	CN	0.0005663	C2	0.0064974	C2H
0.0009285	C2H2	0.0012684	C2N2	0.0000001	C2H3	0.0000000	C2H4
0.0000000	C2H4O	0.0000000	C2H6	0.0019618	C3	0.0060477	C3H
0.0000228	C3H2	0.0000002	C3H3	0.0000000	C3H4A	0.0000000	C3H5
0.0000000	C3O2	0.0000331	C4	0.0063986	C4H	0.0000481	C4H2
0.0000000	C4H3	0.0000000	C4H4A	0.0001094	C4N2	0.0000493	C5
0.0000174	C5H	0.0000003	C5H2	0.0000000	C5H3	0.0000010	C6
0.0003574	C6H	0.0000016	C6H2	0.0000000	C6H3	0.0000000	C6H6
0.0000007	C7	0.0000077	C7H	0.0000000	C7H2	0.0000000	C8
0.0000000	C8H	0.0000000	C8H2	0.0000000	C9	0.0000001	C9H
0.0000000	C9H2	0.0000000	C10	0.0000000	C10H	0.0000000	C10H2
0.0127292	H	0.0000041	HN	0.0000000	HNO	0.0000000	HNO2
0.0000000	HNO3	0.0000000	HO	0.0000000	HO2	1 0.0000457	N
0.0000000	NO	0.0000000	NO2	0.0000000	N2O	0.0000001	O
0.0000000	O2	0.0000001	CO2	0.1105511	CO	0.6051916	HE
0.0032347	H2	0.0000000	H2O	0.2225999	N2		

Figure 8. Typical Output From Equilibrium Surface Thermochemistry (EST) Program

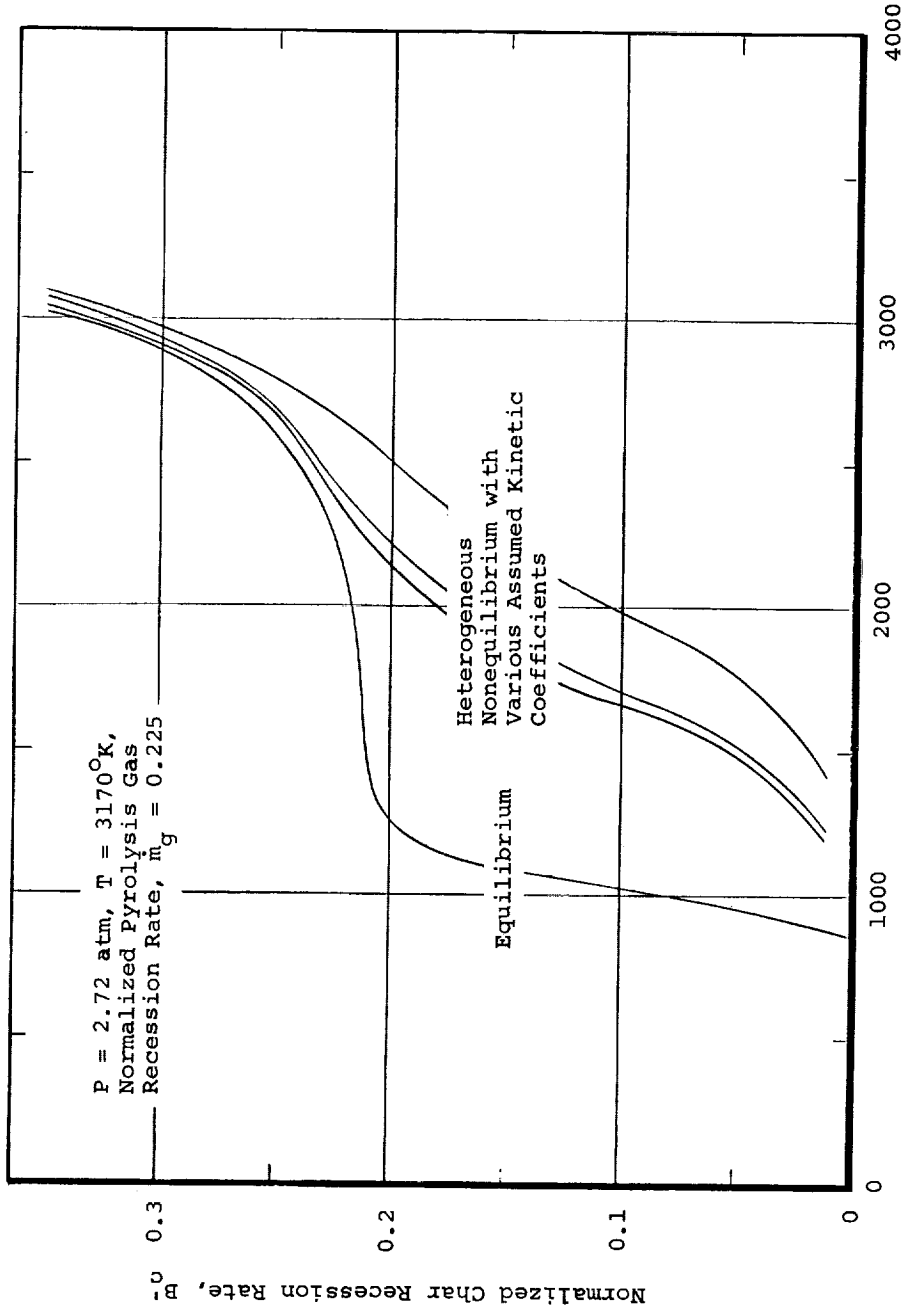

Figure 9. Equilibrium and Nonequilibrium Surface Thermochemical Response of a Graphite Phenolic Ablation Material

The section has discussed in rather general fashion the treatment of general chemical systems. The ultimate program which should evolve from this analysis will be a General Nonequilibrium Ablation Thermochemistry (GNAT) program designed for treating the problems associated with equilibrium and nonequilibrium at and above ablating surfaces.

SECTION 5
COUPLED BOUNDARY LAYER AND CHARRING MATERIAL COMPUTATIONAL PROCEDURES

5.1 INTRODUCTION

The charring material response computation described in Section 3.3 above can, of course, be operated independently of any boundary-layer calculations if the temperature and recession rate are specified as the known boundary condition. In fact, the CMA program has many uses when operated in this way, particularly as a tool for extracting material properties (thermal conductivity, specific heat, and decomposition kinetic parameters) from measured test data.

To make a general predictive tool, however, the CMA program must be coupled to some boundary-layer calculation. For best accuracy, this calculation should be complete in all relevant details. The BLIMP program described in Section 2.3 constitutes such a boundary-layer procedure. The coupled version of BLIMP plus CMA, denoted the CABLE program, thus provides a complete charring ablator analysis procedure. This coupled procedure is discussed in Section 5.3 below.

For greater speed, the CMA program can be coupled, instead, to the ACE or EST programs described in Section 4.4 which approximate the boundary layer by convective transfer coefficients but still retain the essential chemical features of the ablation events including the effects of unequal diffusion coefficients for all species. Section 5.2 below describes the approach utilized for obtaining solutions with these programs.

5.2 CHARRING MATERIAL ABLATION PROGRAM COUPLED TO FILM-COEFFICIENT BOUNDARY-LAYER CHEMISTRY PROGRAM EST OR ACE

5.2.1 General Problem Description

Section 3.2.3 above describes how the CMA in-depth solution routine can be coupled to a surface energy balance procedure to provide the heated surface boundary condition. The surface energy balance was given in normalized form in Eq. (30). It can also be expressed as

$$-q_{a_w} + q_{\substack{rad \\ in}} + \dot{m}_c h_c + \dot{m}_g h_g - q_{\substack{rad \\ out}} - (\rho v)_w h_w - \sum_{\ell} \dot{m}_{r_\ell} h_\ell - q_{cond} = 0 \tag{76}$$

where

$$q_{\substack{rad \\ in}} - q_{\substack{rad \\ out}} \equiv q_r \tag{77}$$

$$(\rho v)_w = \dot{m}_g + \dot{m}_c - \sum_{\ell} \dot{m}_{r_\ell} \tag{78}$$

The $\dot{m}_g$ and $q_{cond} = f(T_w)$ are delivered by the in-depth solution. Other dependencies of interest are

$$h_g = h_g(T_w)$$

$$h_c = h_c(T_w)$$

$$q_{\substack{rad \\ out}} = q_{\substack{rad \\ out}}(T_w)$$

For the other terms

T_w, $-q_{a_w}$, $q_{\substack{rad \\ in}}$, h_w, $\sum_{\ell} \dot{m}_{r_\ell} h_\ell$ = functions of boundary-layer-edge enthalpy, pressure, local boundary-layer solution, laws for conservation of chemical elements, chemical equilibria and/or kinetic relations, upstream events, $\dot{m}_c$ and $\dot{m}_g$

From the standpoint of the surface energy balance solution the desired relationship may be summarized as

$$T_w,\ -q_{a_w},\ q_{\substack{rad \\ in}},\ h_w,\ \sum \dot{m}_{r_\ell} h_\ell = \text{functions of } \dot{m}_c \text{ and } \dot{m}_g \text{ for given P} \tag{79}$$

Equation (76) requires an iterative solution in which T_w and $\dot{m}_c$ are the primary variables of interest, one of them regarded as dependent and the other as independent. It is most convenient to obtain the relations of Eq. (79) outside of the CMA in-depth solution and to provide the resulting information as tables which may be stored and referred to as needed. These tables give $-q_{a_w}$, $q_{rad\ in}$, h_w, $\sum_{\ell} \dot{m}_{r_\ell} h_\ell$, and T_w as functions of $\dot{m}_c$, $\dot{m}_g$, and another variable (essentially time but including all time-dependent aspects such as pressure).

The energy balance solution procedure proceeds as follows. An initial guess of the char consumption rate, $\dot{m}_c$, is obtained in some manner. With this $\dot{m}_c$ and the $\dot{m}_g$ supplied by the in-depth solution, the quantities $-q_{a_w}$, $q_{rad\ in}$, h_w, $\sum \dot{m}_{r_\ell} h_\ell$ and T_w are obtained by table look up in the tables provided by the outside surface solution routine. The quantities h_c, h_g and $q_{rad\ out}$ are then formulated using the T_w so obtained. The surface energy balance (Eq. (76)) is then computed, the q_{cond} as a function of T_w having been provided by the in-depth solution. In general, however, the sum of the terms will not equal zero but some error. An iteration procedure is then used to select successively better estimates of $\dot{m}_c$ which drive the error to zero. Experience shows that Newton's procedure, in which the derivative of the error with respect to $\dot{m}_c$ is used to compute the next guess for $\dot{m}_c$, gives good results.

The following sections describe how the required tables are generated using the film-coefficient model of the boundary layer. First, the film coefficient expressions for $-q_{a_w}$ are presented, followed by a discussion of the chemistry-and-mass-balance solution required for constructing the surface tables.

5.2.2 General Requirements for Energy Flux

Film coefficient correlations of boundary-layer heat-transfer analysis and data have been used for years to predict mass and energy transfer rates at a surface. If no chemical reactions are involved, the adaptation of the film-coefficient model to the mass-transfer problem is rather simple and straightforward. If equilibrium chemical reactions are involved, either in the boundary layer or at the surface, the ultimate form of the film-coefficient adaptation remains relatively simple for the special case of equal mass diffusion coefficients for all species and unity Lewis number. In this case, the diffusive energy flux $-q_{a_w}$ is given by the familiar expression

$$-q_{a_w} = \rho_e u_e C_H (H_r - h_w) \tag{80}$$

where C_H is the Stanton number for heat transfer. This expression has been generalized to include the effects of $C_M \neq C_H$ and unequal mass diffusion coefficients as described in Part II of the present series of reports. In that case the expression for $-q_{a_w}$ becomes more complex and involves more information about the wall state than simply h_w. The extra information automatically is computed in the process of computing the wall state in any case, as noted in the next section, so no extra computation is involved for the more complex case.

5.2.3 Solution Procedure as Related to Tabular Formulation

Construction of the tabular boundary condition to the CMA program basically requires solution for the state of the gas adjacent to the heated wall, given the normalized char rate $B'_c \equiv \dot{m}_c/\rho_e u_e C_M$ and the char chemical composition, the normalized gas injection rate $B'_g \equiv \dot{m}_g/\rho_e u_e C_M$ and the gas chemical composition, and the boundary-layer edge state. Such a solution provides h_w and $-q_{a_w}$ needed for the surface energy balance. The required solution satisfies the necessary mass balances (with mass diffusive fluxes given by film-coefficients analogous to those for the diffusive energy fluxes) and chemical relations, but of course does not attempt to satisfy an energy balance, since this last step is to be performed by the CMA program using the tabulated results of the chemistry-plus-mass-balance solution.

Several computer programs are available for the determination of the wall state tables. The Equilibrium Surface Thermochemistry program (EST) is one such program for the special case of chemical equilibrium at the wall. The Aerotherm Chemical Equilibrium program (ACE) is a later version of the EST program which allows the surface run-off of materials formed at the surface above their fail temperatures. Hence ACE computes $\sum_\ell \dot{m}_{r_\ell} h_\ell$ and lumps it with $-q_{a_w}$ for the later solution of the surface energy balance. Utilization of the KINET subroutine together with the ACE program allows heterogeneous kinetic control of several simultaneous reactions with the surface material as well as surface-catalyzed homogeneous reactions. These routines have been discussed in Section 4.4.

The chemistry-plus-mass-balance solutions provided by the EST or ACE program supply as output tables of T_w, h_w and other quantities needed to compute $-q_{a_w}$, all as functions of B'_c, B'_g, and pressure. During each time step in the course of the in-depth response solution, the CMA program develops an expression $q_{cond} = q_{cond}(T_w)$, substitutes this into the surface energy balance (Eq. (76)), and then searches among the surface tables for a B'_c which yields an energy balance, thus defining a new value for T_w. Then the solution procedure is ready for the next time step.

It may be noted that the tabular approach to the surface chemistry solution is suggested by economy. Without such tables each iteration in the search for a surface energy balance would require a new surface chemistry solution, generally in the near neighborhood of many such previous solutions. In almost all problems, the tabular approach involves fewer surface computations. Furthermore, tables once generated are often useable for many different problems, yielding even greater economy. Finally, without the tabular approach, the occasional nonconvergent surface chemistry solution would stop the entire in-depth solution process. With the tabular approach, such solutions are automatically weeded out of the tables without damage to the subsequent in-depth solution.

5.2.4 Experience with Film-Coefficient Coupling

The in-depth CMA solution routine coupled to the film-coefficient models provided by the EST, ACE, and ACE/KINET programs has been tested on a fairly wide variety of materials and a brief account of these tests may provide some useful orientation for the reader. (It may be noted that it is sometimes difficult to establish whether any discrepancies between predictions and data are due to errors in in-depth properties or models or errors in the surface treatment. Usually a careful testing plan first establishes whether or not the in-depth aspects are being treated correctly by comparing in-depth predictions to in-depth data, such as thermocouple response, where the predictions are made with assigned surface temperature and recession rate to match observed surface data. If the in-depth model can be verified in this manner, calculations may then be done with the general thermochemical boundary conditions. Success in predicting surface temperature and recession under these circumstances constitutes the "good results" referenced to below.)

By suppressing pyrolysis effects, the program has been used for numerous transient ablation problems featuring noncharring refractories. Examples here have included alumina, boron nitride, tungsten, and graphite and have covered problems with liquid layer runoff and kinetic control with generally excellent results.

With regard to charring materials, the program has been run very extensively for graphite-phenolic and carbon-phenolic with good results. Success with nylon-phenolic has been mixed since this material often suffers from mechanical ablation effects not included in the program model; the same remarks apply to asbestos-phenolic. Materials with substantial silica content have been frequently predicted, sometimes with good success, but other times with poor results since materials with large amounts of silica occasionally display such physical events as thick liquid layer runoff and subsurface char reactions (for example, silica-carbon reactions) not accounted for by the program.

In conclusion, the coupled computation procedure constituted by the CMA program plus some film-coefficient based chemistry solution (EST, ACE, or ACE/KINET) has been applied to a wide range of materials of technical interest with excellent to poor correlation depending on the particular material and boundary conditions. Any discrepancies between predictions and data have been clearly attributable to effects not considered by the program or occasionally to ill-judged boundary conditions or material properties. The program appears to be fully checked out and operational for the physical and chemical models currently employed.

5.3 COUPLED ABLATOR/BOUNDARY LAYER/ENVIRONMENT (CABLE) PROGRAM

5.3.1 Introduction

The coupled ablator/boundary layer/environment (CABLE) program is a computational procedure which couples the transient response of a charring heat shield material to a chemically reacting laminar boundary layer appropriate to superorbital reentry. A coupled approach is necessary since the material response affects the structure of the boundary layer, and the boundary layer determines the energy and mass fluxes at the surface which in turn control the heat shield response. The CABLE program incorporates subroutine versions of the BLIMP program (described in Section 2.3) and the CMA program (described in Section 3.3). The features of the CABLE program are summarized in Section 5.3.2, the mechanics of coupling are discussed in Section 5.3.3 and the coupling procedure is demonstrated further by a sample problem presented in Section 5.3.4.

5.3.2 Characteristics of the CABLE Program

All of the features of the BLIMP and CMA programs pertinent to the coupled problem are retained in the CABLE program. In that the characteristics of these subprograms have been described in some detail in preceding sections, the models employed in the CABLE program are presented summarily in Table I. The operational status of the various aspects of the computational procedure are also summarized therein. It can be seen that many considerations are fully operational, including all aspects of the in-depth response of the ablating surface material and the nonablating backup material. Certain aspects of the boundary-layer solution cannot be considered fully operational until such time that the procedure is checked out for the wide variety of materials, environments and flight conditions for which it is presumably applicable. Some aspects of the ultimate boundary-layer program have not been fully implemented at this time. Those areas where additional effort is recommended are discussed in Section 6.

5.3.3 Coupling Procedure

In the present approach, a series of one-dimensional transient charring ablation solutions are directly coupled to time-varying but quasi-steady two-dimensional boundary layers as shown in the following sketch. From a study of the numerical equations associated with the boundary-layer and charring-ablation solution procedures, it is seen that the charring-ablation solution at station ℓ and time θ is dependent upon the boundary-layer solutions at previous stations ℓ-1 and ℓ-2 through the three-point finite difference

TABLE I

COUPLED ABLATOR/BOUNDARY LAYER/ENVIRONMENT (CABLE) COMPUTER PROGRAM

I BOUNDARY-LAYER-EDGE CONDITIONS

	Phenomena	Model	Operational Status
(a)	Flight conditions	Transient or steady-state; boundary-layer-edge conditions around the body can be specified, or pressure distribution around the body and either conditions upstream of the shock or local stagnation conditions can be specified	Fully operational
(b)	Environmental gas	Arbitrary elemental and molecular composition	Fully operational
(c)	Chemical state	General mixed equilibrium-nonequilibrium	See Item II(e)
(d)	Incident radiation	Angular dependent incident radiation from inviscid shock layer	See Item II(g)
(e)	Entropy layer	Edge velocity allowed to be a function of stream function as well as streamwise location	Incorporated into program logic, but option has never been exercised; presently, flow field is considered isentropic or the presence of an entropy layer approximated by assignment of edge velocity as well as pressure but with zero shear at the boundary-layer edge
(f)	Radiation coupled inviscid flow field	Total enthalpy allowed to be a function of stream function as well as streamwise location	Requires rearrangement of some program logic before option can be implemented; presently flow field is considered adiabatic or nonadiabatic flow field approximated by assignment of total enthalpy but with zero heat flux at the boundary-layer edge

TABLE I (Continued)

II BOUNDARY LAYER

	Phenoemna	Model	Operational Status
(a)	Boundary-layer type	Laminar nonsimilar with discontinuous mass injection	Fully operational
(b)	Nature of solution	Numerical procedure capable of yielding accurate solutions	Fully operational; three to four place accuracy obtained with relatively few nodal points
(c)	Body geometry	General planar or axisymmetric flow around blunt or sharp bodies; three-dimensional boundary layers can be approximated by streamtube considerations	Fully Operational
(d)	Chemical system	Arbitrary elemental and molecular composition	Fully operational
(e)	Chemical state	General mixed equilibrium-nonequilibrium with arbitrary homogeneous and heterogeneous (surface) reaction kinetics	Fully operational for equilibrium; some solutions have been obtained for partially frozen boundary layers with rate-controlled surface reactions or surface-catalyzed reactions; general nonequilibrium model not implemented requiring rather extensive additional program logic
(f)	Transport properties	Incorporates bifurcation approximations for unequal diffusion and thermal diffusion coefficients and approximations for mixture viscosity and thermal conductivity of the Sutherland-Wassilijewa type	Fully operational for equal diffusion coefficients; convergence can be slow and some nonconvergences have occurred in problems with unequal diffusion coefficients due, apparently, to inexact derivatives in the Newton-Raphson iteration procedure.
(g)	Radiation absorption and emission	One-dimensional radiation absorption and emission with accurate frequency integrations for molecular, ionic, and atomic species resulting from ablation products and their interaction with boundary-layer edge gas	Not implemented; requires some additional programming, compilation of radiation data, debug, and checkout; presently, incident flux considered to pass through boundary layer without attenuation.

TABLE I (Continued)

III SURFACE PHENOMENA

Phenomena	Model	Operational Status
(a) Coupling considerations	The boundary layer and charring ablator solution fully coupled; transient solution at a given streamwise station completed before proceeding to next station	One solution has been obtained; some further checkout is required before the coupling can be considered fully operational for all materials and environments for which it is presumably applicable
(b) Chemical interactions	Chemical reactions between char, pyrolysis gas, and boundary-layer species allowed; these reactions are assumed to be in equilibrium except for specified rate-controlled reactions	Equilibrium operational; some solutions have been obtained for selected rate-controlled reactions
(c) Mechanical removal mechanisms	Each candidate surface condensed phase material (e.g., SiO_2*,C*,SiC*) assigned a fail temperature, above which that species cannot appear as the surface material (this is equivalent to specifying, for example, a zero liquid viscosity for SiO_2* and zero strength for C* above their respective fail temperatures)	Operational for those surface materials which have been considered; occasionally leads to chemistry convergence difficulties
(d) Other considerations	Velocity slip and temperature jump at the surface not allowed	---

IV IN-DEPTH RESPONSE OF EXPOSED (ABLATING) MATERIAL

Phenomena	Model	Operational Status
(a) Class of materials	Any charring or noncharring material for which thermochemical data are available or can be estimated	Fully operational
(b) Geometry	One-dimensional conduction but area change due to material curvature taken into account in a generalized manner, with planar, cylindrical, and spherical geometries as special cases	Fully operational

TABLE I (Continued)

IV IN-DEPTH RESPONSE OF EXPOSED (ABLATING) MATERIAL (Continued)

	Phenomena	Model	Operational Status
(c)	Thermal properties	Temperature dependent	Fully operational
(d)	Pyrolysis kinetics and subsequent internal chemical events	Pyrolysis can be specified by three independent kinetic reactions; thermal equilibrium between the char and pyrolysis gas assumed; formulation consistent with general pyrolysis-gas cracking, the user employing pyrolysis-gas enthalpy as function of temperature; char density buildup due to coking not calculated	Fully operational
(e)	Internal pressure distribution	Pressure distribution through the char calculated a posteriori using Darcy's law with momentum correction, the user specifying char permeability as a function of temperature to simulate char-density buildup due to coking reactions	Fully operational
(f)	Numerical technique	Implicit finite-difference, except that gas generation is partially explicit	Fully operational
(g)	Other numerical considerations	Variable grid spacing with nodelets used in decomposition zone. Nodes dropped from rear of ablation material	Fully operational

V IN-DEPTH RESPONSE OF BACKUP MATERIALS

Phenomena	Model	Operational Status
General	Several noncharring materials with variable thermal properties are allowed, with interfacial contact resistance (including air gaps) between materials, and variable rear surface boundary conditions	Fully operational

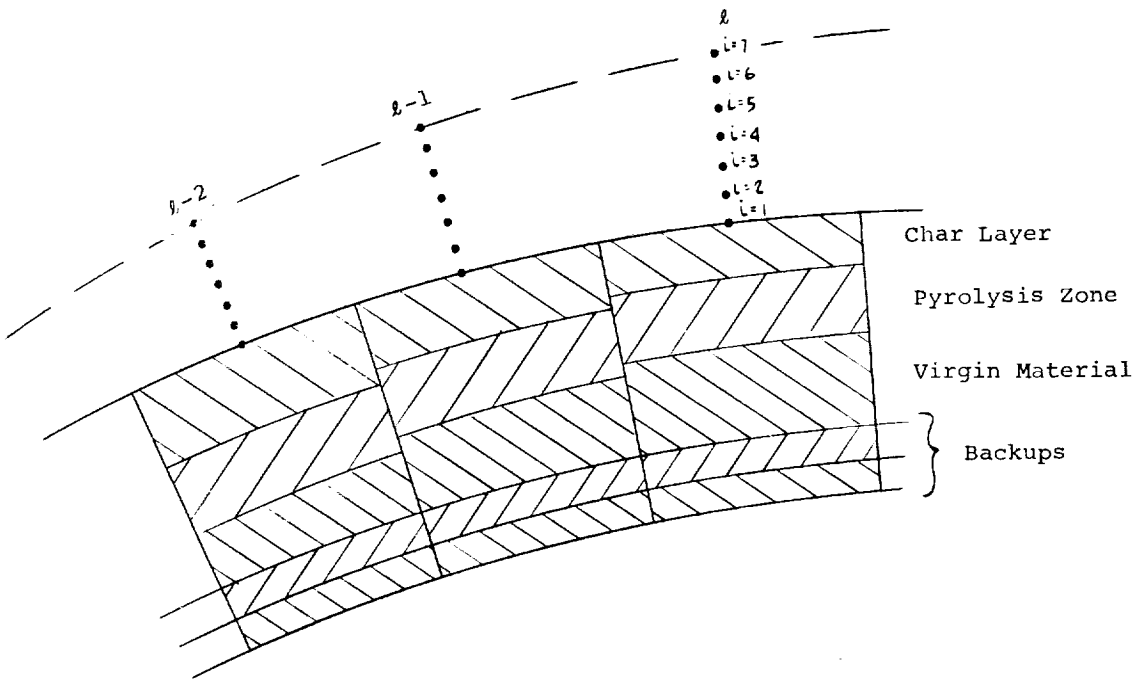

relations for the streamwise derivatives, is dependent upon the $\theta - \Delta\theta$ solution of the internal response of the ablation material at ℓ through the charring ablator finite-difference relations, and is implicitly dependent upon itself and the current boundary-layer solution.

Several approaches for coupling the boundary layer and charring ablation solutions were considered in the present study. The method which was finally adopted was selected on several bases: it makes use of options of existing programs which are well exercised and known to perform well, it avoids extrapolation of surface boundary conditions, and it avoids repeated (iterative) solution of the boundary layer and transient charring ablation response. The various other methods which were considered were inferior in one or more of these considerations. Furthermore, storage requirements and computational time are improved relative to most if not all of the other methods considered.

In the procedure which has been adopted, the transient charring ablation solution is effectively the controlling program. The charring ablation solution at a given station proceeds noniteratively, calling the boundary-layer procedure as needed to supply the surface boundary condition. The complete transient history at each axial station is performed prior to advancing to the next axial station. This is accomplished by performing sets of nonsimilar boundary-layer solutions at the current station for a discrete array of times (θ), normalized pyrolysis-gas mass flow rates ($\dot{m}_g^*$), and normalized char mass

flow rates ($\dot{m}_c^*$) (or surface temperatures, T_w, when $\dot{m}_c^* = 0$) which bracket the current values for these parameters. Calculations for intermediate times and intermediate values of $\dot{m}_g^*$ and $\dot{m}_c^*$ (or T_w) are then performed by interpolation as they are needed for the charring ablation solution. It is significant that only those members of the $\dot{m}_g^*$, $\dot{m}_c^*$ array needed to contain current values are considered, and that at any instant, these are required for only a pair of times.

The procedure is demonstrated by the example illustrated in the following sketch which is a planar representation of three-dimensional ($\dot{m}_g^*$, $\dot{m}_c^*$, θ) space.

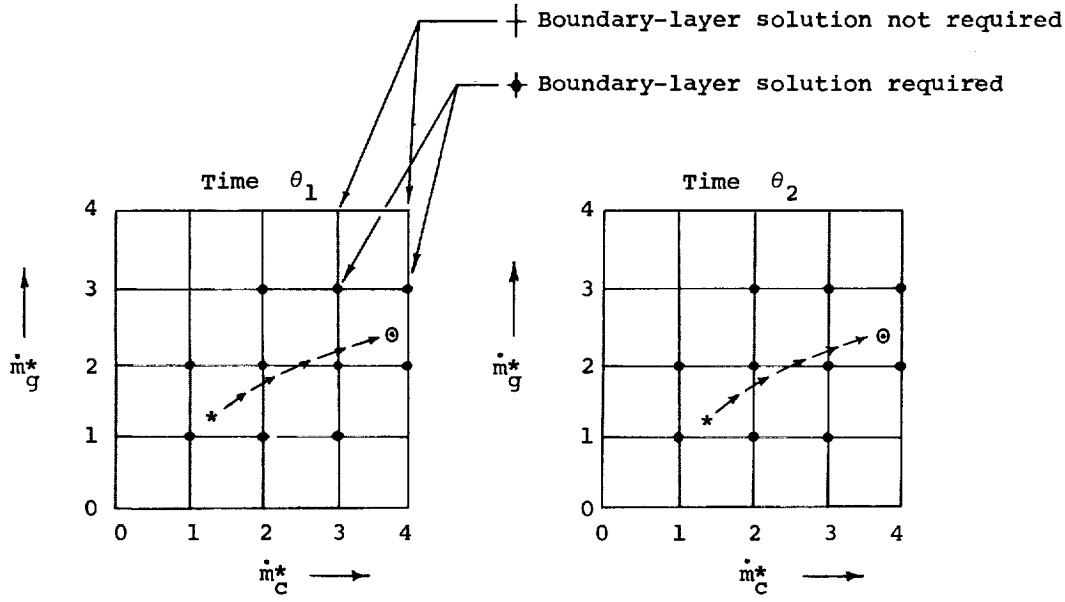

The lines of arrows shown in the sketches are the projections in the time planes $\theta = \theta_1$ and $\theta = \theta_2$ of a hypothetical history of $\dot{m}_g^*$ and $\dot{m}_c^*$ in a coupled boundary layer and charring ablation solution between times θ_1 and θ_2, where $\theta_2 > \theta_1$. The solution at time θ_1 is indicated by asterisks, whereas the solution at time θ_2 is indicated by circles. The times θ_1 and θ_2 and the grid values for $\dot{m}_g^* = 0,1,2,\ldots$ and $\dot{m}_c^* = 0,1,2,\ldots$ are preselected values for these parameters at which parametric boundary-layer solutions are conducted if and when needed. Based on the point (*) at time θ_1, boundary-layer solutions are generated for the $\dot{m}_g^*$, $\dot{m}_c^*$ points 1,1; 1,2; 2,1; and 2,2

at times θ_1 and θ_2.* Charring ablation solutions can be obtained for times $\theta_1 \le \theta \le \theta_2$ by linear interpolation as long as $\dot{m}_g^*$ and $\dot{m}_c^*$ stay within these values. Suppose that the course of the calculation between times θ_1 and θ_2 are as indicated in the sketch. Then, additional solutions at $\dot{m}_g^*$, $\dot{m}_c^*$ of 1,3 and 2,3; then 3,2 and 3,3; and finally 2,4 and 3,4 would be required, each at both times. When time θ_2 (point ⊙) is approached, the BLIMP program is called upon for solution at time θ_2 for the exact values of $\dot{m}_g^*$ and $\dot{m}_c^*$. This boundary-layer solution is printed out and that information needed for future reference (at downstream stations) is saved on tape. Solutions are then performed for time θ_3 for the current bracketing values of $\dot{m}_g^*$, $\dot{m}_c^*$ (in the present example, values of $\dot{m}_g^*$, $\dot{m}_c^*$ of 2,3; 3,3; 2,4; and 3,4). These boundary-layer solutions at time θ_3 are placed over those for θ_1 by a tape flip-flop since the latter are no longer needed. The charring ablation solution next proceeds from time θ_2 to time θ_3, calling the BLIMP program only in the event that this range of $\dot{m}_g^*$, $\dot{m}_c^*$ is exceeded.

By the use of this procedure, storage requirements are nominal. In the first place, the charring ablation solutions are noniterative and the complete transient solution at a station is accomplished and the results printed out before advancing to the next station. Thus no historic information relative to the charring ablation solution has to be stored. With regard to the boundary layer, only two times with four $\dot{m}_g^*$, $\dot{m}_c^*$ combinations at each of these times need be considered at the same time. The only quantities in the boundary layer which need to be dimensioned for the full time array are three input quantities of time, total pressure, and total enthalpy. Edge conditions are computed around the body at the time of the stagnation-point calculation since the necessary integrations are performed by curve fitting. This necessitates that streamwise dimension, static pressure, edge velocity, edge density, edge viscosity, edge temperature, body curvature parameter (r_o^{κ}), transformed streamwise dimension ($\bar{\xi}$), pressure gradient parameter (β), and the flux normalizing parameter (α^*) be dimensioned for the number of streamwise positions (but not for time). About 300 numbers must be stored during the flip-flop operation associated with the two times which are being considered simultaneously, whereas about 500 numbers must be stored on tape to reenter the boundary layer at the

*This simple example applies only after char recession has commenced, that is, $\dot{m}_c^* > 0$. In the early portion of a trajectory when $\dot{m}_c^* = 0$, $\dot{m}_c^*$ is replaced by T_w as an independent parameter. Furthermore, it is then necessary for each θ and $\dot{m}_g^*$ of current interest to compute the T_w above which char recession would occur. This is illustrated in the sample problem presented in Section 5.3.4.

same time but at the next downstream station (used for first guesses and for calculation of nonsimilar terms). Thus, both permanent machine storage requirements and tape storage requirements are not excessive as a consequence of coupling.

This coupling approach has the important feature that the CMA program operates very nearly as it does when used in conjunction with the ACE program (see Section 5.2). In the CMA/ACE approach, complete surface tables are computed a priori and independently with the ACE or EST program and these are available to the CMA solution. In the coupled approach, these surface tables are initialized with the word VOID. When the CMA program encounters this word, the BLIMP program is called to supply the requisite information for that θ, $\dot{m}_g^*$ and $\dot{m}_c^*$ (or T_w). It is thus significant that the CMA/EST and CMA/ACE approaches have been used extensively and very successfully for a wide variety of materials and environments. Likewise, the boundary-layer calculations are performed with assigned $\dot{m}_g^*$ and $\dot{m}_c^*$ or assigned $\dot{m}_g^*$ and T_w, together with the requirement of surface equilibrium (with possible specified rate-controlled surface reactions), options of the BLIMP program which also have been exercised extensively with success. Furthermore, this replacement of the wall mass and energy balances by these simple assignment statements adds stability to the boundary-layer solution.

5.3.4 Coupled Solution for Apollo SA 202 Trajectory

As a demonstration of the coupling procedure, a trace of $\dot{m}_g^*$ versus T_w at the stagnation point of the Apollo heat shield during the first 76 seconds of the Apollo SA 202 reentry trajectory is presented in Figure 10. In this problem the time-table entries were selected to be 4310, 4348, 4375 and 4400 seconds; $\dot{m}_g^*$ entries as 0, 0.1, 0.2, 0.3; T_w entries as 500, 1000, 1500, 2000, and 2500°R; and $\dot{m}_c^*$ as 10^{-5}, 10^{-3} and 10^{-2}. Boundary-layer solutions were performed at combinations of these independent parameters as they were required and are numbered in the sequence in which they were performed.

The first step in the coupled solution was to initialize the charring ablation solution at the assumed initial temperature of 530°R. This was followed by a boundary-layer solution at this initial nonablating condition (θ_1 = 4310 sec, T_w = 530°R, $\dot{m}_g^*$ = 0). This is identified as Solution 1 in Figure 10. The next step was to find the wall temperatures at which ablation would start for the initial time of 4310 seconds and the second entry in the time table, 4348 seconds, each for the first two entries in the $\dot{m}_g^*$ table, namely 0 and 0.1 (Solutions 2 through 5). This was accomplished by computing the surface temperatures required to maintain surface equilibrium for these boundary-layer edge conditions (i.e., times), these normalized pyrolysis gas

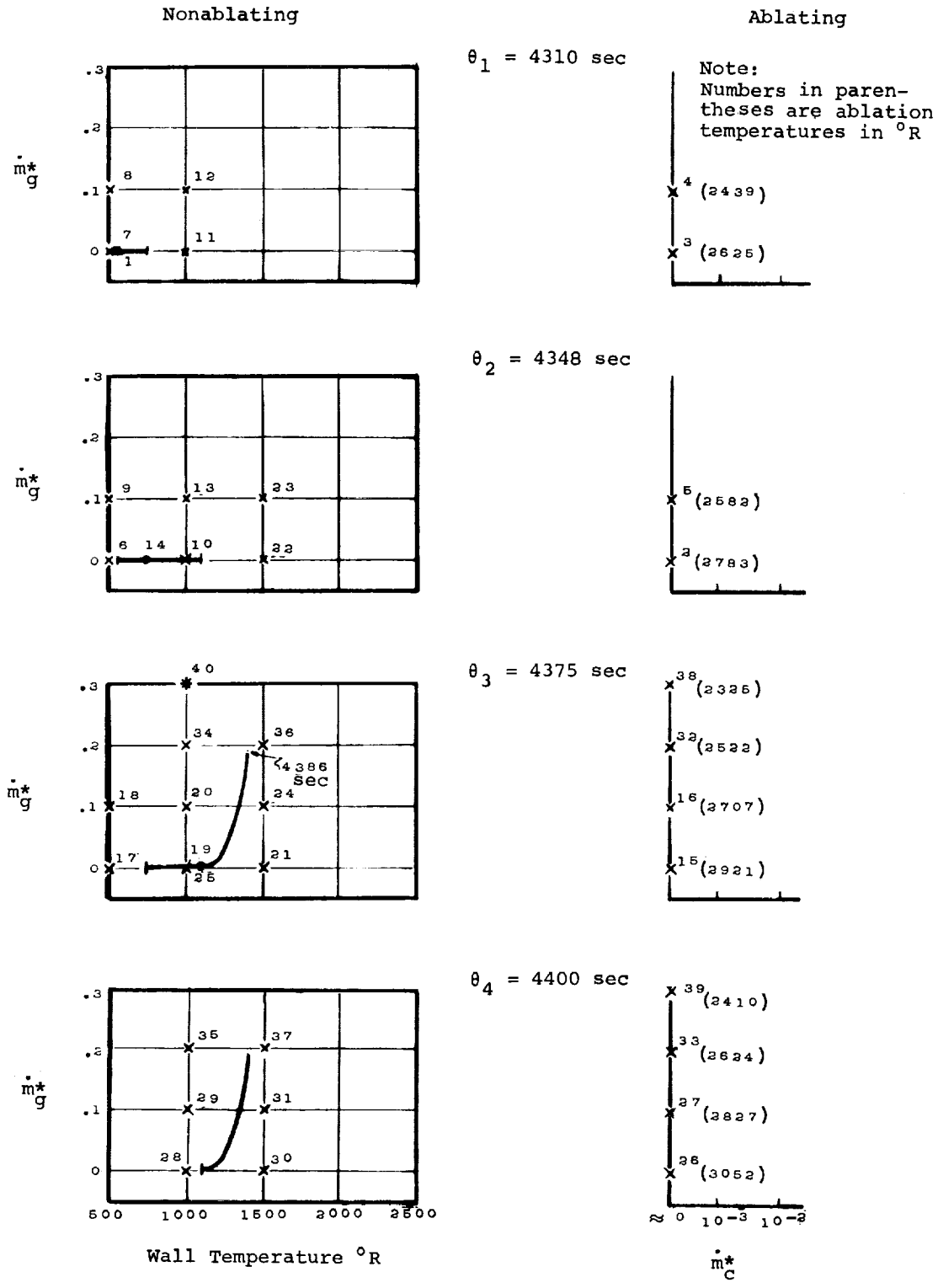

Figure 10. Demonstration of Coupling Procedure for Apollo Stagnation Point During SA 202 Trajectory

flow rates, and a very small normalized surface recession rate ($\dot{m}_c^*$ of 10^{-5} was used in these boundary-layer calculations). It can be seen that these "ablation temperatures" are all higher than the first two entries in the T_w table of 500 and 1000°R. Therefore, T_w is the appropriate independent parameter (rather than $\dot{m}_c^*$) during this portion of the trajectory. Boundary-layer solutions were then obtained at the eight corners of the θ, $\dot{m}_g^*$, T_w cube (Solutions 6 through 13). At this point the transient charring-ablation solution was able to commence, interpolating between the bracketing values of θ, $\dot{m}_g^*$ and T_w.

The transient charring-ablation solution then proceeded to $\theta_2 = 4348$ seconds, the time steps being determined by various controls built into the implicit finite-difference procedure. A charring-ablation solution was performed at precisely 4348 seconds, and this was followed by a boundary-layer solution at that time, wall temperature, $\dot{m}_g^*$ and $\dot{m}_c^*$ (Solution 14). The next order of business was to obtain the ablation temperatures (Solutions 15 and 16) at the next entry in the time table, $\theta_3 = 4375$ seconds, for the two current $\dot{m}_g^*$ of 0 and 0.1, and to obtain boundary-layer solutions at this new time for the two current T_w and $\dot{m}_g^*$ (Solutions 17 through 20).

The transient charring-ablation solution was then able to recommence and continue until a surface temperature of 1000°R was attained. It was then necessary to perform boundary-layer solutions at the next T_w entry of 1500°R for the current bracketing values of time and $\dot{m}_g^*$ (Solutions 21 through 24). The charring-ablation solution then recommenced and continued until the tabular entry time of 4375 seconds, at which point a boundary-layer solution was obtained (Solution 25). In order to proceed further with the charring-ablation solution, it was necessary to obtain the ablation temperatures (Solutions 26 and 27) and current $\dot{m}_g^*$ and T_w entries (Solutions 28 through 31) for the next time entry, $\theta_4 = 4400$ seconds.

Returning to the transient charring-ablation solution, it can be seen that substantial pyrolysis was beginning to occur. When an $\dot{m}_g^*$ of 0.1 was attained, it was necessary to compute ablation temperatures (Solutions 32 and 33) for the next $\dot{m}_g^*$ entry of 0.2 for the two currently bracketing times, and to compute boundary layers for this new $\dot{m}_g^*$ at the current T_w and times (Solutions 34 through 37). Returning again to the charring-ablation solution, an $\dot{m}_g^*$ of 0.2 was soon reached. Again, it was necessary to perform boundary-layer solutions to obtain ablation temperatures for the new $\dot{m}_g^*$ of 0.3 (Solutions 38 and 39)* and to obtain boundary-layer solutions at the current

*Computer printout for boundary-layer Solution 39 is presented as Figure 3 of this report.

bracketing times and wall temperatures for this new $\dot{m}_g^*$. Boundary-layer Solution 40 was nonconvergent and the run was terminated at this point.

The reason for this nonconvergent boundary-layer solution was that inadequate convergence damping was applied for this particular problem. The combination of a high mass injection rate and low surface temperature produced a large equilibrium concentration of CH_4 in the boundary-layer which, in turn, produced a pronounced temperature reversal. A convergent solution for this boundary-layer point has since been obtained by use of a different damping scheme. This convergence difficulty has been brought to light to demonstrate the fact that the boundary-layer procedure and in turn the chemistry subroutines must be one hundred percent reliable for all potential flight conditions to be encountered in order to obtain a coupled solution without interruption.

Temperature distributions through the charring-ablation material and boundary layer are presented in Table II for θ = 4310, 4348 and 4375 seconds, respectively. Note that there is a substantial temperature change between the wall and the first node out into the boundary layer, suggesting that it might be advisable to add a few nodes or rearrange nodal spacing.

The heat flux available to the charring-ablation program at an intermediate time is computed by linear interpolation of information derived from the boundary-layer solutions at the tabulated times. This is compared to the heat flux calculated by the boundary-layer procedure for the actual $\dot{m}_g^*$, $\dot{m}_c^*$ and T_w in the following tabulation. It can be seen that the interpolated

Time, Sec	Surface Heat Flux, Btu/sec ft^2	
	From CMA Interpolation of BLIMP Calculations	From Direct BLIMP Calculation
4310	0.154	0.1541
4348	0.570	0.5688
4375	1.58	1.581

values agree very closely with the actual values, indicating that the interpolation has been very accurate.

The above-described coupled run, including 40 boundary-layer solutions, required 16 minutes and 33 seconds on the Univac 1108 computer. It is estimated that this is only 15 percent of the entire SA 202 reentry trajectory. At this rate a stagnation point solution for the entire trajectory would require 1 hour and 50 minutes and the calculation of the nonsimilar boundary layer around the Apollo reentry vehicle would require 18 hours and 20 minutes. This figure is misrepresentative for three reasons, two having to do with

TABLE II

TEMPERATURE DISTRIBUTION FROM THE BACKWALL TO THE EDGE OF THE BOUNDARY LAYER FROM COUPLED SOLUTION: APOLLO STAGNATION POINT; SA 202 TRAJECTORY

Nodal Point	Nodal Temperatures, °R for Trajectory Times of		
	4,310 sec	4,348 sec	4,375 sec
Boundary Layer			
7 (edge)	7,877	8,584	9,228
6	7,504	8,215	8,858
5	6,995	7,634	8,213
4	6,651	7,226	7,742
3	6,046	6,500	6,891
2	3,493	3,803	4,087
1 (wall)	530.0	748.4	1,099
Charring Ablator			
1 (wall)	530.0	748.4	1,099.0
2		737.4	1,070.3
3		717.2	1,018.6
4		698.7	971.8
5		681.7	929.4
6		666.2	890.8
7		651.9	855.8
8		638.9	824.1
9		627.1	795.4
10		616.4	769.4
11		606.7	745.9
12		598.0	724.7
13		590.1	705.4
14		583.0	688.0
15		576.7	672.1
16		571.0	657.8
17		564.7	641.4
18		558.3	624.6
19		553.0	610.2
20		548.6	597.8
.		--	--
.			
.			
36		530.2	531.9
37		530.1	531.1
38 (backwall)	530.0	530.0	530.7

the number of chemistry iterations per boundary-layer iteration. In the present series of 40 boundary-layer solutions, an average of 14.3 iterations per solution was required. This is substantially greater than the 4 to 6 iterations usually required for a stagnation point solution, an uninspired uniform damping factor of 0.6 having been applied to all corrections to improve reliability.* With an improved damping scheme it is reasonable to expect an average of 6 iterations per stagnation solution to be adequate. Since the boundary-layer calculations control the computational time, this would reduce the time required to achieve a complete stagnation point history to 46 minutes. Experience has shown that boundary-layer solutions for downstream stations converge very rapidly (about 2 to 4 iterations per solution), and, furthermore, that the chemistry iteration is faster by a factor of two or so, both because the residual values for dependent variables provide good first guesses. This latter point is significant since the boundary-layer program spends about 70 percent of its time in the chemistry iteration. Applying these corrections to the original estimate, the computational time for the nine downstream stations could be expected to be reduced to 2 hours and 20 minutes. Thus, the total computational time for a coupled transient nonsimilar solution around the Apollo heat-shield during an 800 second reentry trajectory would be approximately 3 hours on the Univac 1108. On the other side of the ledger, if one were to increase the number of nodal points across the boundary layer from 7 to 10 to insure accuracy, the computational time would increase to 4 hours and 30 minutes, since the computational time is approximately proportional to the number of nodal points with this number of nodes.**

At the time of this writing, this is the only coupled transient charring ablation problem which has been attempted. It is significant, therefore, that the logic of the CABLE program (which calls the CMA and BLIMP programs as subroutines) and the coupling mechanics are really quite straightforward. Furthermore, the CMA program operates very nearly as it has on hundreds of occasions in the CMA/ACE approach and the BLIMP program is also called upon to perform for the same classes of boundary conditions for which considerable experience has been gained. Therefore, it is fair to say that the CABLE program is reasonably well checked out. The major concerns are the improvement of computational time and increase in reliability of the boundary layer and chemistry procedures. Recommendations for improvements are presented in Section 6.

---

*This is very uneconomical in general but, as discussed previously, was inadequate for the fortieth boundary-layer solution.

**If a considerably larger number of nodes were to be used, say 15 or more, the computational time would become proportional to the cube of the number of nodal points, since matrix inversion would then be controlling.

SECTION 6
SUMMARY, CONCLUSIONS AND RECOMMENDATIONS

In the Parts II through VI of this series of reports and in this summary report (Part I) a substantial analytical effort has been described. In order to bring this effort into perspective, this section presents (1) a brief summary of the analytical studies and their product computer codes, (2) the conclusions which can be drawn relative to the methods adopted and their applicability, and (3) recommendations for broader applications of the techniques and further analytical and numerical developments.

6.1 SUMMARY

The overall goal of this study has been the development of advanced theoretical techniques and their implementation in the form of computer programs for the evaluation of ablation-material performance. The thorough treatment of the intimate thermal-chemical coupling between boundary-layer and ablative surface mechanisms has been the primary specific goal.

The development of generalized and comprehensive predictive tools has been a dominant goal of the study, a factor which has necessitated the development of several novel analytical and numerical procedures. These procedures involve both the component parts of the analysis and the means whereby the parts are coupled.

The general status of the procedures developed or extended during the current effort are summarized in Table I. The status of the analyses presented in this series of reports is entered under "Model" in the table, whereas the status of the computer programs is indicated under "Operational Status." The table is directed specifically toward the Coupled Ablator/Boundary Layer/Environment (CABLE) master program. This program utilizes three major components, namely, the evaluation of the in-depth response of the charring ablator and its backup materials (Charring Material Ablation (CMA) program), the characterization of the nonsimilar laminar multicomponent chemically-active boundary layer (Boundary Layer Integral Matrix (BLIMP) program), and the evaluation of the chemical state in both open and closed systems (subroutine version of the Aerotherm Chemical Equilibrium (ACE) program). The reader is referred to Table I for an overview of the developments. In the remainder of this section some of the highlights are reviewed.

As a consequence of the ultimate coupling goal of this effort, computational speed, reliability, compatibility and generality were significant factors in the development of both theoretical and numerical techniques. Thus new boundary-layer and chemical-state procedures were developed. These have

demonstrated to be major improvements (as judged by the above-listed factors) over existing procedures in all four areas. However, further improvements in computational speed and reliability of the boundary-layer and chemistry programs are desirable and are discussed in Section 6.3

The boundary layer is solved by an integral matrix solution procedure which yields accurate solutions with relatively few nodal points and thus relatively few entries into the conservation equations. Because of the major computational time associated with the evaluation of the state-dependent parameters in a general chemical system, speed is significantly enhanced by this minimization of nodal points. This numerical procedure possesses a high degree of mathematical formality and is applicable to a broad range of problems with varied input and boundary conditions. An equilibrium chemistry model is incorporated into the computer programs which is applicable to all chemical systems. An analysis for extending this to general mixed equilibrium-nonequilibrium chemical systems is presented which should avoid the pitfalls often experienced as equilibrium is approached. Newly developed models for multicomponent transport properties including unequal diffusion and thermal diffusion coefficients for all species have demonstrated that accurate and time-saving approximations can be adopted with no significant loss of accuracy. Finally, an implicit finite difference procedure is employed which accurately characterizes the in-depth response of the charring ablator.

Two approaches have been developed for obtaining coupled solutions. The boundary layer and charring ablator numerical procedures can be coupled by use of the CABLE calling routine, or the CMA program can be operated independently utilizing input for the surface thermochemical boundary condition as provided by ACE (which represents the boundary layer by bulk transfer coefficients).

In the fully coupled procedure, the transient charring ablation response at a particular streamwise station is completed prior to advancing to the next station. Thus historic (i.e., upstream) boundary-layer information required for a starting solution and for calculation of nonsimilar terms is stored, whereas no charring ablation information at stations other than the one under current consideration is stored. The approach which has been adopted has the primary advantages that (1) it provides an implicit solution while avoiding extrapolations of surface boundary conditions and iterative repetition of charring ablation and boundary-layer solutions, (2) the CMA program operates very nearly the same as it does in the convective transfer coefficient approach, the BLIMP program providing tabular input data as needed (full tables being supplied a priori in the transfer coefficient approach), and

(3) the BLIMP program operates with assigned wall conditions (a more direct option than the alternative of introducing overall wall mass and energy balances into the boundary-layer solution).

6.2 CONCLUSIONS

The following major conclusions can be drawn regarding the research described in this report:

1. Theoretical analyses and computational techniques have been developed which are believed to extend substantially the state of the art for the characterization of: (a) nonsimilar, laminar, chemically-reacting boundary layers with unequal diffusion and thermal diffusion coefficients for all species and radiation absorption and emission; (b) mixed equilibrium-nonequilibrium, homogeneous or heterogeneous chemical systems; and (c) the transient response of ablating materials which decompose in depth, considering a general internal decomposition model (including coking kinetics) and with detailed consideration of chemical interactions at the surface. The specific models which have been employed are summarized in Table I. These procedures are self-consistent such as to permit full coupling.

2. The computational techniques have been incorporated for the most part into a set of computer programs which can either be operated independently to yield solutions for the boundary layer, the chemical state, and/or the charring ablator, or be operated simultaneously to yield fully coupled solutions. The operational status of the program components are also summarized in Table I.

3. These computer codes are applicable to all chemical systems and thus can be used to obtain solutions for any environment, ablation-material combination. These solutions should compare favorably with experimental data obtained in laminar flows as long as surface thermochemical considerations control the ablation process and if material and gas-phase properties are adequately known.

4. For those material-environment combinations where subsurface chemistry and/or surface mechanical removal mechanisms are not adequately described by the models currently employed, agreement with experimental data cannot be assured.

6.3 RECOMMENDATIONS

Recommendations for further work can be divided into three general categories: recommendations on the use of the computer programs in their present

form, recommendations for improving certain computational aspects of the solution procedures, and recommendations pertaining to the inclusion of additional physicochemical phenomena in the computer codes. These three groups are discussed in the following subsections.

6.3.1 Program Employment

As mentioned previously, the programs in their present form are adequate for many materials and environments, in particular those where surface thermochemical considerations control the ablation process and where material and gas-phase properties are adequately known. When this is the case, utilization of the programs is straightforward. However, when other considerations are significant, some "education" of the programs may be required for the specific material(s) of interest. The following approach is recommended to accomplish this objective:

1. Perform transient charring ablation calculations with the CMA program, Option 2 (assigned surface temperatures and ablation rates as measured during static test operation) and correlate with experimental internal temperature distributions as a check on thermal property data. Post-test chemical and physical analyses, in-depth, might also indicate the necessity for inclusion of such mechanisms as coking or erosion within the char layer or condensed phase reactions in-depth.

2. Perform transient charring ablation calculations with CMA/EST or CMA/ACE programs (which represent the boundary layer by bulk transfer coefficients) after first obtaining the necessary transfer coefficients from calorimetric data, from separate operation of the BLIMP program, or if possible, from cross-correlation of the results of both methods. With these calculations, attempt to correlate surface recession and surface temperature with experimental data. To achieve satisfactory correlation it may be necessary to extend these programs to include such considerations as the allowance of multiple condensed phase surface materials (e.g., liquid droplets on an otherwise carbon surface, or liquid solutions), and surface reaction kinetics. The latter can be taken into account by construction of a specialized KINET subroutine for the ACE program. The proper introduction of any of the mechanisms mentioned above is dependent on both the formulation of valid models and the experimental or theoretical evaluation of the appropriate properties.

3. Once reasonably good correlation is obtained, incorporate any changes in the ACE (or ACE-KINET) program into the surface chemistry routines of the BLIMP subroutine to the CABLE program, and utilize the CABLE

program to obtain coupled nonsimilar solutions. Again, the predictions should be correlated with experimental data.

In the event that a large number of calculations are to be made, parametric solutions using the CABLE program should be generated. The results should then be used to develop formulations for convective transfer coefficients specific to the particular materials and applications of interest for use with the more economical and more expedient CMA/ACE or CMA/ACE-KINET programs.

6.3.2 Improved Computational Details

The CMA program for in-depth response does not appear to require any extensive upgrading in computational details. For rapid transients, during which it is desirable to reduce the time-step size (in order to follow the transient more accurately) to values below the maximum which would be allowed by an explicit solution, it would be of value to be able to switch to a full-explicit in-depth energy scheme in order to minimize computation time. This could be simply done. For transients involving extremely high heat fluxes, on the other hand, it appears that neither a full-explicit scheme nor the mixed implicit-energy, explicit-density scheme presently used in the CMA program is always adequate. For these transients, both the energy equation and the decomposition equation appear to require implicit treatment to prevent the solution from disintegrating. This problem deserves further attention.

With regard to the BLIMP program, it is recommended that effort be directed to the development of a general convergence damping scheme. In those instances where inexact analytic derivatives are currently employed in the Newton-Raphson iteration process, it may be desirable to compute exact analytical derivatives or to approximate at least some of these derivatives by finite-difference relations. These are especially important if the BLIMP program is to be used extensively as a subroutine to the CABLE program because 100 percent reliability is required. Finally, for the purpose of computational economy, a streamlined CABLE program should be developed where considerably fewer boundary-layer solutions are required, interpolation between these solutions being guided by the considerably faster film-coefficient approach.

6.3.3 Additions to the Physical Model

Since the CMA in-depth computation includes only the physics of the basic pyrolysis problem, specific materials with important additional subsurface

events are not all well described by the program. Physical events here include coking and subsurface char erosion due to interaction with the pyrolysis gas, chemical kinetics of pyrolysis-gas cracking reactions as the gas flows through the char, thick liquid layer run-off (the present chemical programs account for only thin, nonviscous liquid-layer removal), additional subsurface chemical reactions such as carbon-silica reactions, thermal expansion effects, and mechanical damage to weak chars.

For many materials none of these additional effects is of interest. For other materials, the relative importance of these additional events has generally not been determined. For such materials the probable importance of the various physical events should be defined through well-planned experimentation and post-test model examination coupled with performance prediction with the existing computer programs. Such an approach has been outlined in Section 6.3.1. Only after such experimentation and study can additional analysis and programming efforts be undertaken with real confidence. In this regard, an approach for considering coking reactions in-depth, presented in Part VI of this series of reports, will be useful in the event that char density buildup appears to be an important process. A rather extensive programming effort would be required to incorporate this model into the CMA program.

The assessment of the applicability of the boundary-layer procedure in its present operational form for a particular ablation material in a specific application is much more straightforward since it is possible to estimate under what conditions phenomena not currently considered come into play. The following computer program developments may be required depending primarily upon the flight conditions of interest: extension to a turbulent boundary layer, to include radiation absorption and emission within the boundary layer, to include general nonequilibrium, to include an entropy layer, or to allow a nonadiabatic inviscid flow field. The effort required to accomplish each of these extensions is discussed briefly in the remaining paragraphs.

The boundary layer computational procedure could be extended to turbulent boundary layers by the use of eddy transport properties based, for example, on the laws of the wall and the wake adopted in Ref. 21. Radiation absorption and emission could be included by the use of the one-dimensional model presented in Section 2.1.3 and discussed in more detail in Appendix E to Part III.

The first step to the inclusion of nonequilibrium effects within the boundary layer could be to perform boundary-layer calculations while considering the kinetically controlled reactions to be frozen within the boundary layer, but including these reactions at the boundary-layer edge and including surface catalyzed and heterogeneous reactions at the wall. All equilibrium reactions would then be included during all aspects of the calculations. Subsequently nonequilibrium streamtube calculations would then be performed to obtain the

complete nonequilibrium flow field. This is permissible as a first approximation since ablation rates are generally fairly insensitive to nonequilibrium effects within the boundary layer. The extension of the boundary-layer procedure to include the general mixed equilibrium-nonequilibrium model presented in Section 4 and described in more detail in Part V of this series of reports is believed to be practical but would require a rather extensive programming effort.

The BLIMP program is presently programmed to include entropy-layer effects but this option has never been activated. Consideration of a nonadiabatic flow field would require the reorganization of some program logic, but this could be done without major difficulty.

REFERENCES

1. Aerotherm Corporation, Palo Alto, California: User's Manual, Boundary Layer Integral Matrix Program (BLIMP), in preparation.

2. Lees, L.: Laminar Heat Transfer Over Blunt-Nosed Bodies at Hypersonic Flight Speeds. Jet Propulsion, Vol. 26, No. 4, April 1956, pp. 259-269, 274.

3. Bird, R. B.: Diffusion in Multicomponent Gas Mixtures. 25th Anniversary Congress Society of Chemical Engineers (Japan), Nov. 6-14, 1961. Published in abbreviated form in Kagaku Kogaku, Vol. 26, 1962, pp. 718-721.

4. Hirschfelder, J. O., Curtiss, C. F., and Bird, R. B.: Molecular Theory of Gases and Liquids, Second printing, corrected, with notes added, John Wiley and Sons, Inc., New York, 1964.

5. Cess, R. D.: Radiation Effects upon Boundary-Layer Flow of an Absorbing Gas. J. Heat Transfer, Vol. 83, No. 4, Nov. 1964, pp. 469-475.

6. Scala, S. M. and Gilbert, L. M.: Sublimation of Graphite at Hypersonic Speeds. AIAA J., Vol. 3, No. 9, Sept. 1965, pp. 1635-1644.

7. Smith, A. M. O. and Clutter, D. W.: Machine Calculation of Compressible Laminar Boundary Layers. AIAA J., Vol. 3, No. 4, April 1965, pp. 639-647.

8. Blottner, F. G.: Nonequilibrium Laminar Boundary Layer Flow of Ionized Air. AIAA J., Vol. 2, No. 11, Nov. 1964, pp. 1921-1927.

9. Leigh, D. C. F.: The Laminar Boundary Layer Equation: A Method of Solution by Means of an Automatic Computer. Cambridge Phil. Soc. Proc., Vol. 51, 1955, pp. 320-332.

10. Pallone, A. J.: Nonsimilar Solutions of the Compressible-Laminar-Boundary Layer Equations with Applications to the Upstream-Transpiration Cooling Problem. J. Aerospace Sci., Vol. 28, No. 6, June 1961, pp. 449-456, 492.

11. Dorodnitsyn, A. A.: General Method of Integral Relations and its Application to Boundary Layer Theory. Advances in Aeronautical Sciences, Vol. 3, MacMillan, New York, 1960, pp. 207-219.

12. Aerotherm Corporation, Palo Alto, Calif.: User's Manual, Aerotherm Charring Material Ablation Program, Version 2, January 1966.

13. Aerotherm Corporation, Palo Alto, Calif.: Fortran Variable Names, Aerotherm Charring Material Ablation Program, Version 2, February 1966.

14. Aerotherm Corporation, Palo Alto, Calif.: Flow Charts, Aerotherm Charring Material Ablation Program, Version 2, April 1966.

15. Blumenthall, J. L., Santy, M. F., and Burns, E. A.: Kinetic Studies of High-Temperature Carbon-Silica Reactions in a Charred Silica-Reinforced Phenolic Resin. AIAA J., Vol. 4, No. 6, June 1966, pp. 1053-1057.

16. Schneider, P. J., Dolton, T. A., and Reed, G. W.: Char-Layer Structural Response in High-Performance Ballistic Reentry. AIAA Paper No. 66-424, June 29, 1966.

17. Kratsch, K. M., Hearne, L. F., and McChesney, H. R.: Thermal Performance of Heat Shield Composites During Planetary Entry. Lockheed Missiles and Space Company, Sunnyvale, Calif., Report LMSC-803099, October 1963.

18. Liston, E. M.: Experimental and Analytical Studies of Radiation Only Pyrolysis Of Model Char-forming Polymers. Stanford Research Institute Annual Summary Report No. 1, Contract NAS7-341, July 20, 1966.

19. Schaefer, J. W.: A Study of Composite Material Chunking Mechanisms. Vidya Progress Report, Aerojet-General P.O. No. 450342-0800, January 31, 1965.

20. Aerotherm Corporation, Palo Alto, California.: User's Manual, Aerotherm Equilibrium Surface Thermochemistry Program, Version 2, June 1966.

21. Kendall, R. M., Rubesin, M. W., Dahm, T. J., and Mendenhall, M. R.: Mass, Momentum, and Heat Transfer within a Turbulent Boundary Layer with Foreign Gas Mass Transfer at the Surface. Part I - Constant Fluid Properties. Vidya Division of Itek Corp., Vidya Final Report No. 111, Feb. 1, 1964 (AD 619 209).